From resistance to sensitivity and back – the full circle of resisting the inescapable

Tonći Šuštić

The research described in this thesis was performed at the Division of Molecular Carcinogenesis of the Netherlands Cancer Institute (Amsterdam, The Netherlands) and was financially supported by the Dutch Cancer Society (KWF), Euroean Research Council (ERC), Cancer Genomics Center (CGC) and the Oncode institute.

ISBN: 9789464022230
Printed by: Gildeprint
Copyright © 2020 Tonći Šuštić. All rights reserved.

Cover design by: Liana Silvey

From resistance to sensitivity and back – the full circle of resisting the inescapable

Van resistentie tot gevoeligheid en terug - de complete cirkel om het onvermijdelijke te weerstaan

(met een samenvatting in het Nederlands)

Proefschrift

ter verkrijging van de graad van doctor aan de
Universiteit Utrecht
op gezag van de
rector magnificus, prof.dr. H.R.B.M. Kummeling,
ingevolge het besluit van het college voor promoties
in het openbaar te verdedigen op

dinsdag 16 juni 2020 des middags te 12.45 uur

door

Tonći Šuštić

geboren op 21 februari 1984
te Split, Kroatië

Promotor:

Prof. dr. R. Bernards

Table of contents

Chapter 1 General introduction **7**

Chapter 2 A functional genetic screen identifies the phosphoinositide 3-kinase pathway as a determinant of resistance to fibroblast growth factor receptor inhibitors in *FGFR* mutant urothelial cell carcinoma. **27**
European Urology (2017)

Chapter 3 A role for the Unfolded Protein Response stress sensor ERN1 in regulating the response to MEK inhibitors in *KRAS* mutant colon cancers. **43**
Genome Medicine (2018)

Chapter 4 RUNX2/CBFB modulates the response to MEK inhibitors through activation of receptor tyrosine kinases in *KRAS* mutant colorectal cancer. **77**
Translational Oncology (2020)

Chapter 5 General discussion **107**

Appendix
Nederlandse samenvatting **127**
Summary *(in English)* **131**
Curriculum vitae **134**
Publication list **136**
Acknowledgments **138**

Chapter 1

General introduction

A short history of nearly everything on molecular cancer genetics

Cancer evolved as an umbrella term for more than 100 distinct diseases with diverse risk factors originating from various cell types and organs of the human body. It is therefore challenging to make a firm definition of cancer, but we can say that cancer cells are characterized by their ability to undergo unrestrained proliferation and often also by invasion beyond tissue boundaries and metastasis to distant organs. Much of cancer research efforts over the last couple of decades is founded on a premise that cancer results from a deranged genome. This idea originated in the late nineteenth and early twentieth century with seminal studies by David von Hansemann (Hansemann, 1890) and Theodor Boveri (Boveri, 1914) who were examining dividing cancer cells under the microscope. They reported that cancer cells harbor abnormalities of the hereditary material which they saw as aberrant chromosomes in various stages of mitosis. In the ensuing decades, chemical nature of this hereditary material was defined as deoxyribonucleic acid (DNA) (Avery, 1944), its structure was discovered (Watson and Crick, 1953) and its rearrangements were linked to human disease.

The first specific and recurrent genomic abnormality directly and causally linked with cancer was reported in 1973 by Rowley *et al.* who described the translocation between chromosomes 9 and 22 in chronic myeloid leukemia, defining the so called "Philadelphia chromosome" (Rowley, 1973). About one decade later, in 1982, the first naturally occurring somatic point mutation in cancer was identified. This was a single base substitution in codon 12 of the *HRAS* gene (Reddy et al., 1982; Tabin et al., 1982). This finding marked the onset of an era of molecular cancer genetics and sparked the relentless search for the abnormal genes underlying the development of human cancer. In the first 25 years since the discovery of the *HRAS* point mutation, approximately 100.000 additional somatic mutations have been identified in the cancer genome (Stratton et al., 2009), and this number continues to increase. Some of these point mutations were found in already known cancer-promoting genes such as *BRAF*, *PIK3CA*, *EGFR*, and *HER2*, and some were more surprising such as mutations in *IDH1*, isocitrate dehydrogenase, which is an essential enzyme of the Krebs cycle of oxidative phosphorylation.

Interestingly, a whole series of somatic point mutations was found in genes coding for kinases that become constitutively activated by the specific mutation found in cancer. This initiated carefully orchestrated drug discovery efforts to find inhibitors that could serve as anticancer therapeutics. Thanks to these efforts we now have access to both large-scale sequencing of cancer genomes and the drugs necessary to experimentally interrogate the phenotypic behavior of cancer cells in the presence and absence of such drugs. Together, these efforts resulted in a fine-grained picture of the various genetic alterations that underlie cancer development coupled with their functional consequences. It is our challenge now to integrate this complex information to deepen our understanding of the biological mechanisms that promote cancer cell growth and invasion, in the hope to chart new directions for treatment of cancer.

Cancer as an evolutionary process that can be mimicked *in vitro*

In our current understanding, malignant outgrowth is a result of an elaborate two-step evolutionary process. First, the acquisition of heritable genetic variation in individual cells, and second, natural selection, which weeds out cells that have acquired deleterious mutations or mutations that do not confer growth or survival advantage. When cells gradually accumulate these mutations during the course of a lifetime they are called somatic mutations, as opposed to germline mutations that are inherited from parents and transmitted to offspring. Current DNA sequencing technologies have confirmed the causal link between cancers and the mutations in the DNA sequence of the genomes of cancer cells. However, only a minority of somatically acquired changes present in cancer genome have been directly linked with cancer development. These changes have been dubbed ‘driver’ mutations, to differentiate them from the plethora of underlying ‘passenger’ mutations that made no measurable contribution to the process of carcinogenesis. A driver mutation is one that confers growth or survival advantage to the cancer cell and has been positively selected in the pre-malignant and malignant microenvironment. On the other hand, passenger mutations have not been selected because they do not confer selective advantage, but are still abundantly present in the cancer genome, presumably due to the accrual of random somatic mutations that occur during cell division, or due to exposure to carcinogens such as benzo[a]pyrene, aflatoxins, or tobacco smoke (Loeb and Harris, 2008). In either case, while the damage in a particular segment of the DNA occurs randomly, the phenotypes of associated carcinogenic changes are determined by selection.

Any somatic mutation that impairs cell survival will be subject to negative selection in the cancer evolution. Contrary to that, any mutation that is beneficial to the survival of cancer cells will be actively maintained due to positive selection. These dynamic processes of positive and negative selection can be mimicked *in vitro* using elaborate experimental setup called functional genetic screen. A screen is called functional if it has a functional, and often binary readout, of growth *vs.*

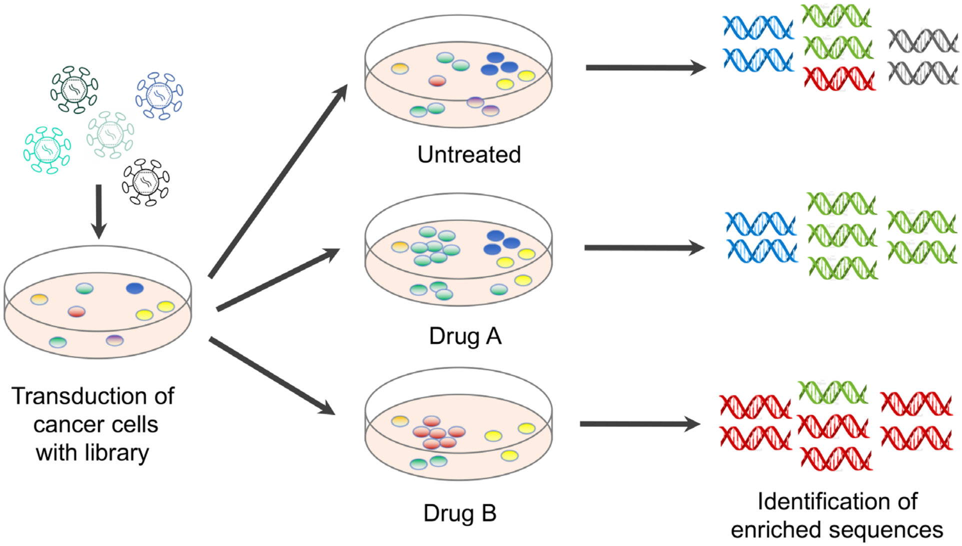
Untreated
Drug A
Drug B
Transduction of cancer cells with library
Identification of enriched sequences

Figure 1. Experimental setup of a functional genetic screen. If a genetic screen is analysed as a positive selection screen, then we measure the relative enrichment of specific sequences in drug-treated scenario compared to untreated control cell population. For example, green and red sequences are enriched in the presence of drugs A and B, respectively. However, if a screen is analysed as a negative selection screen, then we are looking for the absence of specific DNA sequences, for example the absence of red sequences in Drug A, and the absence of blue sequences in Drug B.

no growth, survival *vs.* death, positive *vs.* negative selection. If positive selection resulting from overcoming drug-induced growth inhibition has been the primary focus of a screen, we call it a resistance screen. On the other hand, negative selection screens are also called dropout screens, because the aim is to find the specific sequences that are missing from the test scenario (Figure 1). In this thesis, I have applied both approaches to understand the molecular mechanisms underlying responses of cancer cells to drugs.

Targeted therapeutics and acquired resistance

As it became clear that cancer arises primarily as a result of somatically acquired changes in the genetic material, a lot of focus has been directed towards large cancer genome-sequencing projects. These studies have yielded profound insights into the mutations that contribute to malignant growth. Some of the mutations identified cause aberrant and constant activation of genes that drive uncontrolled proliferation and govern metastatic or immune-evading properties of cancer cells. Comprehensive sequencing efforts have revealed ~140 genes that can promote or "drive" tumorigenesis, when altered by specific intragenic mutations (Vogelstein et al., 2013); and these genes have been termed oncogenes.

Considering that a typical tumor contains only two to eight of these "driver" mutations (the remaining mutations are passengers that confer no selective growth advantage), and that cancer cells can become addicted to the activity of a single oncogene, which is known as "oncogene addiction" (Weinstein, 2002), much effort has been placed in designing small molecule inhibitors directed against individual oncoproteins. These inhibitors, called targeted therapeutics, resulted in clinical improvement in cancers driven by specific genetic events, such as $BRAF^{V600E}$ mutant melanomas, chronic myeloid leukemias driven by *BCR-ABL* translocations, *HER2* amplified breast cancers, *EGFR* mutant lung cancers and several others (Sun and Bernards, 2014).

However, advanced cancers are far more complex than clonal outgrowths of a single transformed cell; they are highly heterogenous in nature and possess adaptive mechanisms that help cells survive under changing physiological and/or pharmacological circumstances. It is for this reason that resistance occurs almost invariably when advanced stage disease is treated with agents that act on an oncogenic driver. Intrinsic resistance is a rapid adaptive response of a majority of cancer cells within the tumor. On the other hand, adaptive or acquired resistance requires comprehensive rewiring of cell signaling and often involves additional (epi) genetic alterations that become prominent over the course of clonal selection. This is the reason why adaptive resistance emerges after an initial period of response.

To tackle this problem, it is essential to gain a comprehensive mechanistic understanding of these adaptive mechanisms which emerge as a result of the dynamic and genetic flexibility of intracellular signaling pathways. As our understanding deepens, new possibilities for intervention are being discovered, and applied in the clinic, as demonstrated by the phenomenon of synthetic lethality, as well as more recently described genetic interactions termed collateral dependencies. These topics are discussed in more detail below.

Synthetic lethality

Inhibitors against protein products of most druggable oncogenes have already been developed and are commercially available. Moreover, effective targeted agents are emerging even against certain variants of mutant *RAS* that have previously been considered undruggable (Janes et al., 2018; Ostrem et al., 2013). It is therefore of paramount importance to learn how to successfully apply these agents to forestall or avoid the emergence of resistant clones. One example of a successful approach is synthetic lethality (SL), a situation in which neither drug (or mutation) is lethal to a cell when applied in isolation, but administered together they result in lethality (Figure 2A). Synthetic lethality is a particularly important concept because cancers can be initiated through a series of loss-of-function mutations in tumor-suppressor genes, such as *PTEN* or *TP53*. While it is impossible to pharmacologically target the missing or inactivated gene, it is possible to discover specific vulnerabilities that arise in the given loss-of-function genetic context. In other words, it is possible to find a druggable synthetic lethal partner of a mutationally inactivated tumor-suppressor gene. This was formally proven in 2005, when two seminal papers demonstrated that *BRCA1* or *BRCA2* deficient tumor cells are hypersensitive to inhibitors of Poly-ADP ribose Polymerase (PARP) (Bryant et al., 2005; Farmer et al., 2005). Several mechanisms have since been proposed, neither of which fully explaining the extent and potency of the observed phenotype (D'Andrea, 2018). Simplistically speaking, *BRCA*-deficient tumors are defective in homologous-recombination-mediated DNA repair which makes them dependent on PARP-mediated base-excision repair of damaged DNA. This vulnerability can be therapeutically exploited using PARP inhibitors in various *BRCA*-mutant cancers, such as ovarian, breast or prostate cancer (Audeh et al., 2010; Fong et al., 2009; Tutt et al., 2010). The encouraging outcomes of these clinical trials were confirmed by follow up studies which led to the approval of three different PARP inhibitors (olaparib, rucaparib, and niraparib) by the U.S. Food and Drug Administration (FDA) for clinical use in patients with *BRCA*-mutant ovarian and breast cancer (Lord and Ashworth, 2017).

The BRCA-PARP synthetic lethal interaction is an example of a “gene-drug” synthetic lethality, as it arises as a consequence of interaction between the mutated gene (*BRCA*) and a small molecule (PARP inhibitor). If small molecules are used to inhibit both of the gene products of the two genes that are in a synthetic lethality relationship relative to one another, this interaction can be considered a “drug-drug” synthetic lethality. One of the clinically most successful examples is synthetic lethal interaction between EGFR and BRAF in *BRAF* mutant colorectal cancer (Prahallad et al., 2012). It is important to note that EGFR and BRAF inhibitors, applied as single agents, are largely ineffective in this malignancy, but administered together display drug synergy. This finding, based on an unbiased functional genetic approach (synthetic lethality screen), provided a mechanistic rationale for several clinical trials where *BRAF (V600E)* metastatic colorectal cancer (CRC) patients received either a dual combination of BRAF and EGFR inhibitors or a triple combination with the addition of MEK or PI3K inhibitors (Corcoran et al., 2018; van Geel et al., 2017). The results of these studies conclusively demonstrated that the combination treatment improved response rates and outcome as compared with single agent treatment strategies. The same combination of EGFR and BRAF inhibition was also studied in the presence of chemotherapeutic agent irinotecan. There also, the addition of BRAF inhibitor showed an increase in response rate and progression-free survival when compared with the combinations without the BRAF inhibitor (Hong et al., 2016; Kopetz et al., 2017). Finally, a phase 3 trial confirmed the safety of triple combination containing BRAF inhibitor encorafenib, MEK inhibitor binimetinib and an anti-EGFR antibody cetuximab (Kopetz et al., 2019). These results will most likely lead to the FDA approval of this triple combination as second-line treatment for patients with *BRAF (V600E)* metastatic CRC. However, the beneficial outcome was not observed in the entire patient cohort and there were documented cases of secondary resistance. This is most likely due to intratumor heterogeneity and clonal evolution of mutations leading to the reactivation of the MAPK pathway (Oddo et al., 2016).

Importantly, a drug combination that is clinically superior might not necessarily meet the criteria of a quantitative test of synergistic pharmacological interaction. The pharmacological assays designed to identify and validate synergistic drug combinations are based on Loewe Additivity (used in Chapter 2) or Bliss independence score, and are applicable to cell culture experiments, but not to clinical trials. If a pharmacological drug interaction assay confirms a given drug combination as synergistic, the clinical benefit that might arise in combination treatment is due to drug interaction within tumor cells. On the other hand, in some clinically superior combinations the benefit is only visible on the level of patient populations due to variability in drug responses (Palmer and Sorger, 2017). Distinguishing between the two is important for the interpretation of clinical trial data and for making the choice between sequential and simultaneous treatment.

A remarkable example of a combination synergy effect that was not based on a synthetic lethality screen is given by phase 3 clinical trial combining a small-molecule inhibitor of CDK4 and CDK6 palbociclib with an aromatase inhibitor letrozole in the treatment of postmenopausal women with estrogen-receptor (ER)-positive, human epidermal growth factor receptor 2 (HER2)-negative advanced breast cancer. The study concluded that palbociclib combined with letrozole resulted in significantly longer progression-free survival compared to letrozole alone, although the rates of myelotoxic effects were higher in combination treatment arm (Finn et al., 2016). Another clinically successful example of a “drug-drug” combination that would not necessarily qualify as a synthetic lethality is co-inhibition of BRAF and MEK in the treatment of BRAF-mutant melanoma, which was also validated in a phase 3 clinical trial (Long et al., 2014), although it provides only a few months of progression-free survival compared to BRAF inhibitor alone.

In recent years, the gene-centric efforts to identify synthetic lethal effects associated with individual cancer driver genes have been complemented by a series of genetic screens aiming to map the genetic dependencies of large panels of tumor cell lines. One such study described as many as 501 genome-scale loss-of-function screens performed in a wide range of human cell lines (Tsherniak et al., 2017), while another focused specifically on profiling kinase dependencies (Campbell et al., 2016). Thanks to these and other similar studies, such as (McDonald et al., 2017), we now have access to an overview of the genes necessary for the growth of individual cell lines. In combination with genotype information, we can now search for specific synthetic lethal effects with the ultimate goal to identify vulnerabilities in human cancers that can be provoked using small molecules. However, the fact remains that now, after more than a decade of concentrated effort to identify and utilize synthetic lethality in the treatment of cancer, there are still only a handful of clinically successful examples. One of the plausible hypotheses explaining this is the issue of incomplete penetrance of synthetic lethality due to the intra-tumor heterogeneity or context dependency of the phenotype. In other words, only a fraction of tumor cells in a lesion undergo cell death program when an associated synthetic lethal target is inhibited (Ryan et al., 2018) or the phenotype is only apparent in a subset of cancers, making the clinical development less attractive. The cell death only happens in a fraction of tumor cell clones that contain a specific genetic alteration that renders that specific cell population susceptible to a given synthetic lethality. In order to overcome this problem, a combination of various strategies would need to be applied, either simultaneously or intermittently. These issues gave rise to the idea of higher-order synthetic lethality interactions (collateral dependencies) and collateral vulnerabilities which will be discussed below.

Collateral dependency

Hard lessons learned from a series of clinical trials that failed to reach target have thought us that oncogene-dependent cancer cells will engage previously dispensable genes and pathways when treated with an inhibitor specific to their oncogenic driver. This seemingly subtle yet precise shift in signaling flux enables cancer cells to survive and proliferate in an oncogene-inhibited state. A number of non-mutational bypass mechanisms of drug resistance have already been described, and carefully reviewed (Garraway and Jänne, 2012), concluding that a thorough understanding of resistance mechanisms is imperative in order to avoid the pre-existing resistance and overcome acquired resistance to targeted therapeutics. Any putative synthetic lethal dependencies with the driving oncogene are contingent on the overactivated signaling induced by that oncogene. If the product of that oncogene is inhibited by a small molecule, the bypass pathways capable of sustaining cancer cell survival in this new situation of acute deprivation of a driver oncogene's activity are likely distinct from direct synthetic lethal interactions. For this reason, Lou and coworkers have recently proposed a new term, dubbed collateral dependency (CD) to describe a class of genetic interactions that support the driver-limited cancer cell state (Lou et al., 2019). They made use of the genome-scale CRISPR interference functional genomics platform (Gilbert et al., 2014; Horlbeck et al., 2016) and the new KRAS^{G12C} specific inhibitor (Janes et al., 2018; Lito et al., 2016; Ostrem et al., 2013; Patricelli et al., 2016) to search for collateral dependency-type genetic interactions in cellular models of *KRAS*^{G12C} mutant lung and pancreatic cancer. They identified diverse mechanisms by which CDs influence *KRAS*^{G12C}-driven growth upon oncogene inactivation and tested these interactions in a large panel of *KRAS*^{G12C}-driven cancer cells. Their results show that vast majority of newly identified genetic interactions are not synthetic lethal (SL) with mutant *KRAS*, thus demonstrating that CDs are biologically distinct from SL dependencies. Moreover, this work revealed that optimal targeting of *KRAS*-driven cancers requires combination of inhibitory activities, against the driver oncogene and any of its collateral dependencies.

Collateral dependencies are, in a nutshell, synthetic lethality-like genetic interactions that arise specifically in an oncogenic driver-limited state (Figure 2B). While synthetic lethal genes are dependent on hyperactive signaling downstream of the driving oncogene, collateral dependencies arise when this driving oncogene is persistently inhibited by the externally applied targeted agent. Indeed, altered signaling networks in a driver-limited cancer cell state may open novel genetic vulnerabilities that were previously masked by the hyperactive oncogenic signaling. In essence, collateral dependencies can be regarded as higher-order synthetic lethal effects. Although Lou *et al* (Lou et al., 2019) were the first to use the term collateral dependency, their work established a generalizable strategy that can be applied, in retrospect, to any direct inhibitor of an oncogenic driver. In fact, one of the clinically most advanced examples of such higher-order synthetic lethality is the interaction between EGFR and BRAF in *BRAF* mutant colorectal cancer (Prahallad et al., 2012),

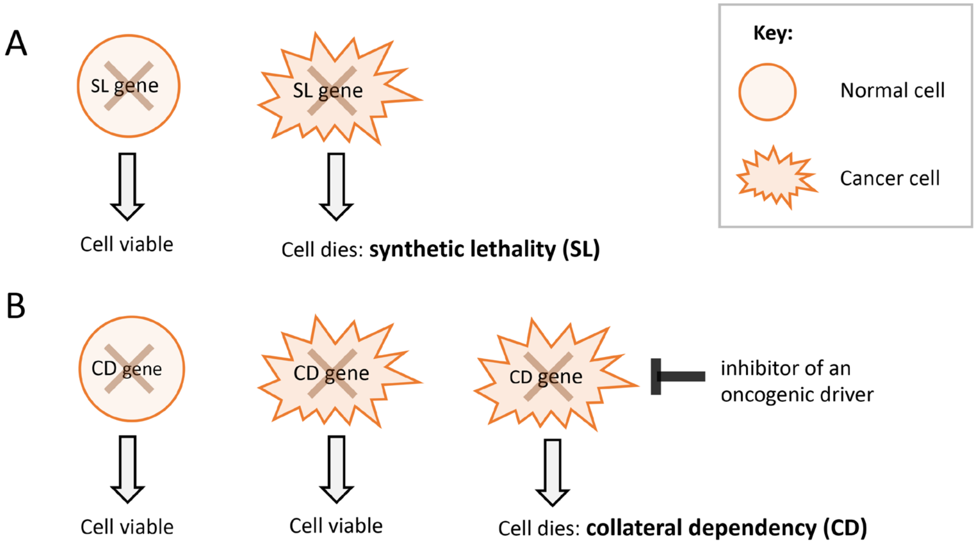
A
SL gene
Cell viable
SL gene
Cell dies: **synthetic lethality (SL)**
Key:
Normal cell
Cancer cell
B
CD gene
Cell viable
CD gene
Cell viable
CD gene
inhibitor of an oncogenic driver
Cell dies: **collateral dependency (CD)**

Figure 2. Synthetic lethality and collateral dependency.

(A) Synthetic lethality arises as a consequence of loss of function or inactivation of a synthetic lethal (SL) gene in an oncogenic context of a cancer cell. If the same gene is deleted or targeted in a non-transformed cell, the cell remains viable.

(B) In an untreated scenario, the loss or inactivation of a collateral dependency (CD) gene is well tolerated by the cancer cell (middle). Collateral dependency is revealed only upon inhibition of an oncogenic driver in cancer cells (right). Figure adapted from Lou *et al.* (Lou et al., 2019) which was already mentioned above in the synthetic lethality section. Here, a driver gene effect is targeted by the BRAF inhibitor while anti-EGFR compounds aim to prevent any synthetic rescue effects that have now been termed collateral dependencies. In this case, active EGFR is therefore a collateral dependency of BRAF-inhibited CRC cells. The incomplete responses and secondary resistance observed in subsequent clinical trials (Hong et al., 2016; Kopetz et al., 2019; 2017) could also be due to the fact that not all *BRAF*-mutant collateral dependencies have been identified and successfully targeted in those studies.

Collateral vulnerability

Acquiring resistance to a targeted agent usually involves rewiring of cellular signaling which may result in specific vulnerabilities to drugs that parental cell population would be innately resistant to. Unlike collateral dependencies, this is not a novel concept; it was known since the 1960s and termed collateral sensitivity (Hutchison, 1963). It is defined as a greater susceptibility of a resistant population, in comparison with the parent population, to another compound, meaning a compound different that the one used to induce resistance. Interestingly, the parent population can be less susceptible than the resistant population to the action of the second agent, but this is not always the case. The resistant population of tumor cells constitutes a reservoir from which drug-resistant tumor clones can emerge. This is why targeting resistant cell population, which is often referred to as the persister cell pool, presents an opportunity to forestall or impede tumor relapse (Oxnard, 2016). The origins of this persister cell pool were a topic of major debates in the field, until two recent publications proved that persister cells can emerge from pre-existing resistant subclones that expand after therapy and also that they emerge *de novo* upon exposure to targeted agent (Hata et al., 2016; Ramirez et al., 2016). Interestingly, in some cells, drug-resistant subclones arise with the same resistance mechanism every time that they are treated with a given compound, while other cells exhibit no predestined resistance mechanism and have the potential to acquire diverse resistant phenotypes. Recent work by Hangauer and coworkers (Hangauer et al., 2017) identified a broad downregulation of antioxidant gene-expression in persister cells. This observation led the authors to identify persister cell vulnerabilities specifically in oxidative stress defense mechanisms and suggest that targeting of these resistance mechanisms may represent a therapeutic strategy to prevent acquired drug resistance. In this thesis, we start with the hypothesis that resistant cell clones harbor specific collateral vulnerabilities that, once uncovered, may represent a potent therapeutic approach.

Thesis overview

In the following chapter; Chapter 2, we describe an unbiased functional genetic approach we designed to search for synthetic lethal interactions with the *FGFR* oncogene in *FGFR*-mutant bladder and lung cancer. Although the growth of *FGFR*-mutant cancers is driven by the constitutively activated FGFRs (fibroblast growth factor receptors), the responses to FGFR kinase inhibitors are moderate at best. Aiming to study the drug-resistance mechanisms and potentially unravel new synthetic lethal partners of the *FGFR* oncogene, we performed an FGFR inhibitor synthetic lethality screen in an *FGFR*-mutant bladder cancer model using a small hairpin RNA (shRNA) library targeting a complete set of human kinases. We discovered that silencing several components of the PI3K pathway (*AKT3*, *PIK3CA* and *PIK3R1*) can enhance the responsiveness to the FGFR inhibition. Moreover, we reported that PI3K reactivation is an important resistance mechanism that can occur upon exposure to FGFR inhibitor. Importantly, the reactivation of PI3K happens through feedback signaling by EGFR and HER2/3. Our work demonstrates that targeting components of the downstream signaling of the FGFR and ERBB family members, such as PI3K, can block the adaptive pathway and convert the response from cytostatic to cytotoxic (Wang et al., 2017). Finally, we formally proved synthetic lethal interaction between FGFR and PI3K inhibitors in various *FGFR*-mutant bladder and lung cancer cell lines (Wang et al., 2017).

While Chapter 2 of this thesis will focus on the concept of synthetic lethality, Chapter 3 will propose a novel and unexpected collateral dependency that arises in *KRAS* mutant colorectal cancer cells via the master regulator of the unfolded protein response, ERN1. ERN1 functions as an endoplasmatic reticulum (ER) membrane-embedded kinase and an endonuclease that sensors the status of unfolded proteins inside the ER lumen and governs the unfolded protein response (Niwa et al., 1999). A series of functional genetic screens performed on yeast cells, demonstrated that loss of *ire1*, a yeast homologue of *ERN1*, represents a collateral vulnerability of hyperactivated Ras signaling in yeast. However, signaling downstream of Ras differs in yeast and mammalian cells. Only upon inhibition of MAPK signaling with the use of allosteric MEK inhibitors, we uncover the genetic interaction between mutant *RAS* and *ERN1* in *KRAS* mutant colorectal cancer cells. To understand the mechanism of this interaction we apply CRISPR-Cas9 based genetic screen genome-wide and uncover specific collateral dependencies of the MEK-inhibited state in our colorectal cancer models (Sustic et al., 2018).

In Chapter 4 we will discuss relatively unexplored players in MEK inhibitor resistance, transcription factor *RUNX2* and its binding partner and transcriptional coactivator *CBFB*. We will present a mechanistic examination of *RUNX2* and *CBFB* negative cells and demonstrate that cells made resistant to MEK inhibitor (by losing *RUNX2* or *CBFB*) gain collateral vulnerability to conjoint SHP2 and MEK inhibition (Sustic et al., 2020). SHP2 is one of the crucial adaptor proteins that relays survival and proliferation signals from the cell membrane and engages downstream pathways such as PI3K or MAPK signaling (Prahallad et al., 2015). The persistent signaling through SHP2, found in resistant cell population, makes *RUNX2* knockout (KO) cells especially vulnerable to small molecules targeting SHP2. This is why SHP2 engagement can be thought of as a collateral vulnerability of MEK inhibitor resistant cells. Moreover, we explore the possibility of using SHP2, as potentially crucial signaling node, to overcome resistance to MEK inhibitors in *KRAS* mutant colon cancer (Sustic et al., 2020).

REFERENCES

Audeh, M.W., Carmichael, J., Penson, R.T., Friedlander, M., Powell, B., Bell-McGuinn, K.M., Scott, C., Weitzel, J.N., Oaknin, A., Loman, N., Lu, K., Schmutzler, R.K., Matulonis, U., Wickens, M., Tutt, A., 2010. Oral poly(ADP-ribose) polymerase inhibitor olaparib in patients with BRCA1 or BRCA2 mutations and recurrent ovarian cancer: a proof-of-concept trial. Lancet 376, 245–251. doi:10.1016/S0140-6736(10)60893-8

Avery, O.T., 1944. Studies on the chemical nature of the substance inducing transformation of Pneumococcal types: induction of transformation by a desoxyribonucleic acid fraction isolated from Pneumococcus type III. Journal of Experimental Medicine 79, 137–158. doi:10.1084/jem.79.2.137

Boveri, T., 1914. Zur Frage der Entstehung maligner Tumoren. Gustav Fischer 1–64.

Bryant, H.E., Schultz, N., Thomas, H.D., Parker, K.M., Flower, D., Lopez, E., Kyle, S., Meuth, M., Curtin, N.J., Helleday, T., 2005. Specific killing of BRCA2-deficient tumours with inhibitors of poly(ADP-ribose) polymerase. Nature 434, 913–917. doi:10.1038/nature03443

Campbell, J., Ryan, C.J., Brough, R., Bajrami, I., Pemberton, H.N., Chong, I.Y., Costa-Cabral, S., Frankum, J., Gulati, A., Holme, H., Miller, R., Postel-Vinay, S., Rafiq, R., Wei, W., Williamson, C.T., Quigley, D.A., Tym, J., Al-Lazikani, B., Fenton, T., Natrajan, R., Strauss, S.J., Ashworth, A., Lord, C.J., 2016. Large-Scale Profiling of Kinase Dependencies in Cancer Cell Lines. CellReports 14, 2490–2501. doi:10.1016/j.celrep.2016.02.023

Corcoran, R.B., André, T., Atreya, C.E., Schellens, J.H.M., Yoshino, T., Bendell, J.C., Hollebecque, A., McRee, A.J., Siena, S., Middleton, G., Muro, K., Gordon, M.S., Tabernero, J., Yaeger, R., O'Dwyer, P.J., Humblet, Y., De Vos, F., Jung, A.S., Brase, J.C., Jaeger, S., Bettinger, S., Mookerjee, B., Rangwala, F., Van Cutsem, E., 2018. Combined BRAF, EGFR, and MEK Inhibition in Patients with BRAFV600E-Mutant Colorectal Cancer. Cancer Discovery 8, 428–443. doi:10.1158/2159-8290.CD-17-1226

D'Andrea, A.D., 2018. Mechanisms of PARP inhibitor sensitivity and resistance. DNA Repair (Amst.) 71, 172–176. doi:10.1016/j.dnarep.2018.08.021

Farmer, H., McCabe, N., Lord, C.J., Tutt, A.N.J., Johnson, D.A., Richardson, T.B., Santarosa, M., Dillon, K.J., Hickson, I., Knights, C., Martin, N.M.B., Jackson, S.P., Smith, G.C.M., Ashworth, A., 2005. Targeting the DNA repair defect in BRCA mutant cells as a therapeutic strategy. Nature 434, 917–921. doi:10.1038/nature03445

Finn, R.S., Martin, M., Rugo, H.S., Jones, S., Im, S.-A., Gelmon, K., Harbeck, N., Lipatov, O.N., Walshe, J.M., Moulder, S., Gauthier, E., Lu, D.R., Randolph, S., Diéras, V., Slamon, D.J., 2016. Palbociclib and Letrozole in Advanced Breast Cancer. N Engl J Med 375, 1925–1936. doi:10.1056/NEJMoa1607303

Fong, P.C., Boss, D.S., Yap, T.A., Tutt, A., Wu, P., Mergui-Roelvink, M., Mortimer, P., Swaisland, H., Lau, A., O'Connor, M.J., Ashworth, A., Carmichael, J., Kaye, S.B., Schellens, J.H.M., de Bono, J.S., 2009. Inhibition of poly(ADP-ribose) polymerase in tumors from BRCA mutation carriers. N Engl J Med 361, 123–134. doi:10.1056/NEJMoa0900212

Garraway, L.A., Jänne, P.A., 2012. Circumventing cancer drug resistance in the era of personalized medicine. Cancer Discovery 2, 214–226. doi:10.1158/2159-8290.CD-12-0012

Gilbert, L.A., Horlbeck, M.A., Adamson, B., Villalta, J.E., Chen, Y., Whitehead, E.H., Guimaraes, C., Panning, B., Ploegh, H.L., Bassik, M.C., Qi, L.S., Kampmann, M., Weissman, J.S., 2014. Genome-Scale CRISPR-Mediated Control of Gene Repression and Activation. Cell 159, 647–661. doi:10.1016/j.cell.2014.09.029

Hangauer, M.J., Viswanathan, V.S., Ryan, M.J., Bole, D., Eaton, J.K., Matov, A., Galeas, J., Dhruv, H.D., Berens, M.E., Schreiber, S.L., McCormick, F., McManus, M.T., 2017. Drug-tolerant persister cancer cells are vulnerable to GPX4 inhibition. Nature 1–13. doi:10.1038/nature24297

Hansemann, von, D., 1890. Ueber asymmetrische Zelltheilung in Epithel-krebsen und deren biologische Bedeutung. Virchows Arch. Path. Anat. 119, 299.

Hata, A.N., Niederst, M.J., Archibald, H.L., Gomez-Caraballo, M., Siddiqui, F.M., Mulvey, H.E., Maruvka, Y.E., Ji, F., Bhang, H.-E.C., Krishnamurthy Radhakrishna, V., Siravegna, G., Hu, H., Raoof, S., Lockerman, E., Kalsy, A., Lee, D., Keating, C.L., Ruddy, D.A., Damon, L.J., Crystal, A.S., Costa, C., Piotrowska, Z., Bardelli, A., Iafrate, A.J., Sadreyev, R.I., Stegmeier, F., Getz, G., Sequist, L.V., Faber, A.C., Engelman, J.A., 2016. Tumor cells can follow distinct evolutionary paths to become resistant to epidermal growth factor receptor inhibition. Nat. Med. 22, 262–269. doi:10.1038/nm.4040

Hong, D.S., Morris, V.K., Osta, El, B., Sorokin, A.V., Janku, F., Fu, S., Overman, M.J., Piha-Paul, S., Subbiah, V., Kee, B., Tsimberidou, A.M., Fogelman, D., Bellido, J., Shureiqi, I., Huang, H., Atkins, J., Tarcic, G., Sommer, N., Lanman, R., Meric-Bernstam, F., Kopetz, S., 2016. Phase IB Study of Vemurafenib in Combination with Irinotecan and Cetuximab in Patients with Metastatic Colorectal Cancer with BRAFV600E Mutation. Cancer Discovery 6, 1352–1365. doi:10.1158/2159-8290.CD-16-0050

Horlbeck, M.A., Gilbert, L.A., Villalta, J.E., Adamson, B., Pak, R.A., Chen, Y., Fields, A.P., Park, C.Y., Corn, J.E., Kampmann, M., Weissman, J.S., 2016. Compact and highly active next-generation libraries for CRISPR-mediated gene repression and activation. Elife 5, 914. doi:10.7554/eLife.19760

Hutchison, D.J., 1963. Cross resistance and collateral sensitivity studies in cancer chemotherapy. Adv. Cancer Res. 7, 235–250.

Janes, M.R., Zhang, J., Li, L.-S., Hansen, R., Peters, U., Guo, X., Chen, Y., Babbar, A., Firdaus, S.J., Darjania, L., Feng, J., Chen, J.H., Li, S., Li, S., Long, Y.O., Thach, C., Liu, Y., Zarieh, A., Ely, T., Kucharski, J.M., Kessler, L.V., Wu, T., Yu, K., Wang, Y., Yao, Y., Deng, X., Zarrinkar, P.P., Brehmer, D., Dhanak, D., Lorenzi, M.V., Hu-Lowe, D., Patricelli, M.P., Ren, P., Liu, Y., 2018. Targeting KRAS Mutant Cancers with a Covalent G12C-Specific Inhibitor. Cell 172, 578–589.e17. doi:10.1016/j.cell.2018.01.006

Kopetz, S., Grothey, A., Yaeger, R., Cuyle, P.-J.A., Huijberts, S., Schellens, J.H.M., Elez, E., Fakih, M., Viladot, C.M., Peeters, M., Desai, J., Yoshino, T., Ciardiello, F., Wasan, H.S., Maharry, K., Christy-Bittel, J., Gollerkeri, A., Van Cutsem, E., Tabernero, J., 2019. Updated results of the BEACON CRC safety lead-in: Encorafenib (ENCO) + binimetinib (BINI) + cetuximab (CETUX) for BRAFV600E-mutant metastatic colorectal cancer (mCRC). Journal of Clinical Oncology 37, 688–688. doi:10.1200/JCO.2019.37.4_suppl.688

Kopetz, S., McDonough, S.L., Van Karlyle Morris, Lenz, H.-J., Magliocco, A.M., Atreya, C.E., Diaz, L.A., Allegra, C.J., Wang, S.E., Lieu, C.H., Eckhardt, S.G., Semrad, T.J., Kaberle, K., Guthrie, K.A., Hochster, H.S., 2017. Randomized trial of irinotecan and cetuximab with or without vemurafenib in BRAF-mutant metastatic colorectal cancer (SWOG 1406). Journal of Clinical Oncology 35, 520–520. doi:10.1200/JCO.2017.35.4_suppl.520

Lito, P., Solomon, M., Li, L.-S., Hansen, R., Rosen, N., 2016. Allele-specific inhibitors inactivate mutant KRAS G12C by a trapping mechanism. Science 351, 604–608. doi:10.1126/science.aad6204

Loeb, L.A., Harris, C.C., 2008. Advances in chemical carcinogenesis: a historical review and prospective. Cancer Research 68, 6863–6872. doi:10.1158/0008-5472.CAN-08-2852

Long, G.V., Stroyakovskiy, D., Gogas, H., Levchenko, E., de Braud, F., Larkin, J., Garbe, C., Jouary, T., Hauschild, A., Grob, J.J., Chiarion Sileni, V., Lebbe, C., Mandalà, M., Millward, M., Arance, A., Bondarenko, I., Haanen, J.B.A.G., Hansson, J., Utikal, J., Ferraresi, V., Kovalenko, N., Mohr, P., Probachai, V., Schadendorf, D., Nathan, P., Robert, C., Ribas, A., DeMarini, D.J., Irani, J.G., Casey, M., Ouellet, D., Martin, A.-M., Le, N., Patel, K., Flaherty, K., 2014. Combined BRAF and MEK inhibition versus BRAF inhibition alone in melanoma. N Engl J Med 371, 1877–1888. doi:10.1056/NEJMoa1406037

Lord, C.J., Ashworth, A., 2017. PARP inhibitors: Synthetic lethality in the clinic. Science 355, 1152–1158. doi:10.1126/science.aam7344

Lou, K., Steri, V., Ge, A.Y., Hwang, Y.C., Yogodzinski, C.H., Shkedi, A.R., Choi, A.L.M., Mitchell, D.C., Swaney, D.L., Hann, B., Gordan, J.D., Shokat, K.M., Gilbert, L.A., 2019. KRAS G12C inhibition produces a driver-limited state revealing collateral dependencies. Sci Signal 12, eaaw9450. doi:10.1126/scisignal.aaw9450

McDonald, E.R., III, de Weck, A., Schlabach, M.R., Billy, E., Mavrakis, K.J., Hoffman, G.R., Belur, D., Castelletti, D., Frias, E., Gampa, K., Golji, J., Kao, I., Li, L., Megel, P., Perkins, T.A., Ramadan, N., Ruddy, D.A., Silver, S.J., Sovath, S., Stump, M., Weber, O., Widmer, R., Yu, J., Yu, K., Yue, Y., Abramowski, D., Ackley, E., Barrett, R., Berger, J., Bernard, J.L., Billig, R., Brachmann, S.M., Buxton, F., Caothien, R., Caushi, J.X., Chung, F.S., Cortés-Cros, M., deBeaumont, R.S., Delaunay, C., Desplat, A., Duong, W., Dwoske, D.A., Eldridge, R.S., Farsidjani, A., Feng, F., Feng, J., Flemming, D., Forrester, W., Galli, G.G., Gao, Z., Gauter, F., Gibaja, V., Haas, K., Hattenberger, M., Hood, T., Hurov, K.E., Jagani, Z., Jenal, M., Johnson, J.A., Jones, M.D., Kapoor, A., Korn, J., Liu, J., Liu, Q., Liu, S., Liu, Y., Loo, A.T., Macchi, K.J., Martin, T., McAllister, G., Meyer, A., Mollé, S., Pagliarini, R.A., Phadke, T., Repko, B., Schouwey, T., Shanahan, F., Shen, Q., Stamm, C., Stephan, C., Stucke, V.M., Tiedt, R., Varadarajan, M., Venkatesan, K., Vitari, A.C., Wallroth, M., Weiler, J., Zhang, J., Mickanin, C., Myer, V.E., Porter, J.A., Lai, A., Bitter, H., Lees, E., Keen, N., Kauffmann, A., Stegmeier, F., Hofmann, F., Schmelzle, T., Sellers, W.R., 2017. Project DRIVE: A Compendium of Cancer Dependencies and Synthetic Lethal Relationships Uncovered by Large-Scale, Deep RNAi Screening. Cell 170, 577–592.e10. doi:10.1016/j.cell.2017.07.005

Niwa, M., Sidrauski, C., Kaufman, R.J., Walter, P., 1999. A role for presenilin-1 in nuclear accumulation of Ire1 fragments and induction of the mammalian unfolded protein response. Cell 99, 691–702.

Oddo, D., Sennott, E.M., Barault, L., Valtorta, E., Arena, S., Cassingena, A., Filiciotto, G., Marzolla, G., Elez, E., van Geel, R.M.J.M., Bartolini, A., Crisafulli, G., Boscaro, V., Godfrey, J.T., Buscarino, M., Cancelliere, C., Linnebacher, M., Corti, G., Truini, M., Siravegna, G., Grasselli, J., Gallicchio, M., Bernards, R., Schellens, J.H.M., Tabernero, J., Engelman, J.A., Sartore-Bianchi, A., Bardelli, A., Siena, S., Corcoran, R.B., Di Nicolantonio, F., 2016. Molecular Landscape of Acquired Resistance to Targeted Therapy Combinations in BRAF-Mutant Colorectal Cancer. Cancer Research 76, 4504–4515. doi:10.1158/0008-5472.CAN-16-0396

Ostrem, J.M., Peters, U., Sos, M.L., Wells, J.A., Shokat, K.M., 2013. K-Ras(G12C) inhibitors allosterically control GTP affinity and effector interactions. Nature 503, 548–551. doi:10.1038/nature12796

Oxnard, G.R., 2016. The cellular origins of drug resistance in cancer. Nat. Med. 22, 232–234. doi:10.1038/nm.4058

Palmer, A.C., Sorger, P.K., 2017. Combination Cancer Therapy Can Confer Benefit via Patient-to-Patient Variability without Drug Additivity or Synergy. Cell 171, 1678–1691.e13. doi:10.1016/j.cell.2017.11.009

Patricelli, M.P., Janes, M.R., Li, L.-S., Hansen, R., Peters, U., Kessler, L.V., Chen, Y., Kucharski, J.M., Feng, J., Ely, T., Chen, J.H., Firdaus, S.J., Babbar, A., Ren, P., Liu, Y., 2016. Selective Inhibition of Oncogenic KRAS Output with Small Molecules Targeting the Inactive State. Cancer Discovery 6, 316–329. doi:10.1158/2159-8290.CD-15-1105

Prahallad, A., Heynen, G.J.J.E., Germano, G., Willems, S.M., Evers, B., Vecchione, L., Gambino, V., Lieftink, C., Beijersbergen, R.L., Di Nicolantonio, F., Bardelli, A., Bernards, R., 2015. PTPN11 Is a Central Node in Intrinsic and Acquired Resistance to Targeted Cancer Drugs. CellReports 12, 1978–1985. doi:10.1016/j.celrep.2015.08.037

Prahallad, A., Sun, C., Huang, S., Di Nicolantonio, F., Salazar, R., Zecchin, D., Beijersbergen, R.L., Bardelli, A., Bernards, R., 2012. Unresponsiveness of colon cancer to BRAF(V600E) inhibition through feedback activation of EGFR. Nature 482, 100–103. doi:10.1038/nature10868

Ramirez, M., Rajaram, S., Steininger, R.J., Osipchuk, D., Roth, M.A., Morinishi, L.S., Evans, L., Ji, W., Hsu, C.-H., Thurley, K., Wei, S., Zhou, A., Koduru, P.R., Posner, B.A., Wu, L.F., Altschuler, S.J., 2016. Diverse drug-resistance mechanisms can emerge from drug-tolerant cancer persister cells. Nature Communications 7, 10690–8. doi:10.1038/ncomms10690

Reddy, E.P., Reynolds, R.K., Santos, E., Barbacid, M., 1982. A point mutation is responsible for the acquisition of transforming properties by the T24 human bladder carcinoma oncogene. Nature 300, 149–152.

Rowley, J.D., 1973. Letter: A new consistent chromosomal abnormality in chronic myelogenous leukaemia identified by quinacrine fluorescence and Giemsa staining. Nature 243, 290–293.

Ryan, C.J., Bajrami, I., Lord, C.J., 2018. Synthetic Lethality and Cancer - Penetrance as the Major Barrier. Trends Cancer 4, 671–683. doi:10.1016/j.trecan.2018.08.003

Stratton, M.R., Campbell, P.J., Futreal, P.A., 2009. The cancer genome. Nature 458, 719–724. doi:10.1038/nature07943

Sun, C., Bernards, R., 2014. Feedback and redundancy in receptor tyrosine kinase signaling: relevance to cancer therapies. Trends Biochem. Sci. 39, 465–474. doi:10.1016/j.tibs.2014.08.010

Sustic, T., Bosdriesz, E., van Wageningen, S., Wessels, L.F.A., Bernards, R., 2020. RUNX2/CBFB modulates the response to MEK inhibitors through activation of receptor tyrosine kinases in KRAS-mutant colorectal cancer. Transl Oncol 13, 201–211. doi:10.1016/j.tranon.2019.10.006

Sustic, T., van Wageningen, S., Bosdriesz, E., Reid, R.J.D., Dittmar, J., Lieftink, C., Beijersbergen, R.L., Wessels, L.F.A., Rothstein, R., Bernards, R., 2018. A role for the unfolded protein response stress sensor ERN1 in regulating the response to MEK inhibitors in KRAS mutant colon cancers. Genome Med 10, 90. doi:10.1186/s13073-018-0600-z

Tabin, C.J., Bradley, S.M., Bargmann, C.I., Weinberg, R.A., Papageorge, A.G., Scolnick, E.M., Dhar, R., Lowy, D.R., Chang, E.H., 1982. Mechanism of activation of a human oncogene. Nature 300, 143–149.

Tsherniak, A., Vazquez, F., Montgomery, P.G., Weir, B.A., Kryukov, G., Cowley, G.S., Gill, S., Harrington, W.F., Pantel, S., Krill-Burger, J.M., Meyers, R.M., Ali, L., Goodale, A., Lee, Y., Jiang, G., Hsiao, J., Gerath, W.F.J., Howell, S., Merkel, E., Ghandi, M., Garraway, L.A., Root, D.E., Golub, T.R., Boehm, J.S., Hahn, W.C., 2017. Defining a Cancer Dependency Map. Cell 170, 564–576.e16. doi:10.1016/j.cell.2017.06.010

Tutt, A., Robson, M., Garber, J.E., Domchek, S.M., Audeh, M.W., Weitzel, J.N., Friedlander, M., Arun, B., Loman, N., Schmutzler, R.K., Wardley, A., Mitchell, G., Earl, H., Wickens, M., Carmichael, J., 2010. Oral poly(ADP-ribose) polymerase inhibitor olaparib in patients with BRCA1 or BRCA2 mutations and advanced breast cancer: a proof-of-concept trial. Lancet 376, 235–244. doi:10.1016/S0140-6736(10)60892-6

van Geel, R.M.J.M., Tabernero, J., Elez, E., Bendell, J.C., Spreafico, A., Schuler, M., Yoshino, T., Delord, J.-P., Yamada, Y., Lolkema, M.P., Faris, J.E., Eskens, F.A.L.M., Sharma, S., Yaeger, R., Lenz, H.-J., Wainberg, Z.A., Avsar, E., Chatterjee, A., Jaeger, S., Tan, E., Maharry, K., Demuth, T., Schellens, J.H.M., 2017. A Phase Ib Dose-Escalation Study of Encorafenib and Cetuximab with or without Alpelisib in Metastatic BRAF-Mutant Colorectal Cancer. Cancer Discovery 7, 610–619. doi:10.1158/2159-8290.CD-16-0795

Vogelstein, B., Papadopoulos, N., Velculescu, V.E., Zhou, S., Diaz, L.A., Kinzler, K.W., 2013. Cancer Genome Landscapes. Science 339, 1546–1558. doi:10.1126/science.1235122

Wang, L., Sustic, T., Leite de Oliveira, R., Lieftink, C., Halonen, P., van de Ven, M., Beijersbergen, R.L., van den Heuvel, M.M., Bernards, R., van der Heijden, M.S., 2017. A Functional Genetic Screen Identifies the Phosphoinositide 3-kinase Pathway as a Determinant of Resistance to Fibroblast Growth Factor Receptor Inhibitors in FGFR Mutant Urothelial Cell Carcinoma. European Urology 71, 858–862. doi:10.1016/j.eururo.2017.01.021

Watson, J.D., Crick, F.H.C., 1953. Molecular structure of nucleic acids. Nature 171, 737–738.

Weinstein, I.B., 2002. Cancer. Addiction to oncogenes--the Achilles heal of cancer. Science 297, 63–64. doi:10.1126/science.1073096

Chapter 2

A functional genetic screen identifies the phosphoinositide 3-kinase pathway as a determinant of resistance to fibroblast growth factor receptor inhibitors in *FGFR* mutant urothelial cell carcinoma

Liqin Wang [1,*], Tonći Šuštić [1,*], Rodrigo Leite de Oliveira [1,*],
Cor Lieftink [1], Pasi Halonen [1], Marieke van de Ven [2],
Roderick L. Beijersbergen [1], Michel M. van den Heuvel [3],
René Bernards [1,#] and Michiel S. van der Heijden [1,3,#]

[*] These authors contributed equally

[#] Corresponding authors

[1] Division of Molecular Carcinogenesis, Cancer Genomics Netherlands. The Netherlands Cancer Institute, Plesmanlaan 121, 1066 CX Amsterdam, The Netherlands.

[2] Mouse Clinic Intervention unit. The Netherlands Cancer Institute, Plesmanlaan 121, 1066 CX Amsterdam, The Netherlands.

[3] Division of Medical Oncology, Antoni van Leeuwenhoek Hospital, Plesmanlaan 121, 1066 CX Amsterdam, The Netherlands.

European Urology (2017); 71 (6); 858-862.

ABSTRACT

Activating mutations and translocations of the *FGFR3* gene are commonly seen in urothelial cell carcinoma (UCC) of the bladder and urinary tract. Several FGFR inhibitors are currently in clinical development and response rates appear promising for advanced UCC. A common problem with targeted therapeutics is intrinsic or acquired resistance of the cancer cells. To find potential drug targets that can act synergistically with FGFR inhibition, we performed a synthetic lethality screen for the FGFR inhibitor AZD4547 using an shRNA library targeting the human kinome in the UCC cell line RT112 (*FGFR3-TACC3* translocation). We identified multiple members of the PI3K pathway and found that inhibition of *PIK3CA* acts synergistically with FGFRi. The PI3K inhibitor BKM120 acted synergistically with inhibition of FGFR in multiple UCC and lung cancer cell lines having *FGFR* mutations. Consistently, we observed an elevated PI3K-AKT pathway activity resulting from EGFR or ERBB3 reactivation caused by FGFR inhibition as the underlying molecular mechanism of the synergy. Our data show that feedback pathways activated by FGFR inhibition converge on the PI3K pathway. These findings provide a strong rationale to test FGFR inhibitors in combination with PI3K inhibitors in cancers harboring genetic activation of *FGFR* genes.

ARTICLE

Molecular pathways activated in urothelial cell carcinoma (UCC) could provide targets for new treatments. Fibroblast Growth Factor Receptors (FGFRs) are activated in a subset of UCC, most commonly by *FGFR3* mutation (hotspot mutation or translocation) or overexpression of *FGFR1* [1]. Clinical trials with FGFR inhibitors (FGFRi), such as AZD4547 and BGJ398, are currently ongoing in UCC. Initial results with BGJ398 showed encouraging response rates [2], though information on durability of these responses is currently lacking. Akin to other molecularly targeted therapies, resistance is likely to be a major concern. Resistance to FGFR inhibition was observed *in vitro* (Fig. 1a; Methods: see supplement): the *FGFR3-TACC3* translocated cell line RT112 responded initially, but cells quickly adapted to AZD4547, an inhibitor of FGFR1, 2 and 3 (weaker activity against FGFR4). As resistance to targeted therapies often develops through feedback activation of additional signaling pathways, it is likely that FGFRi has to be combined with agents targeting additional molecular pathways. One such example is synergy between FGFR inhibitor with inhibitors of EGFR3. Feedback mechanisms that render cells insensitive to kinase inhibition often occur through activation of other kinases. Therefore we set out to screen an shRNA library targeting all 518 human kinases and 17 additional kinase-related genes to find genes whose inhibition enhances the sensitivity to FGFR inhibitor AZD4547 in *FGFR3* mutant UCC (Fig. 1b). RT112 cells were infected with a lentiviral library containing some 5000 shRNAs and cultured in the absence or presence of AZD4547 for 14 days. Cells were then harvested, DNA was isolated and the relative abundance of shRNA vectors was measured by deep-sequencing. The readcounts were normalized and analyzed with DESeq2 to identify shRNAs and their corresponding target genes that show significant depletion in the presence and not in the absence of AZD4547 (supplemental table 1, 2). We observed multiple components of the PI3K signaling pathway including the catalytic component *PIK3CA*, the regulatory subunit *PIK3R1* and the downstream target *AKT3* (Fig. 1c). In addition, with the same criteria, we found *EGFR* for which synergy with FGFR inhibition has been described [3].

Because of the presence of several components of the PI3K pathway, we decided to focus our validation on the central node, the catalytic subunit of PI3K, *PIK3CA*. Three different shRNAs targeting *PIK3CA* were significantly depleted in the drug-treated group compared to the control. This suggested that suppression of *PIK3CA* synergizes with FGFR inhibition in *FGFR3* mutant bladder cancer. To validate this finding, we infected RT112 cells with each of these 3 shRNAs targeting *PIK3CA* and treated with or without AZD4547 for 2 weeks. All three shRNAs against *PIK3CA* induce efficient knockdown of *PIK3CA* protein expression as determined by western blot analysis (Fig. 1d). Parental RT112 cells did not significantly respond to FGFR inhibition or *PIK3CA* suppression alone, but knockdown of *PIK3CA* strongly enhanced the response to the FGFR inhibitor AZD4547 (Fig. 1e).

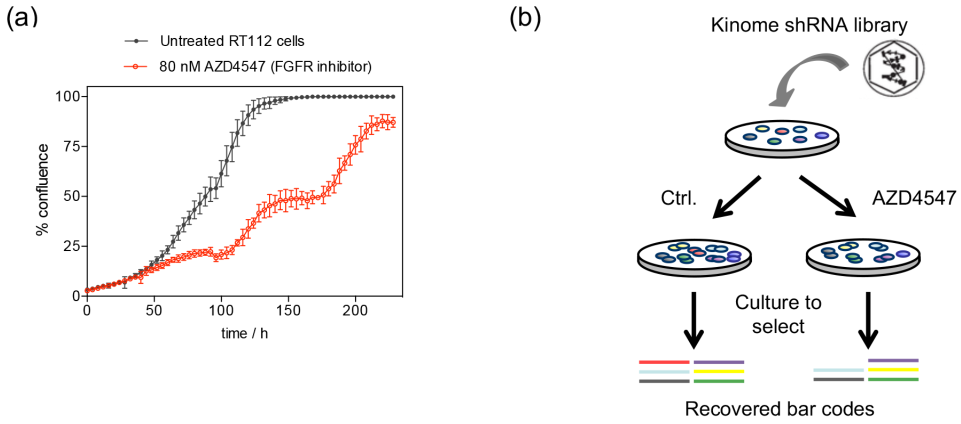

Figure 1: *PIK3CA* suppression enhances sensitivity to FGFR inhibition in UCC.

(a) RT112 cells were treated with AZD4547 (80 nM) and viability was followed using an incucyte assay. Error bars represent 4 biological replicates.

(b) Outline of synthetic lethality shRNA screen for enhancers of AZD4547 sensitivity. Human kinome shRNA library polyclonal virus was produced to infect RT112 cells, which were then left untreated (Ctrl.) for 10 days or treated with 30 nM AZD4547 for 14 days. After selection, shRNA inserts from both arms were recovered by PCR and their abundance was quantified by deep sequencing.

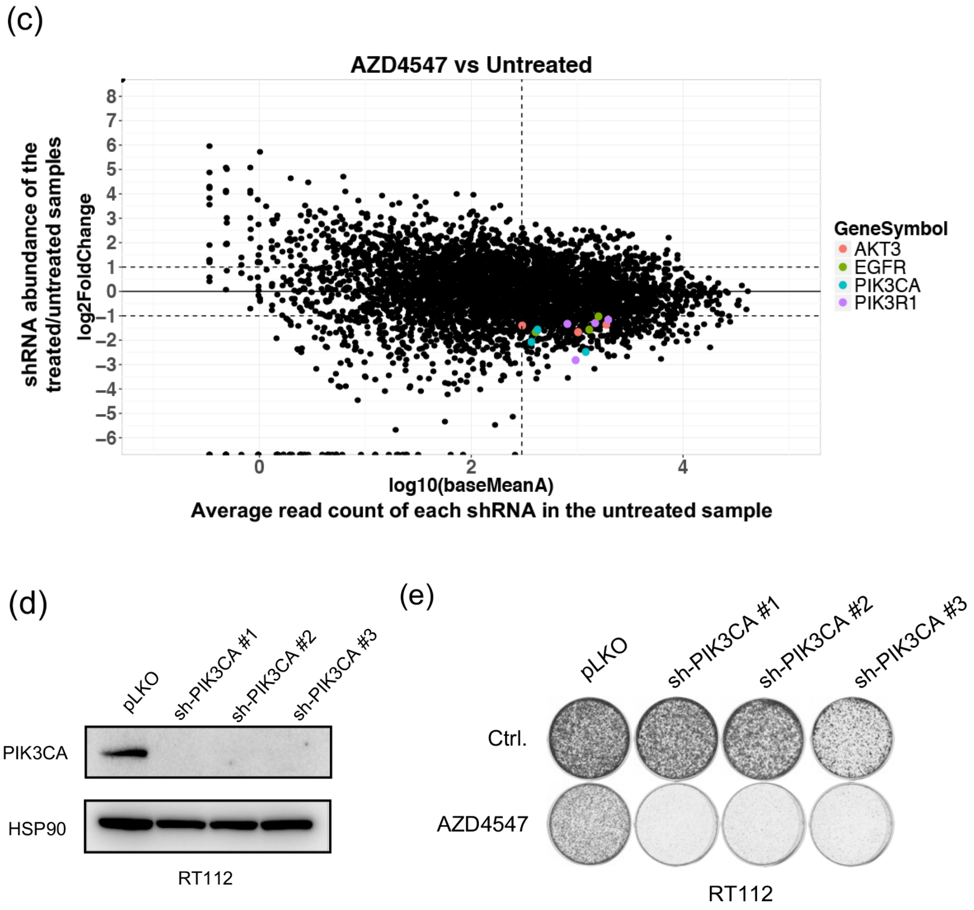

Figure 1: *PIK3CA* suppression enhances sensitivity to FGFR inhibition in UCC.

(c) Representation of the relative abundance of the shRNA barcode sequences from the shRNA screen. The y-axis shows log2 of the fold change of shRNA abundance of the treated and untreated samples. The x-axis indicates the log 10 of the average read count of each shRNA in the untreated sample. shPIK3CA, shPIK3R1, shAKT3 and shEGFR identified as the top hit according to the presence of at least 3 independent shRNAs in 3 biological screen replicates.

(d) The level of knockdown of *PIK3CA* by 3 different shRNAs was measured by PIK3CA protein levels by western blot. HSP90 protein expression is used for normalization.

(e) The functional phenotypes of independent shPIK3CA vectors are indicated by colony formation assay in 50 nM AZD4547. The cells were fixed, stained and photographed after 10 days.

We next investigated whether pharmaceutical inhibition of the PI3K pathway was also synergistic with FGFR inhibition using BKM120, a pan-PI3K inhibitor with modest anti-tumor activity in cancer patients as a single agent. We found that both RT112 (*FGFR3-TACC3* translocation[4]) and JMSU1 (*FGFR1* amplification[5]) were not significantly inhibited by BKM120 or AZD4547 monotherapy. However, synergy was observed with the combination, tested by long-term *in vitro* colony formation assays (Fig. 2a, b), incucyte proliferation assay (Supplementary Fig. 1a, b) and synergy assays (Supplementary Fig. 1c). Moreover, biochemical analysis indicated that the combination resulted in the induction of cleaved poly (ADP-ribose) polymerase (c-PARP), a hallmark of apoptosis (Fig. 2c, d).

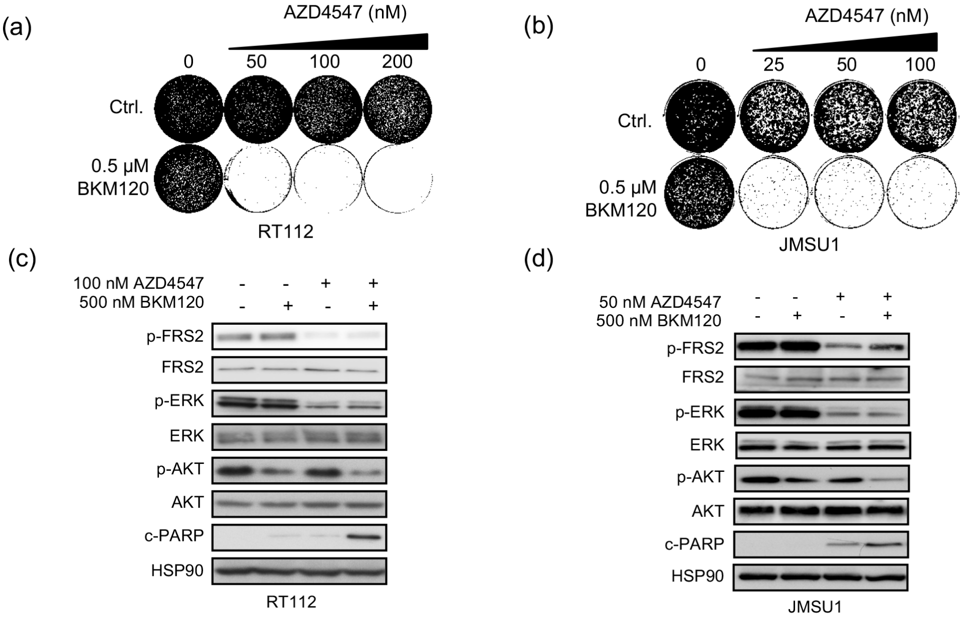
(a)
AZD4547 (nM)
0
50
100
200
Ctrl.
0.5 μM BKM120
RT112
(b)
AZD4547 (nM)
0
25
50
100
Ctrl.
0.5 μM BKM120
JMSU1
(c)
100 nM AZD4547 - - + +
500 nM BKM120 - + - +
p-FRS2
FRS2
p-ERK
ERK
p-AKT
AKT
c-PARP
HSP90
RT112
(d)
50 nM AZD4547 - - + +
500 nM BKM120 - + - +
p-FRS2
FRS2
p-ERK
ERK
p-AKT
AKT
c-PARP
HSP90
JMSU1

Figure 2: Functional and biochemical interaction between FGFR and PI3K inhibition in UCC. (a,b) Synergistic response of RT112**(a)** and JMSU1**(b)** to combinations of FGFR (AZD4547) and PI3K (BKM120) inhibitors. RT112 and JMSU1 cells were cultured in increasing concentrations of FGFR inhibitor AZD4547 alone, PI3K inhibitor BKM120 (0.5 μM) alone, or their combination. The cells were fixed, stained and photographed after 14 days. **(c,d)** Biochemical analysis of combination of FGFR and PI3K inhibitors. RT112 and JMSU1 cells were harvested after 24 hours of drug treatment. Phosphorylated-AKT (p-AKT), total AKT (AKT), cleaved-PARP (c-PARP), phosphorylated-FRS2 (p-FRS2), total FRS2 (FRS2), phosphorylated-ERK (p-ERK) and total ERK (ERK) were measured. HSP90 served as a loading control.

To expand our results to another cancer type with *FGFR* alterations, we tested this drug combination in two independent *FGFR1* amplified lung cancer cell line models: H520 (squamous cell carcinoma) and DMS114 (small cell carcinoma)[6]. As observed in the UCC lines, these two lung cancer cell models showed apoptosis in response to the drug combination, but not to either drug alone (Supplementary Fig. 1d-g). Of note, similar results were recently obtained for ponatinib (an FGFR inhibitor) in combination with mTOR inhibition in NSCLC cells[7].

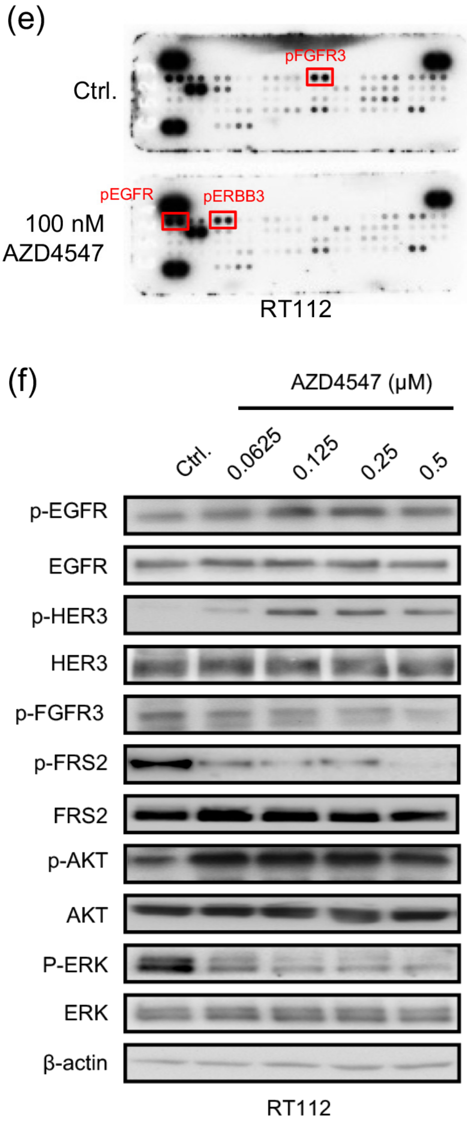
(e)
pFGFR3
Ctrl.
pEGFR
pERBB3
100 nM
AZD4547
RT112
(f)
AZD4547 (μM)
Ctrl.
0.0625
0.125
0.25
0.5
p-EGFR
EGFR
p-HER3
HER3
p-FGFR3
p-FRS2
FRS2
p-AKT
AKT
P-ERK
ERK
β-actin
RT112

Figure 2: Functional and biochemical interaction between FGFR and PI3K inhibition in UCC.

(e) RTK blot analysis of FGFR inhibitor (100nM, 7 days) treated RT112. AZD4547 induced feedback activation of EGFR and ERBB3.

(f) Biochemical analysis indicated the reactivation of EGFR and ERBB3 in association with elevated PI3K-AKT signaling, but not MAPK signaling after treating RT112 cells for 1 week with 50 mM AZD4547. Phosphorylated-EGFR (p-EGFR), Total EGFR (EGFR), phosphorylated-ERBB3 (p-ERBB3), total HER3 (HER3), phosphorylated-FGFR3 (p-FGFR3), phosphorylated-AKT (p-AKT), total AKT (AKT), phosphorylated-FRS2 (p-FRS2), total FRS2 (FRS2), phosphorylated-ERK (p-ERK) and total ERK (ERK) were measured. β-actin served as a loading control.

To address the molecular mechanism underlying the synergy between PI3K and FGFR inhibition, we further analyzed signaling pathways in AZD4547-treated RT112 cells using Receptor Tyrosine Kinase (RTK) phosphorylation blots (Fig. 2e). We found that FGFR inhibition induced a feedback mechanism to activate ERBB3 and to a lesser extent EGFR. As a consequence, PI3K-AKT signaling was activated, thereby presumably blunting the effects of the FGFR inhibitor (Fig. 2f). Feedback activation of RTKs (EGFR3 and ligand-associated ERBB2/ERBB3) has been reported before[8]. Our findings provide a strong rationale that feedback signaling converges on the PI3K pathway, but not on the BRAF-MEK-ERK pathway (Fig. 2f), and resistance could be counteracted by PI3K inhibitors, in order to enhance the FGFR inhibitor sensitivity.

To test the combination treatment *in vivo*, we engrafted RT112 bladder cancer cells into immunodeficient NMRI-nu mice. When tumors reached approximately 100 mm^3, mice were randomized into different cohorts and treated with vehicle, AZD4547, BKM120 or the drug combination. As shown in Fig. 2g, treatment with the single drugs AZD4547 or BKM120 resulted in limited tumor growth inhibition. However, treatment with the combination of AZD4547 and BKM120 resulted in persistent suppression of tumor growth throughout the duration of the experiment. Immunohistochemistry staining of the tumors at the end of the experiment (supplementary Fig. 1i) shows that the combination suppressed tumor proliferation (Ki67) and inducted apoptosis (cleaved caspase 3).

We also found that in two *FGFR3*-activated cell lines, MGHU3 and SW780, synergy was not observed (Supplementary Fig. 1h-j). MGHU3 cells carry an activating mutation in the *AKT1* gene (E17K), causing pathway activation downstream of *PIK3CA*[9]. Indeed, these cells were highly sensitive to mTOR inhibition (AZD8055). This finding suggests that comprehensive genetic profiling remains relevant before initiating combination treatment, in order to establish the best possible treatment. SW780 cells carry a translocation, *FGFR3-BAIAP2L1*[4]. This translocation has not been found in other cancers and the mechanism of FGFR activation is unknown, though cells appear to be dependent on FGFR signaling[10]. Other resistance pathways could therefore be active in this cell line.

In conclusion, our data show that resistance pathways to FGFR inhibition often converge on the PI3K pathway. In addition to upstream RTK activation, *FGFR*-activated tumors can have co-occurrence of mutations in the *PIK3CA* gene. These activating mutations would not be targeted by addition of upstream RTK inhibitors. Our data provide a strong rationale to treat *FGFR3*-altered UCC with a combination of FGFR and PI3K inhibitors (Fig. 2h). These results may apply to other cancer types as well, for example squamous NSCLC.

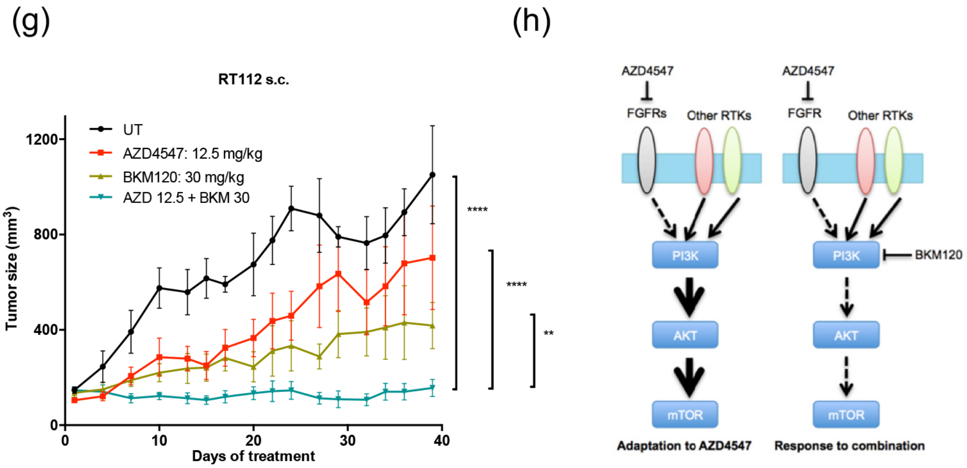

Figure 2: Functional and biochemical interaction between FGFR and PI3K inhibition in UCC.

(g) FGFR inhibitor (AZD4547) in combination with the PI3K inhibitor (BKM120) significantly suppresses tumor growth in RT112 xenograft model.
(**** $p<0.0001$, ** $p<0.01$ ANOVA)

(h) FGFR altered tumors initially respond to FGFR inhibition. However, the tumor cells are able to up-regulate other RTKs that result in enhanced signaling through the PI3K-AKT pathway, leading to drug resistance. Combining FGFR inhibition with a PI3K inhibitor eliminates the PI3K-AKT activity and synergistically kills cancer cells.

REFERENCES

1. Cancer Genome Atlas Research N. Comprehensive molecular characterization of urothelial bladder carcinoma. Nature 2014;507:315-22.
2. Nogova L, Sequist LV, Perez Garcia JM, et al. Evaluation of BGJ398, a Fibroblast Growth Factor Receptor 1-3 Kinase Inhibitor, in Patients With Advanced Solid Tumors Harboring Genetic Alterations in Fibroblast Growth Factor Receptors: Results of a Global Phase I, Dose-Escalation and Dose-Expansion Study. J Clin Oncol 2016:JCO2016672048.
3. Herrera-Abreu MT, Pearson A, Campbell J, et al. Parallel RNA interference screens identify EGFR activation as an escape mechanism in FGFR3-mutant cancer. Cancer Discov 2013;3:1058-71.
4. Williams SV, Hurst CD, Knowles MA. Oncogenic FGFR3 gene fusions in bladder cancer. Hum Mol Genet 2013;22:795-803.
5. Pearson A, Smyth E, Babina IS, et al. High-Level Clonal FGFR Amplification and Response to FGFR Inhibition in a Translational Clinical Trial. Cancer Discov 2016;6:838-51.
6. Weiss J, Sos ML, Seidel D, et al. Frequent and focal FGFR1 amplification associates with therapeutically tractable FGFR1 dependency in squamous cell lung cancer. Sci Transl Med 2010;2:62ra93.
7. Singleton KR, Hinz TK, Kleczko EK, et al. Kinome RNAi Screens Reveal Synergistic Targeting of MTOR and FGFR1 Pathways for Treatment of Lung Cancer and HNSCC. Cancer research 2015;75:4398-406.
8. Wang J, Mikse O, Liao RG, et al. Ligand-associated ERBB2/3 activation confers acquired resistance to FGFR inhibition in FGFR3-dependent cancer cells. Oncogene 2015;34:2167-77.
9. Davies BR, Guan N, Logie A, et al. Tumors with AKT1E17K Mutations Are Rational Targets for Single Agent or Combination Therapy with AKT Inhibitors. Mol Cancer Ther 2015;14:2441-51.
10. Wu YM, Su F, Kalyana-Sundaram S, et al. Identification of targetable FGFR gene fusions in diverse cancers. Cancer Discov 2013;3:636-47.

SUPPLEMENTARY: Materials and methods

Synthetic lethality screen

A kinome shRNA library targeting the complete 518 human kinases and 17 kinase related genes with 5 shRNA's on average per gene were constructed from The RNAi Consortium (TRC) human genome-wide shRNA collection. The kinome library was used to generate a single pool of lentiviral shRNAs to infect RT112 cells. After infection and selection for lentiviral integration, cells were treated with or without 30 nM AZD4547 for 10 days. Next-generation sequencing was used to determine the relative abundance of each shRNA in the different populations. The read count data was analyzed using DESeq2. The analysis was restricted to those shRNAs with a read count >300 in the untreated sample, a log2 fold change treated/untreated of less than -1 and a adjusted p-value of <0.1. For hit selection, we selected those genes that were represented with 3 or more different shRNAs in the hit list as defined above. This resulted in a final hit list of 18 genes. The detailed screen procedure is described in Prahallad *et al* [1]. Screen data is provided in supplementary table 1 and the data of DESeq normalized counts is provided in supplementary table 2.

Long-term colony formation assay and IncuCyte® cell proliferation assays

Cells were seeded into 6-well plates (20,000-50,000 cells per well) and cultured both in the absence and presence of drugs as indicated for 10-15 days. At the end of the assay, cells were fixed with 4% of formaldehyde (#1.04002, Millipore) diluted in PBS, stained with 2% of crystal violet (#HT90132 Sigma-Aldrich) diluted in water and photographed. For IncuCyte® proliferation assays, cells were seeded in 96-well plate (2000 cells per well) and cultured in absence or presence of drugs as indicated. Cell confluence was measured and quantified by the IncuCyte® imaging system (Essen Bioscience).

Protein lysate preparation and immunoblotting

Cells were seeded in DMEM-based medium containing 10% fetal bovine serum (FBS) in the absence or presence of drug for indicated time. The drugs were refreshed every 3 days. Afterwards, the cells were washed with PBS and lysed with RIPA buffer supplemented with protease inhibitors (cOmplete, Roche) and phosphatase inhibitor cocktails II and III (Sigma). All lysates were freshly prepared and processed with Novex NuPAGE Gel Electrophoresis Systems (Invitrogen). Antibodies against HSP90 (sc-33755), p-FGFR3 (SC-33041), p-ERK (SC-16982), ERK and β-actin (SC-47778) were from Santa Cruz Biotechnology; cleaved-PARP (#5625), p-AKT (#4046), AKT (#4691), p-HER3 (#4791), HER3 (#12708), PIK3CA (#4254), p-MEK (#9154), ERK (#9102) and MEK (#4694) were from Cell Signaling; p-EGFR (ab5644) and p-FRS2 (ab193363) were from Abcam; FRS2 (11503-1-AP) was from Proteintech.

RTK blot assay

Cells were cultured in the absence or presence of drugs for 1 week, every 3 days refreshed. Phosphorylation of RTKs was measured using Human Phospho-Receptor Tyrosine Kinase Array Kit (ARY001B, R&D system) according to the manufacturer's instructions.

Synergy assay

To assess whether combined effect of the FGFR and PI3K inhibitor treatment is additive or synergistic, RT112 and H520 cells were plated in 384-well plates and treated with a series of drug concentrations. After 5 days cell viability was measured by Cell Titre Blue assay. Synergy score was determined by subtracting the Loewe additivity matrix scores (calculated from the single drug treatments) from the experimental values of the FGFR and PI3K inhibitor combinations. A positive score indicates that the reduction in cell viability induced by the combination of the two compounds surpasses the effect that can be obtained by increasing concentrations of either two compounds alone.

Mouse xenografts and *in vivo* drug study

All animal procedures were approved by the Ethical commission of the Netherlands Cancer Institute. One million RT112 bladder cancer cells were injected subcutaneously into 7-week-old immunodeficient NMRI-nu mice (6 mice per group). Tumor volume was monitored three times a week, based on caliper measurements calculated with the formula: tumor volume = ½ (length × width^2). When tumors reached a volume of approximately 100 mm^3, mice were randomized and treated daily by oral gavage with AZD4547 12.5 mg/kg, BKM120 30 mg/kg, combination of both drugs, or vehicle solution.

Immunohistochemistry

Fixed tissues were dehydrated and embedded in paraffin. Sections of 2–4 µm were prepared and immunostained with anti-Ki67 (rabbit polyclonal, 1:3000, Abcam AB15580) and anti-cleaved caspase 3 (rabbit polyclonal, 1:400 Cell Signaling #9661) for subsequent histopathological analyses.

SUPPLEMENTARY: Reference

1. Prahallad A, Sun C, Huang S, et al. Unresponsiveness of colon cancer to BRAF(V600E) inhibition through feedback activation of EGFR. Nature 2012;483:100-3.

Online Content

All additional methods, tables, display items and Source Data are available in the online version of the paper.

https://www.sciencedirect.com/science/article/pii/S0302283817300374?via%3Dihub

SUPPLEMENTARY FIGURES

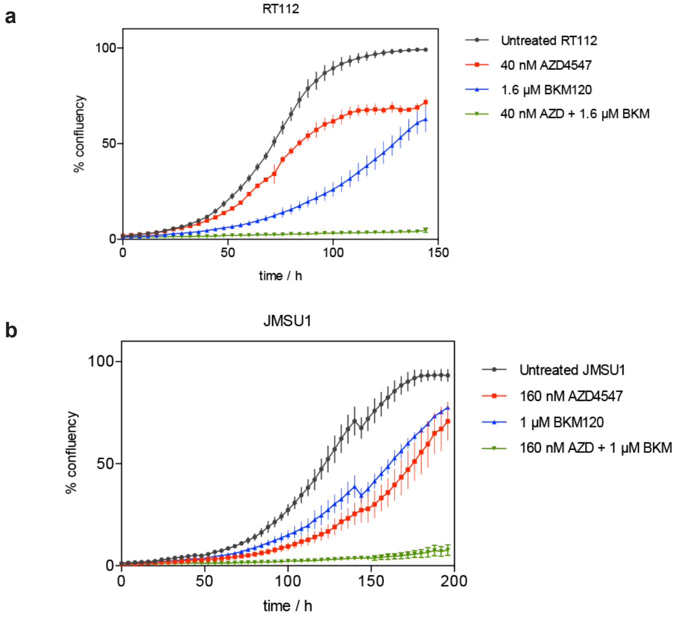

Supplementary Figure 1: Functional and biochemical interaction between FGFR and PI3K inhibition in *FGFR*-activated cancer models.

(a,b) IncuCyte® assay of RT112 **(a)** and JMSU1 **(b)**. The cells were treated with AZD4547 and BKM120 at the indicated drug concentrations.

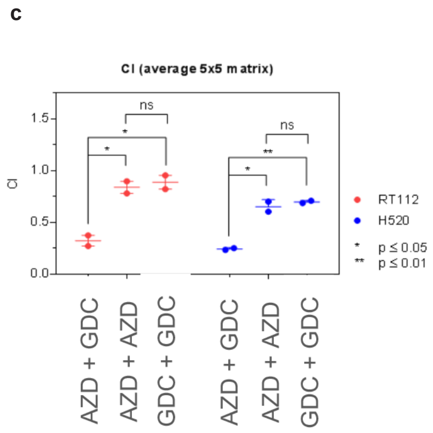

Supplementary Figure 1:

(c) Synergy assay of RT112 and H520, the cells were treated with AZD4547 and GDC0941 at a range of concentrations. Cell titer blue was used as the read-out.

(d,e) Synergistic response of H520 **(d)** and DMS114 **(e)** to the combination of FGFR and PI3K inhibitors. H520 and DMS114 cells were cultured in increasing concentration of FGFR inhibitor AZD4547 alone, PI3K inhibitor BKM120 (0,5 µM) alone, or their combination. The cells were fixed, stained and photographed after 14 days.

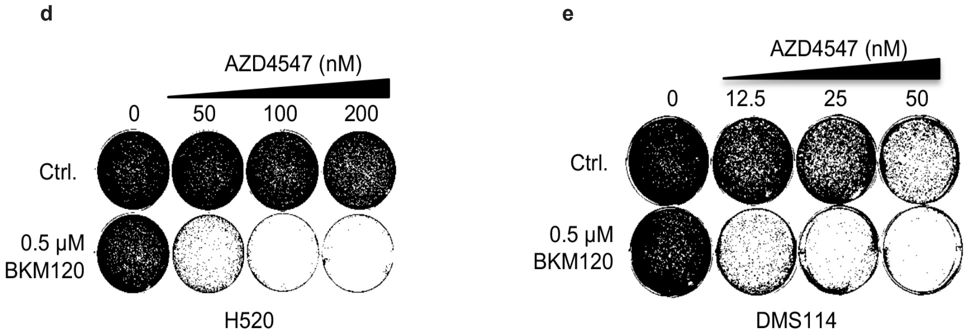
d
AZD4547 (nM)
0
50
100
200
Ctrl.
0.5 µM
BKM120
H520
e
AZD4547 (nM)
0
12.5
25
50
Ctrl.
0.5 µM
BKM120
DMS114

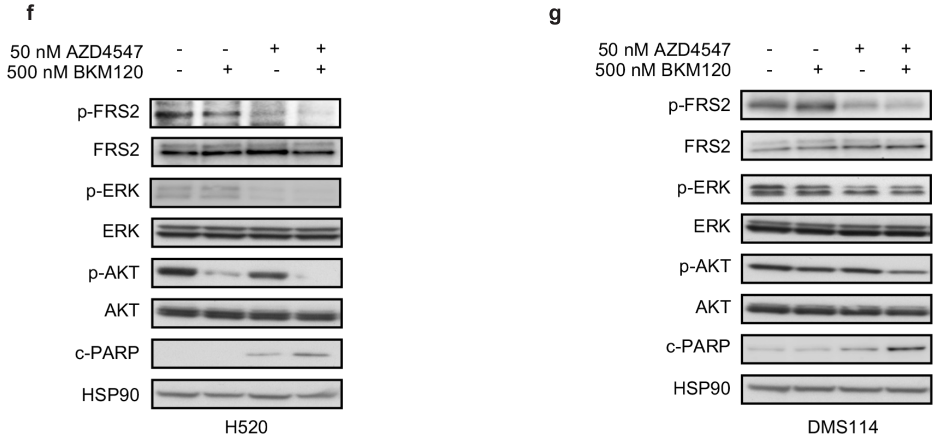
f
50 nM AZD4547 - - + +
500 nM BKM120 - + - +
p-FRS2
FRS2
p-ERK
ERK
p-AKT
AKT
c-PARP
HSP90
H520
g
50 nM AZD4547 - - + +
500 nM BKM120 - + - +
p-FRS2
FRS2
p-ERK
ERK
p-AKT
AKT
c-PARP
HSP90
DMS114

Supplementary Figure 1:

(f,g) Biochemical analysis of the combination of FGFR and PI3K inhibitors. H520 **(f)** and DMS114 cells lysis **(g)** were harvested 24 hours after drug treatment. Phosphorylated-AKT (p-AKT), total AKT (AKT), cleaved-PARP (c-PARP) phosphorylated-FRS2 (p-FRS2), total FRS2 (FRS2) were measured. HSP90 served as a loading control.

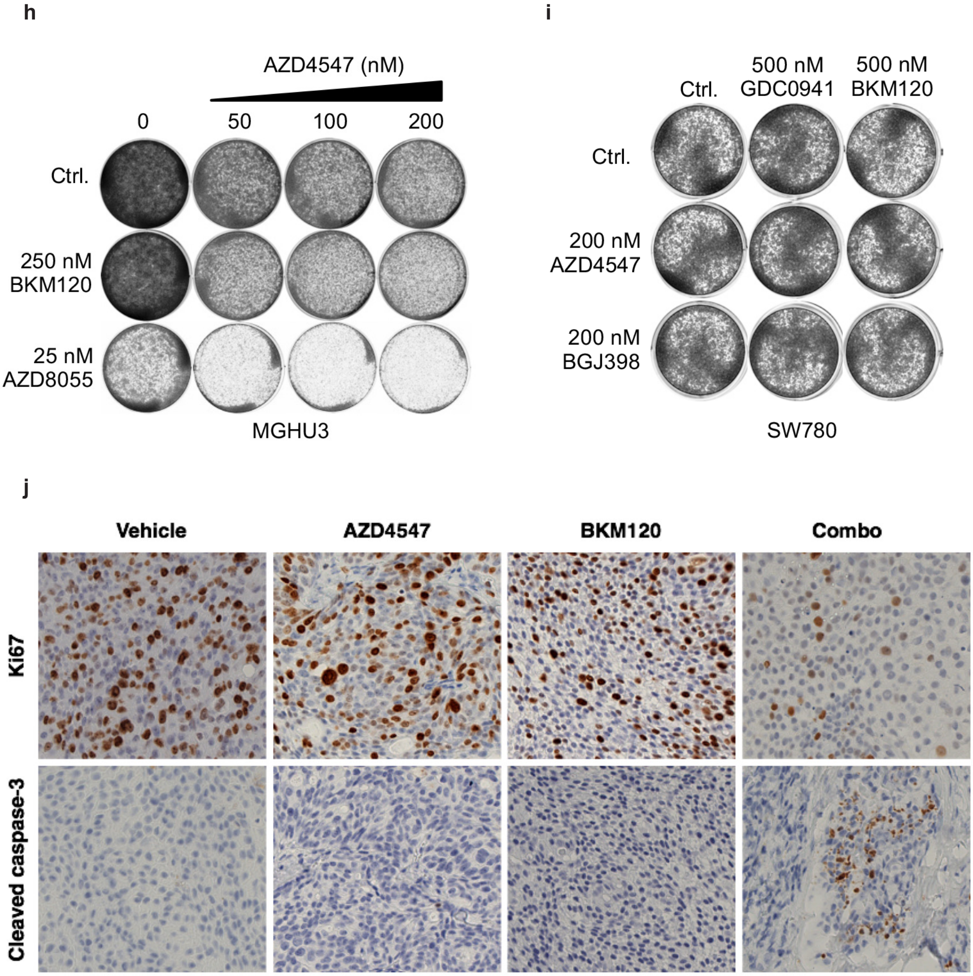
h
AZD4547 (nM)
0
50
100
200
Ctrl.
250 nM BKM120
25 nM AZD8055
MGHU3
i
Ctrl.
500 nM GDC0941
500 nM BKM120
Ctrl.
200 nM AZD4547
200 nM BGJ398
SW780
j
Vehicle
AZD4547
BKM120
Combo
Ki67
Cleaved caspase-3

Supplementary Figure 1:

(h) Non-synergistic response of MGHU3 to the combination of FGFR and PI3K inhibitors. MGHU3 cells were cultured in increasing concentrations of FGFR inhibitor AZD4547 alone, PI3K inhibitor BKM120 (0,25 µM) alone, or their combination. Targeting downstream molecule mTOR by AZD8055 sensitized MGHU3 cells to FGFR inhibition. The cells were fixed, stained and photographed after 14 days.

(i) Non-synergistic response of SW780 to the combination of FGFR and PI3K inhibitors. Cells were cultured in indicated concentrations of FGFR inhibitor AZD4547 or BGJ398 alone, PI3K inhibitor BKM120 or GDC0941 alone, or their combination.

(j) Fixed tissues were dehydrated and embedded in paraffin. Sections of 2–4 µm were prepared and immunostained with Ki67 and cleaved caspase 3.

Chapter 3

A role for the unfolded protein response stress sensor ERN1 in regulating the response to MEK inhibitors in *KRAS* mutant colon cancers

Tonći Šuštić [1, #], Sake van Wageningen [1, 2, #],
Evert Bosdriesz [1], Robert J.D. Reid [2], John Dittmar [2], Cor Lieftink [1],
Roderick L. Beijersbergen [1], Lodewyk F.A. Wessels [1],
Rodney Rothstein [2, *] and René Bernards [1, *]

[1] Division of Molecular Carcinogenesis and Oncode Institute, The Netherlands Cancer Institute, Plesmanlaan 121, Amsterdam 1066 CX, The Netherlands

[2] Department Genetics and Development, Columbia University Vagelos College of Physicians & Surgeons, New York, New York 10032, USA

[#] These authors contributed equally to this work

[*] Corresponding authors

Genome Medicine (2018); 10 (1): 90

ABSTRACT

Background: Mutations in *KRAS* are frequent in human cancer, yet effective targeted therapeutics for these cancers are still lacking. Attempts to drug the MEK kinases downstream of KRAS have had limited success in clinical trials. Understanding the specific genomic vulnerabilities of *KRAS* driven cancers may uncover novel patient-tailored treatment options.

Methods: We first searched for synthetic lethal (SL) genetic interactions with mutant *RAS* in yeast with the ultimate aim to identify novel cancer-specific targets for therapy. Our method used selective ploidy ablation, which enables replication of cancer-specific gene expression changes in the yeast gene disruption library. Second, we used a genome-wide CRISPR/Cas9-based genetic screen in *KRAS* mutant human colon cancer cells to understand the mechanistic connection between the synthetic lethal interaction discovered in yeast and downstream RAS signaling in human cells.

Results: We identify loss of the endoplasmic reticulum (ER) stress sensor *IRE1* as synthetic lethal with activated *RAS* mutants in yeast. In *KRAS* mutant colorectal cancer cell lines, genetic ablation of the human ortholog of *IRE1*, *ERN1*, does not affect growth but sensitizes to MEK inhibition. However, an ERN1 kinase inhibitor failed to show synergy with MEK inhibition, suggesting that a non-kinase function of ERN1 confers MEK inhibitor resistance. To investigate how ERN1 modulates MEK inhibitor responses, we performed genetic screens in *ERN1* knockout *KRAS* mutant colon cancer cells to identify genes whose inactivation confers resistance to MEK inhibition. This genetic screen identified multiple negative regulators of JUN N-terminal kinase (JNK) /JUN signaling. Consistently, compounds targeting JNK/MAPK8 or TAK1/MAP3K7, which relay signals from ERN1 to JUN, display synergy with MEK inhibition.

Conclusions: We identify the ERN1-JNK-JUN pathway as a novel regulator of MEK inhibitor response in *KRAS* mutant colon cancer. The notion that multiple signaling pathways can activate JUN may explain why *KRAS* mutant tumor cells are traditionally seen as highly refractory to MEK inhibitor therapy. Our findings emphasize the need for the development of new therapeutics targeting JUN activating kinases, TAK1 and JNK, to sensitize *KRAS* mutant cancer cells to MEK inhibitors.

Keywords: Ire1, ERN1, MEK inhibitor, colon cancer, JNK, JUN

BACKGROUND

Mutation of specific codons in one of the three *RAS* genes *HRAS, KRAS or NRAS* converts these genes into oncogenes. These mutations are found in a wide variety of tumors, with very high incidences (>50%) in pancreas and colon cancers [1]. Despite decades of research, generation of selective inhibitors of mutant RAS has proven to be difficult. Recently, allosteric inhibitors of KRAS G12C have been developed [2,3], but the clinical effectiveness of these compounds remains to be established.

RAS genes are highly conserved in evolution. The yeast *Saccharomyces cerevisiae* has two *RAS* genes; *RAS1* and *RAS2*. These two genes are individually not required for cell viability. However, the double deletion mutant is inviable, indicating that the genes share an essential function [4]. A yeast *ras1*Δ *ras2*Δ deletion mutant can be rescued by ectopic expression of a human *RAS* gene [5]. Vice versa, mutating codon 19 into a valine converts yeast RAS into a constitutively active protein and this mutant yeast RAS can induce malignant transformation of mouse fibroblasts [6].

We searched for synthetic lethal (SL) genetic interactions with mutant *RAS* in yeast to identify novel cancer-specific targets for therapy. Our method uses SPA (selective ploidy ablation), and allows us to mimic cancer-specific gene expression changes in each of the 4800 nonessential deletion mutant strains in the yeast gene disruption library [7]. Using this approach, we found that inhibition of yeast Unfolded Protein Response (UPR) genes is synthetic lethal with mutant *RAS*.

The UPR in yeast is mediated by Ire1 and Hac1 [8]. Ire1 is an endonuclease that upon endoplasmic reticulum (ER) stress splices *HAC1* mRNA. Hac1 is a transcription factor that executes the UPR by activating genes involved in ER homeostasis. The UPR, and the mechanism of activation by splicing of a specific mRNA, is conserved from yeast to humans. Mammalian cells have an *IRE1* ortholog named *ERN1*. Likewise, *HAC1* has a functional human homolog, *XBP1* [9]. In mammalian *KRAS* mutant colon cancer, we find that inhibition of MEK kinases is synthetic lethal with inhibition of the UPR. Our findings establish an unexpected link between MEK kinase signaling and the UPR executor ERN1 in human cancer.

METHODS

Yeast screen

Wild-type *RAS* alleles were cloned into pWJ1512 using the A and B adaptamers [10]. Primers to obtain mutant *RAS* alleles (mutant sequence underlined) were;

RAS1(V19)-pWJ1512-F 5’ gaattccagctgaccaccATGCAGGGAAATAAATCAACTATAAGAGAGTATAAGATAGTAGTTGTCGGTGGAGTAGGCGTTGGTAAATCTGCTTTAAC, RAS2(V19)-pWJ1512-F 5’ gaattccagctgaccaccATGCCTTTGAACAAGTCGAACATAAGAGAGTACAAGCTAGTCGTCGTTGGTGGTGTTGGTGTTGGTAAATCTGCTTTG, pWJ1512-R 5’ gatccccgggaattgccatg.

The SPA protocol [7] was used to transfer plasmids into the arrayed gene disruption library [11]. Briefly, SPA is a yeast mating-based protocol that allows transfer of a plasmid from a special donor strain into a recipient strain followed by destabilization and counter-selection of the donor yeast chromosomes. The method was adapted for the RAS screen by adding 2% raffinose in addition to 2% galactose as a carbon source for the last two selection steps. In addition, selection steps for RAS2(V19) cells were 1 day longer because overall growth is slower in these strains.

Cell culture, transfection and lentiviral infection

HEK293 cells were cultured in DMEM. All other cell lines were maintained in RPMI1640 medium containing 10% FBS and 1% penicillin/streptomycin at 37ºC and 5% CO2. All cell lines were purchased from the American Type Culture Collection (ATCC), STR profiled (by Eurofins Medigenomix Forensik GmbH, Ebersberg, Germany) and routinely tested negative for mycoplasma.

Transfection of HEK293 cells with linear Polyethylenimine (PEI) 25K from Polysciences (cat# 23966-2) and subsequent infection of target cells was done as described previously [12]. For knockout of individual genes, the following single guide (sg) RNAs were cloned in the lentiCRISPR version 2.1 (LC2.1) vector by Gibson cloning: sgERN1-A, 5’-ACATCCCGAGACACGGTGGT-3’; sgERN1-B, 5’-GATGGCAGCCTGTATACGCT-3’; sgDET1, 5’-ACGTGCAGCAGTGTCGCATA-3’; sgCOP1, 5’-AAGCTCCTTCTCCATCACAC-3’. Non-targeting (NT) sgRNA 5’-ACGGAGGCTAAGCGTCGCAA-3’ was used as a control.

Cell proliferation assays and growth curves

For long-term cell proliferation assays cells were seeded in 6 well plates at densities ranging from 1 to 2×10^4 cells per well and cultured with or without inhibitors, as indicated. When control cells reached confluency, all cells were fixed in 4% formaldehyde and stained with 0.1% crystal violet (in water).

Live cell growth was measured by automated determination of confluency every 4 hours using IncuCyte Zoom (Essen Bioscience). Between 600 and 800 cells were plated per well of a 96 well plate and experiments were carried out in triplicates.

MEK inhibitors selumetinib (AZD6244) and trametinib (GSK1120212) were purchased from Selleck chemicals and kept as 10mM stock solutions in DMSO. ERN1 inhibitor (compound 18) and JNK inhibitor SR-3306 were kindly provided by Astex pharmaceuticals. TAK1 inhibitor was purchased from Merck as (5Z)-7-Oxozeaenol (CAS 66018-38-0).

Protein lysate preparation and western blot analysis

Cells were lysed and western blots performed as described previously [12]. Primary antibodies against HSP90 (sc-13119), p-JUN (sc-822), and ERK2 (sc-154) were purchased from Santa Cruz. Antibodies against ERN1 (#3294), GAPDH (#5174), p-ERK1/2 (#9101), and JUN (#9165) were from Cell Signaling. Antibodies against COP1 (Genentech, 28A4) and DET1 (Genentech, 3G5) were a gift from Vishva Dixit, Genentech. Secondary antibodies were obtained from Bio-Rad Laboratories.

Total RNA isolation and quantitative RT-PCR

Total RNA was isolated and purified using Quick-RNA™ MiniPrep (Zymo Research) and reverse transcription was performed with Maxima Universal First Strand cDNA Synthesis Kit (Thermo Fisher Scientific, #K1661).

The 7500 Fast Real-Time PCR System from Applied Biosystems was used to measure mRNA levels, which were normalized to the expression of GAPDH, in triplicates. The following primer sequences were used in the SYBR® Green master mix (Roche):

GAPDH-Fw, AAGGTGAAGGTCGGAGTCAA; GAPDH-Rev, AATGAAGGGGTCATTGATGG;
ERN1-Fw, AGCAAGCTGACGCCCACTCTG; ERN1-Rev, TGGGGCCCTTCCAGCAAAGGA;
CD59-Fw, CAGTGCTACAACTGTCCTAACC; CD59-Rev, TGAGACACGCATCAAAATCAGAT;
JUN-Fw, AACAGGTGGCACAGCTTAAAC; JUN-Rev, CAACTGCTGCGTTAGCATGAG;
JNK1-Fw, TGTGTGGAATCAAGCACCTTC; JNK1-Rev, AGGCGTCATCATAAAACTCGTTC;
JNK2-Fw, GAAACTAAGCCGTCCTTTTCAGA ; JNK2-Rev, TCCAGCTCCATGTGAATAACCT.

TodetecthumanXBP1mRNAweusedhXBP1-Fw,GAAGCCAAGGGGAATGAAGT; and hXBP1-Rev, GCTGGCAGGCTCTGGGGAAG. To detect human spliced Xbp1, hXBP1-Rev was used with hXBP1spl-Fw, TGCTGAGTCCGCAGCAGGTG; as designed previously [13].

CRISPR-Cas9 resistance screen

To generate ERN1 knockout cells that would not contain the same tracer sequence as currently available CRISPR libraries and thus be suitable for subsequent genome-wide screening, we used a dual vector doxycycline inducible CRISPR/Cas9 system made on the basis of FH1tUTG [14], as previously described [15]. Single cell clones were tested for ERN1 knockout by western blot and by measuring the levels of spliced XBP1 using quantitative RT-PCR as described above.

Version 2 of the human genome-scale CRISPR-Cas9 knockout (GeCKO) half-library A – consisting of 65,383 sgRNAs in lentiviral vectors [16] (Addgene #1000000048) – was used to infect LoVo ERN1 knockout cells with a transduction efficiency of 20% in a sufficient cell number to achieve a 180-fold library coverage. After 48 hours, cells were replated and viral supernatant was replaced by medium containing puromycin (2 µg/ml) to select for infected cells for two days. After additional four days of growth, cells were harvested, a T0 sample was taken, and the rest of the cells were reseeded and cultured in the presence or absence of MEK inhibitors selumetinib and trametinib, in 2 biological replicates each, for 4 weeks. Genome-integrated sgRNA sequences were PCR amplified and their respective abundance was determined as described previously [17]. The abundance of each sgRNA in the treated versus untreated pools was determined by massively parallel sequencing on an Illumina HiSeq 2500 platform. Statistical analysis was performed using DESeq version 1.24.0. The hit selection was based on the overlap between selumetinib and trametinib screens for the genes for which at least one of the sgRNAs meet the following criteria (A) log2 fold change (of treated over untreated samples) >=7, (B) baseMeanA (mean number of reads in the untreated sample) >= 50, and (C) adjusted p-value <= 0.1. The results overview of the CRISPR screen can be found in the Supplementary Tables S5 and S6.

RESULTS

RAS synthetic lethality screens in yeast

To discover genetic interactions with mutant yeast *RAS*, we expressed the constitutively active *RAS* alleles, *RAS1(V19)* and *RAS2(V19)*, in the collection of ~4800 yeast strains in which each individual nonessential gene is deleted [11]. To discriminate between effects due to ectopic expression of the *RAS* alleles and those due to the specific *RAS* gene mutations, we also screened the wild-type *RAS1(wt)* and *RAS2(wt)* alleles. Additionally, we screened cells harboring an empty vector as a control. Median-normalized growth values were used to calculate the growth ratios between experimental and vector control colonies (Additional file 1: Figure S1A) [18]. We have shown previously that a screen organizes related genes based on phenotype and these genes exhibit a high density of interactions within the group. The CLIK algorithm plots this density of interactions from the ranked screen results to determine a cutoff for the screen [19]. CLIK analysis of the *RAS1(V19)* and *RAS2(V19)* screens yielded respectively 151 and 450 strains with a growth defect, which corresponds to a 2-fold difference in growth compared to the population median in both screens (Additional file 2: Table S1). Although no CLIK groups were identified for the *RAS1(wt)* and *RAS2(wt)* screens, the same 2-fold growth difference cutoff was applied, which yields 14 affected strains from each screen (Additional file 1: Figures S1B-E) indicating that the majority of SL interactions are specific to the activated *RAS* mutants. Interestingly, most SLs from the *RAS1(V19)* were also found in the *RAS2(V19)* screen (Additional file 1: Figure S1F). The growth effects in the *RAS1(V19)* and *RAS2(V19)* screens were highly correlated although the effect was more severe in the *RAS2(V19)* screen (Additional file 1: Figure S1G). This finding suggests that the yeast *RAS* genes form a quantitative redundant pair [20].

To validate the deletion mutants from the SL screens, the strains that showed an SL interaction were rescreened with a mutant or wild-type *RAS* allele. 46% of the *RAS1(V19)* and 79% of the *RAS2(V19)* SLs from the primary screen also had a growth defect (>2 times smaller than control) in the validation screen (Additional file 2: Tables S2-5). 90% of the validated hits of the *RAS1(V19)* screen overlapped

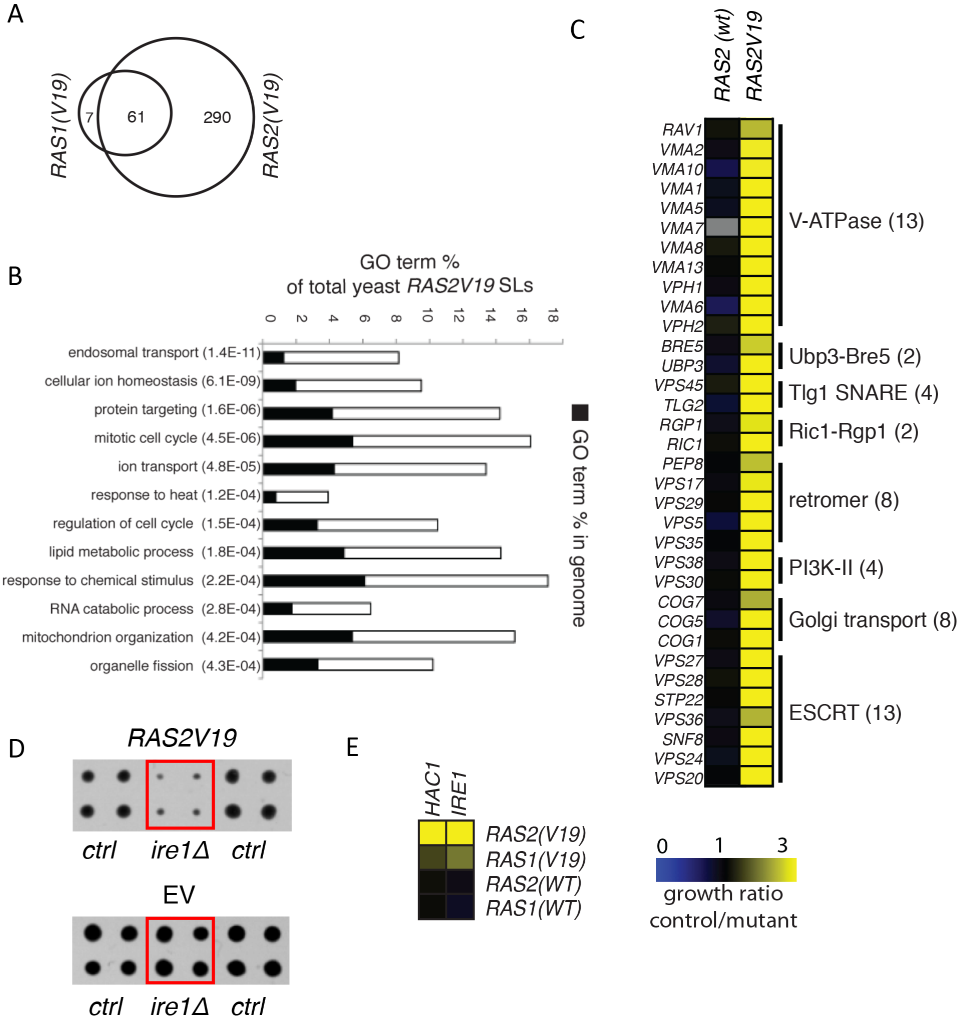

Figure 1. Unfolded Protein Response (UPR) executors are synthetic lethal with mutant *RAS* in *S. cerevisiae*. (A) Venn diagram showing the overlap of the *RAS* synthetic lethal (SL) gene deletion strains identified in the *RAS1(V19)* and *RAS2(V19)* genetic screens. **(B)** Gene Ontology (GO) enrichment analysis on the SL gene deletion strains from the *RAS2(V19)* screen identifies a variety of biological processes, including endosomal transport and protein targeting. **(C)** List of genes coding for protein complexes among the validated list of *RAS2(V19)* SL gene deletion mutants. Higher values correspond to stronger growth arrest in the presence of mutant *RAS*. The pathways and complexes in which the genes are involved are indicated. **(D)** The effect of the deletion of the UPR stress sensor *ire1 (ire1Δ)* in *RAS2(V19)* screen (top) and in the empty vector (EV) control background (bottom). **(E)** Control vs mutant growth ratios of the UPR genes *ire1* and *hac1*. Higher values correspond to stronger growth arrest in the presence of mutant *RAS*.

with the *RAS2(V19)* screen. The gene deletions from the *RAS1(wt)* and *RAS2(wt)* screens did not validate in a second screen, indicating that the SLs are specific to the mutant alleles and that *RAS1(V19)* interacts with a subset of the *RAS2(V19)* SLs (Figure 1A). We decided to focus on the genes from the *RAS2* mutant screen due to the higher number of interactions and the higher validation rate. In addition, almost all of the *RAS1* mutant gene deletions were also found and validated in the *RAS2* screen.

An encouraging sign of the validity of our screen was the recapitulation of the synthetic lethal interaction between *RAS2(V19)* and *SIN4*. *SIN4* is a component of the mediator transcription complex (MED16) and its interaction with *RAS2(V19)* has been described before [21]. Additionally, we found that another mediator component, *PGD1* (MED3), is synthetic lethal with *RAS2(V19)*.

We performed a Gene Ontology (GO) enrichment analysis on the SLs from the *RAS2(V19)* screen, which identified a variety of biological processes enriched in this screen, including endosomal transport and protein targeting (Figure 1B). This finding indicates that cells expressing *RAS2(V19)* are highly dependent on intracellular protein transport. We further analyzed the validated list of *RAS2(V19)* SLs by identifying protein complexes from which 2 or more members were present, based on *Benschop et al* [22]. Again, in this analysis we recovered several complexes involved in endosomal transport (Figure 1C). Based on the dependence of cells expressing *RAS2(V19)* on intracellular transport, we hypothesized that ER homeostasis was disturbed in these cells, which would be consistent with the work of *Leber et al* [23]. To test this hypothesis, we compared our list of *RAS2(V19)* SLs to lists of strains that are sensitive to ER stress agents [24]. We confirmed a significant overlap with strains sensitive to β-mercaptoethanol, DTT and tunicamycin ($P = 3.07E-05$, hypergeometric test; Additional file 2: Table S6), suggesting that ER homeostasis is disturbed by *RAS2(V19)*.

Mutant RAS is known to inhibit the production of GPI-anchors at the ER [25]. This inhibition likely contributes to permanent ER stress in cells expressing *RAS2(V19)*. To test this theory, we compared the effect of expressing *RAS2(V19)* with directly inhibiting GPI-anchor production by analyzing the synthetic lethal genetic interactions of *ERI1*, a non-essential component of the GPI-GnT enzyme [26]. Again, we found a significant overlap between the *RAS2(V19)* SLs lists and the list of *ERI1* genetic interactions (P = 8.60E-09, hypergeometric test; Additional file 2: Table S7). The strongest negative genetic interaction of *ERI1* is with *IRE1*, an important regulator of the UPR. Additionally, *ERI1* shows a strong negative genetic interaction with *HAC1*, a downstream target of Ire1. The UPR is a signaling route that restores ER homeostasis and *ire1Δ* and *hac1Δ* strains are highly sensitive to ER stress agents (Additional file 2: Table S6). Importantly, we found both *IRE1* and *HAC1* are *RAS2(V19)* SLs (Figures 1D, E), indicating that ER homeostasis is disturbed in *RAS2(V19)* expressing cells and that these cells are dependent on the UPR.

Genetic ablation of *ERN1* in *KRAS* mutant colon cancer cells

The UPR, and the mechanism of activation by splicing of a specific mRNA, is conserved from yeast to humans (Figure 1F). Mammalian cells have an *IRE1* ortholog, named *ERN1*, while *HAC1* has a functional human homolog named *XBP1*, whose mRNA is spliced by the ERN1 endonuclease domain to form the active, protein-coding XBP1 spliced (XBP1s) form [9]. To test whether *ERN1* is essential

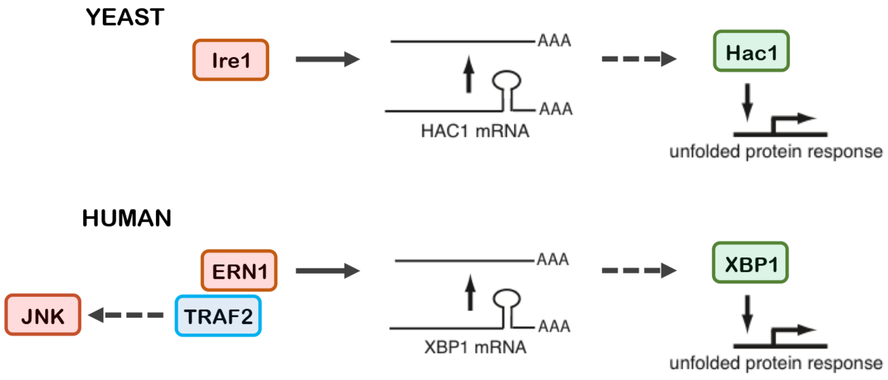

Figure 1. Unfolded Protein Response (UPR) executors are synthetic lethal with mutant *RAS* in *S. cerevisiae*.

(F) Schematic representation of the evolutionary conserved mechanism of UPR execution in yeast (top) and humans (bottom). Ire1 is responsible for the editing of *HAC1* mRNA which produces an active executor of the UPR. *ERN1* is the human ortholog of yeast *ire1*, *XBP1* is a functional human homolog of *hac1*.

in cells with active RAS signaling, we created *ERN1* knockout (KO) LoVo, HCT-116, SW480 and DLD1 *KRAS* mutant colon cancer cells using lentiviral CRISPR-Cas9 vectors. *ERN1* KO cells had an absence of ERN1 protein and a strong decrease in spliced XBP1 (XBP1s) (Figures 2A-D). We found that the proliferation of *ERN1* KO cells was similar to control cells expressing non-targeting (NT) gRNA, indicating that the synthetic lethal interaction between RAS and the UPR is not conserved between yeast and human cells. However, since yeast cells are missing the RAF/MEK/ERK MAPK cascade, we investigated the proliferation of the *KRAS* mutant *ERN1* KO cells in the presence of the MEK inhibitor selumetinib (AZD6244). Interestingly, we found increased MEK inhibitor sensitivity in all *ERN1* KO LoVo, HCT-116 and SW480 cell clones, both in short term and in long term assays (Figures 2E-G and Additional file 1: Figures S2A-C). In DLD1 cells, no effect on selumetinib response was observed upon *ERN1* KO (Additional file 1: Figures S2D-F). These data indicate that a subset of *KRAS* mutant colon cancer cells can be sensitized to MEK inhibition by loss of *ERN1*.

Pharmacologic inhibition of ERN1

The ERN1 protein contains both an endonuclease and a kinase domain. A specific inhibitor of ERN1 kinase activity has been developed that results in allosteric inhibition of the endonuclease activity, referred to as compound 18 by Harrington *et al* [27]. We tested the potency of this inhibitor in LoVo cells by measuring XBP1s levels 24 hours after treatment with increasing amounts of ERN1 inhibitor. The compound proved effective with an IC50 of approximately 100nM (Figure 2H). Next, we tested whether treatment with this potent ERN1 inhibitor would increase the sensitivity of LoVo cells to the MEK inhibitor. To our surprise, inhibition of ERN1 endonuclease activity was not sufficient to recapitulate the phenotype of the genetic ablation of *ERN1* (Figure 2I).

ERN1 is able to cleave other mRNAs besides XBP1, a process termed Regulated IRE1-Dependent Decay (RIDD) [28]. We tested whether the ERN1 inhibitor interfered with RIDD by stressing LoVo cells with the ER stress-inducing agent thapsigargin (Tg) both in the absence and presence of the ERN1 kinase inhibitor. One of the RIDD targets is *CD59* [29]. As expected, XBP1s levels increased and *CD59* mRNA levels decreased upon treatment with

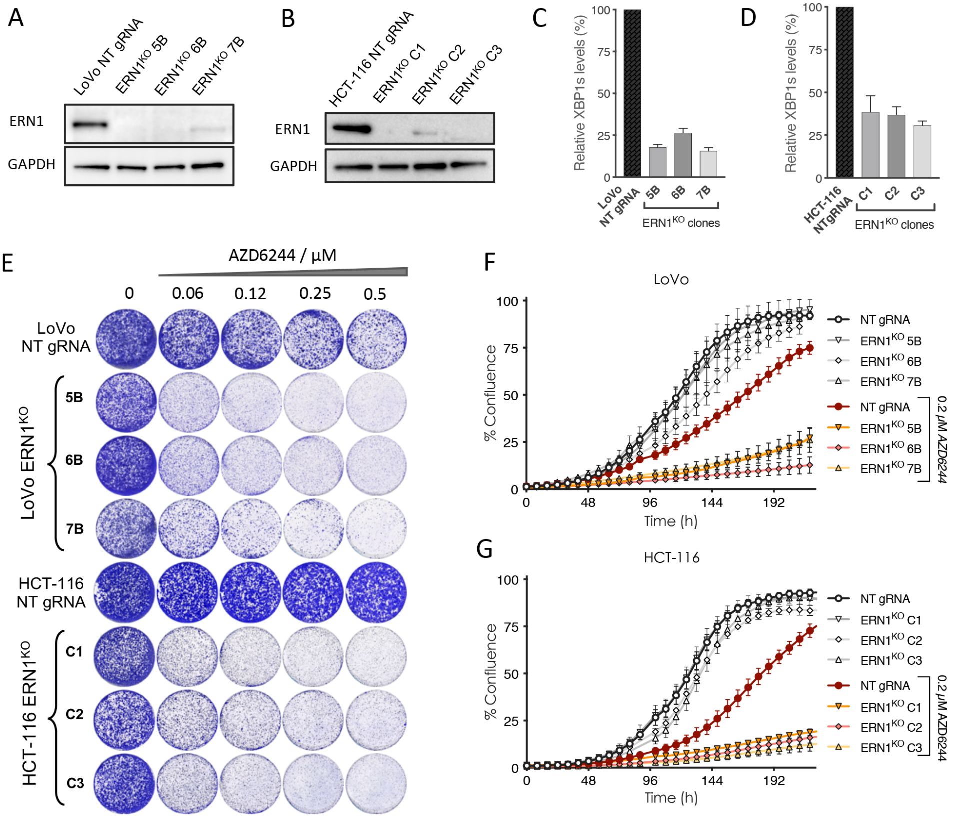

Figure 2. Effects of ERN1 inhibition in *KRAS* mutant human colon cancers.

(A and B) Western blot analysis of *ERN1* expression in control cells expressing non-targeting (NT) gRNA and LoVo *ERN1* KO clones 5B, 6B and 7B **(A)** and HCT-116 *ERN1* KO clones C1, C2 and C3 **(B)**.

(C and D) qPCR analysis of spliced XBP1 mRNA (XBP1s) in control cells expressing non-targeting (NT) gRNA and LoVo *ERN1* KO clones 5B, 6B and 7B **(C)** and HCT-116 *ERN1* KO clones C1, C2 and C3 **(D)**. Error bars indicate standard deviation calculated from three biological replicates.

(E) Representative colony formation assays of three different *ERN1* KO clones compared to the non-targeting (NT) gRNA expressing control cells in the *KRAS* mutant LoVo (top) and HCT-116 colon cancer cells (bottom). Cells were maintained in the indicated range of concentrations of the MEK inhibitor selumetinib (AZD6244) for 10 days, stained and photographed.

(F and G) Live cell proliferation assay (IncuCyte®) of control (NT gRNA) and *ERN1* KO cells following exposure to the MEK inhibitor AZD6244. Error bars indicate standard deviation of three replicate experiments.

Tg. In the presence of the ERN1 inhibitor, XBP1 splicing was not increased and *CD59* mRNA levels did not decrease upon treatment with Tg (Figures 2J and K). These data show that RIDD is effectively inhibited by the ERN1 inhibitor and that RIDD targets are unlikely to be involved in the sensitization of *ERN1* KO cells to the MEK inhibitor.

Genome wide screen reveals ERN1-JNK-JUN signaling axis

To identify a mechanistic link between ERN1 and the RAF/MEK/ERK signaling pathway, we performed a genome-scale CRISPR/Cas9 MEK inhibitor resistance screen using *ERN1* KO LoVo cells. We screened in the presence and absence of two different MEK inhibitors, selumetinib and trametinib (Figure 3A) and used differential analysis to identify the genes whose knockout confers resistance to MEK inhibitors. Considering that the CRISPR library used contained only three sgRNAs per gene target, we decided not to impose the criterion of multiple sgRNAs per

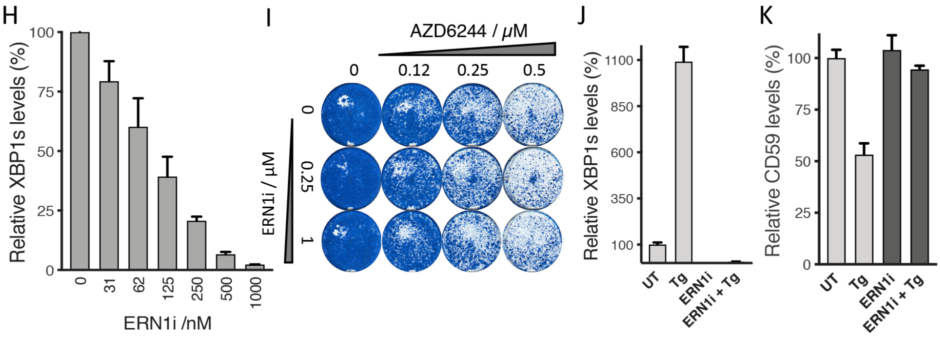

Figure 2. Effects of ERN1 inhibition in *KRAS* mutant human colon cancers.

(H) qPCR analysis of spliced XBP1 mRNA (XBP1s) levels following exposure of LoVo cells to increasing concentrations of the ERN1 kinase inhibitor. Error bars indicate standard deviation calculated from three replicate experiments.

(I) Colony formation assay showing the effect of ERN1 kinase inhibitor on the proliferation of *KRAS* mutant LoVo cells in the presence of the indicated concentrations of the MEK inhibitor AZD6244.

(J) Quantification of spliced XBP1 mRNA (XBP1s) levels following one hour treatment with 100 nM of ER stress inducer thapsigargin (Tg) in the presence and absence of the ERN1 kinase inhibitor.

(K) Quantification of the mRNA levels of the RIDD target CD59 after one hour treatment with 100 nM thapsigargin (Tg) in the presence and absence of the ERN1 kinase inhibitor.

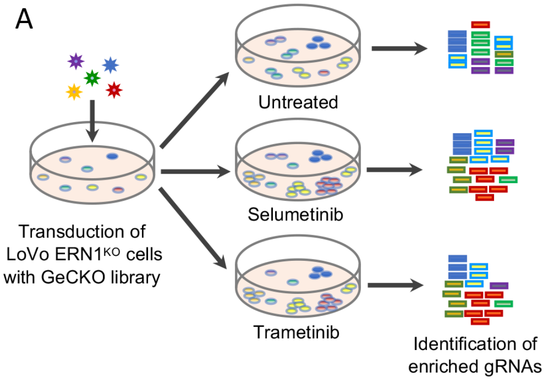
A
Untreated
Selumetinib
Trametinib
Transduction of
LoVo ERN1KO cells
with GeCKO library
Identification of
enriched gRNAs

Figure 3. A genetic screen for resistance to MEK inhibitors in *ERN1* knockout colon cancer.

(A) Schematic outline of the genome-scale CRISPR/Cas9 knockout screen for resistance to MEK inhibition. Two different MEK inhibitors, selumetinib and trametinib, were used, each in two replicates, and compared to the untreated control population.

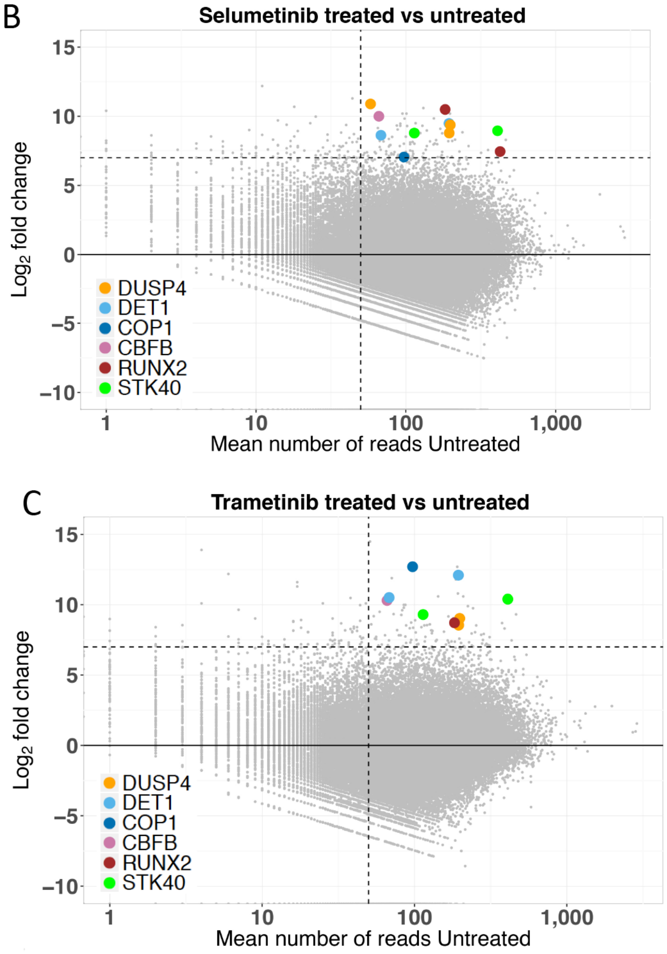

(B and C) MA plots of the selumetinib **(B)** and trametinib screens **(C)**. Horizontal dashed line indicates an arbitrarily imposed threshold of log2 (fold change of treated over untreated) of 7 and vertical dashed line indicates mean number of reads in untreated samples of 50. Highlighted in color are the sgRNAs targeting *DUSP4*, *DET1*, *COP1*, *CBFB*, *RUNX2* and *STK40*, that are found above these two thresholds (with the p adjusted of <= 0.1) in both the selumetinib **(B)** and the trametinib **(C)** screen.

gene. Nevertheless, we found that four hits (*DET1*, *DUSP4*, *RUNX2* and *STK40*) were represented by multiple different sgRNAs, while two hits (*COP1* and *CBFB*) each scored with a single sgRNA both in selumetinib and in trametinib screen (Figures 3B and C). A complete list of screen results can be found in Additional file 2: Tables S8 and S9.

Dual specificity phosphatase-4 (*DUSP4*) has been previously implicated in regulating the response to MEK inhibitors, validating the screen performed here [30,31]. Serine/threonine kinase 40 (*STK40*) is a negative regulator of NF-κB [32,33], and NF-κB activity was already shown to directly modulate resistance to several different MAPK pathway inhibitors [34]. In contrast, the remaining four genes (*DET1*, *COP1*, *CBFB* and *RUNX2*) have not previously been implicated in MAPK signaling or MEK inhibitor resistance. Interestingly, these four genes code for proteins that act pair-wise in complex with each other. The functional and physical interaction between RUNX2 (also known as core-binding factor subunit alpha-1 or CBFA1), and its transcriptional co-activator CBFB (core-binding factor subunit beta) has been well documented using various *in vitro* [35] and *in vivo* model systems [36-39]. DET1 and COP1 are part of an E3 ubiquitin ligase complex that promotes ubiquitination and degradation of the proto-oncogenic transcription factor JUN [40]. Because of a previously established link between ERN1 and JNK [41], we studied DET1 and COP1 further to understand the effects of *ERN1* loss on the response to MEK inhibitors.

DET1 and COP1 are regulators of MEK inhibitor response

To validate the results of the genetic screen, we knocked out *DET1* and *COP1* in *ERN1*-deficient LoVo cells. Importantly, both in long term assays (Figure 3D, and Additional file 1: Figure S3) and in short term assays (Figure 3E) loss of either *DET1* or *COP1* conferred resistance to selumetinib and trametinib in these cells. Both vectors were effective in knocking out their respective targets in a polyclonal knockout cell population (Figure 3F). In addition, biochemical analysis revealed higher basal JUN levels in *DET1* and *COP1* negative cell populations, consistent with the fact that DET1 and COP1 are part of an E3 ubiquitin ligase complex that degrades JUN [40]. Moreover, computational analyses of drug response data in a large cancer cell line panel [42] further supports that high *DET1* or *COP1* expression is correlated with low IC50 values (i.e. sensitivity) for five different MEK inhibitors across a colorectal cancer cell line panel (Figure 3G).

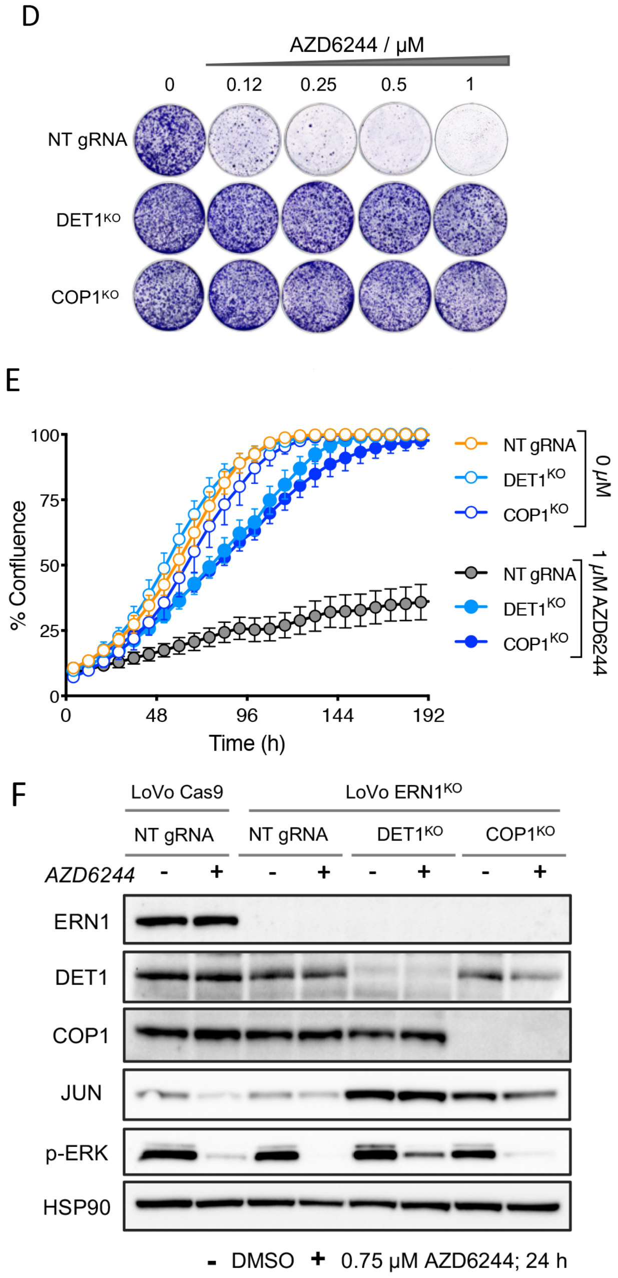

Figure 3. (D and E) Functional validation of *DET1* and *COP1* in LoVo *ERN1* KO background.

(D) Colony formation assays of *DET1* and *COP1* KO cells in the presence and absence of the MEK inhibitor AZD6244 (selumetinib) are shown relative to control cells having NT gRNA. Shown is a representative example of at least three biological replicates.

(E) Live cell proliferation assay of *DET1* and *COP1* KO cells in the presence and absence of 1µM AZD6244 compared to control cells expressing NT gRNA. Error bars indicate standard deviation calculated from three replicate experiments.

(F) Western blot analysis of *DET1* and *COP1* expression in *DET1* and *COP1* knockout cells using antibodies against ERN1, DET1, COP1, JUN, p-ERK and HSP90 as control both in the presence and absence of the MEK inhibitor AZD6244.

Besides an endonuclease and a kinase function, human ERN1 regulates JNK signaling through binding of the adaptor protein TRAF2 [41], which activates JNK to phosphorylate the transcription factor JUN. We tested if active JNK signaling is important for MEK inhibitor sensitivity by directly knocking down *JUN* using shRNAs. We found that LoVo cells are dependent on JUN for proliferation upon treatment with MEK inhibitor. Importantly, the sensitivity of the LoVo cells to treatment with MEK inhibitor correlated with the levels of JUN protein (Figure 4A). To investigate if ERN1 is required for the activation of JUN, we compared JUN phosphorylation in *ERN1* KO cells to control cells, in the presence and absence of MEK inhibitor. We observed a strong increase in JUN phosphorylation in *ERN1* wt cells, compared to *ERN1* KO cells, after 4 hours of MEK inhibitor treatment (Figure 4B). Consistently, we found that JUN expression is increased by MEK inhibitor in parental cells, but not in *ERN1* KO cells, which is not caused by expression changes of either *JNK1* or *JNK2* mRNA (Additional file 1: Figures S4 and S5). These results indicate that ERN1 deficient cells are unable to fully activate JUN signaling, which may explain the MEK inhibitor sensitivity of *ERN1* KO cells. Moreover, we found that MEK inhibitor treatment induces ERN1 activity, an effect not seen in *ERN1* KO cells (Figure 4C).

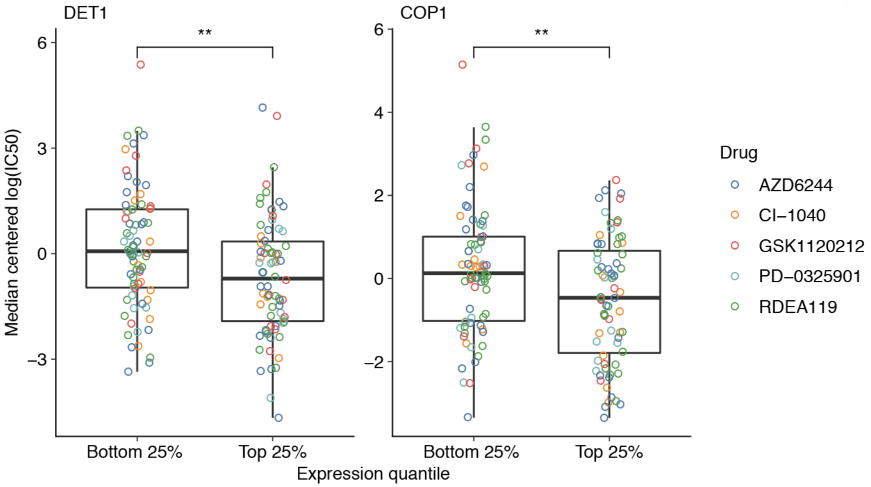

Figure 3. (G) Median centered log(IC50) of five different MEK1 inhibitors in high (top 25%) and low (bottom 25%) expressing *DET1* (left) and *COP1* (right) CRC cell lines in the GDSC100 data set [42]. Cell lines with high *DET1* or *COP1* expression have significantly lower IC50s (p=0.004 for both DET1 and COP1). Log(IC50) estimates were median-centered over all cell lines to make them comparable between MEK inhibitors.

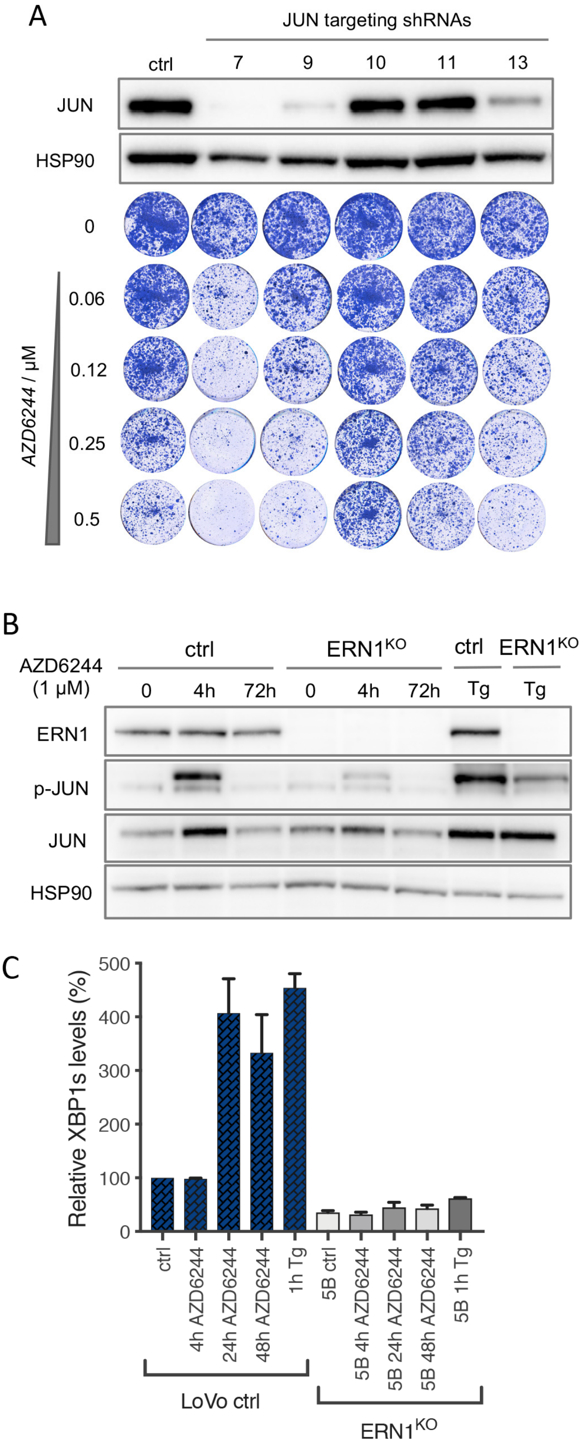

Figure 4. Effect of genetic and pharmacologic downregulation of *JUN* on response to MEK inhibition.

(A) Five different *JUN* targeting shRNAs were used to downregulate *JUN* in LoVo cells. JUN protein levels were quantified by Western blotting (top), and the response to increasing concentrations of the MEK inhibitor AZD6244 on *JUN* knockdown cells is shown in colony formation assay (bottom). Empty vector infected control (ctrl) cells are shown here for comparison.

(B) Biochemical analysis comparing *ERN1* KO cells with their control counterparts (ctrl) in the presence and absence of the MEK inhibitor AZD6244 for the indicated number of hours. One-hour thapsigargin treatment (Tg) at 0.1 µM was used as a control for p-JUN induction.

(C) Quantification of spliced XBP1 mRNA (XBP1s) in the presence and absence of 1 µM AZD6244 at indicated time points. Error bars indicate standard deviation calculated from three replicate experiments.

Finally, we tested if directly inhibiting JNK kinase signaling with a JNK kinase inhibitor would sensitize LoVo cells to MEK inhibition. The potency and specificity of the JNK inhibitor SR-3306 was tested by measuring phosphorylated JUN levels upon treatment of cells with the ER stress-inducing agent thapsigargin (Tg) (Figure 4D). We found that LoVo cells were sensitive to the combination of JNK and MEK inhibition (Figures 4E and F). This effect was also found by blocking TAK1, a kinase upstream of JNK (Figures 4G-I).

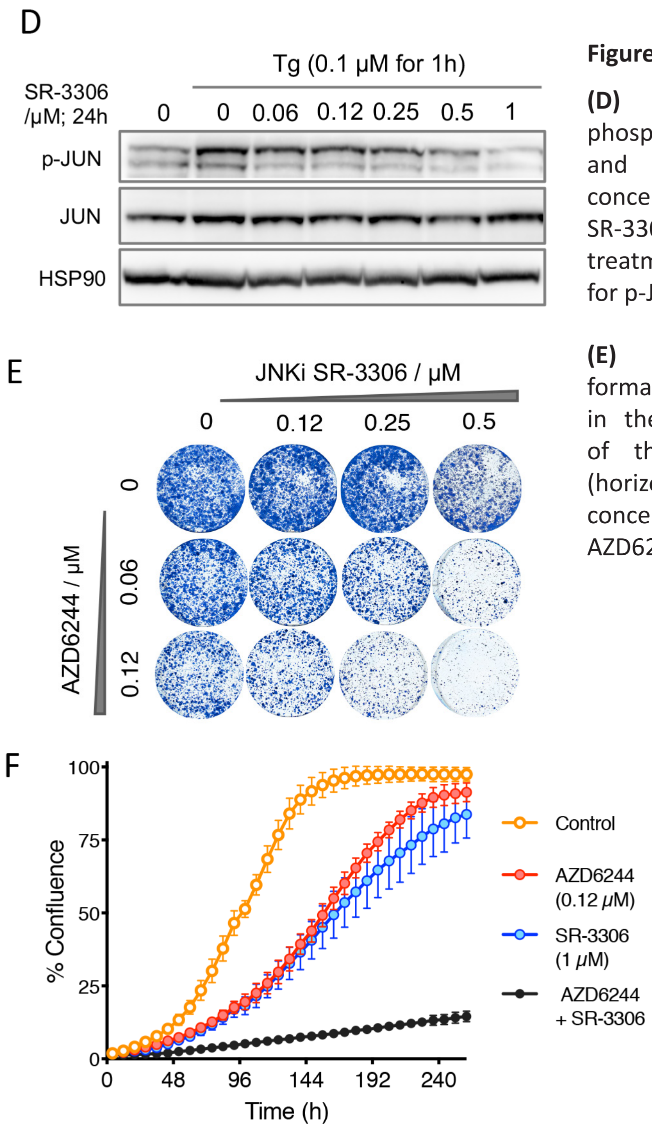

Figure 4.

(D) Biochemical analysis of JUN phosphorylation in the presence and absence of increasing concentrations of the JNK inhibitor SR-3306. One-hour of thapsigargin treatment (Tg) at 0.1 μM was used for p-JUN induction.

(E) A representative colony formation assay of LoVo cells grown in the increasing concentrations of the JNK inhibitor SR-3306 (horizontally) and the increasing concentrations of the MEK inhibitor AZD6244 (vertically).

(F) Live cell proliferation assay for the combination of the MEK inhibitor AZD6244 and the JNK inhibitor SR-3306 (black), each inhibitor individually (red and blue), and vehicle treated control cells (yellow line). Error bars indicate standard deviation calculated from three replicate experiments.

DISCUSSION

Although the yeast and human *RAS* genes have many properties that are interchangeable, the signaling pathways that are controlled by them differ. Here, we find that both yeast and human RAS share a link with the UPR. The shared interaction suggests that an analogous genetic network structure evolved connecting both yeast and human RAS to the ER stress signaling. Using genome-wide synthetic lethality screens in yeast, we identified multiple genes necessary for ER homeostasis, including the UPR stress sensor *IRE1*, to be SL with mutant *RAS*. This genetic interaction was not observed in *KRAS* mutant colon cancer cells, which are unaffected by genetic ablation of *ERN1*, the human ortholog of *IRE1*. However, in contrast to yeast, human cells possess a RAF/MEK/ERK MAPK pathway, and inhibiting this pathway uncovers the SL interaction between *ERN1* KO and mutant *KRAS*. Although we conclude that *ERN1* itself is dispensable for cell growth and proliferation, we find that its loss can sensitize *KRAS* mutant colon cancer cells to MEK inhibition. Considering unsatisfactory performance of MEK inhibitors in clinical trials [43-45], we used *ERN1* knockout colon cancer cells as a model to study resistance mechanisms to MEK inhibition. As small molecule ERN1 inhibitors failed to enhance sensitivity to MEK inhibition, we resorted to genetic screens to explore the mechanism responsible for the observed synthetic lethality effect. Our genome-wide CRISPR/Cas9 screen identified a series of genetic events that can reinstate MEK inhibitor resistance in *ERN1* knockout colon cancer cells. One of the most prominent hits in this screen was dual specificity phosphatase-4 (*DUSP4*), a well-established tumor suppressor that negatively regulates JUN N-terminal kinase JNK. Upon loss of *DUSP4*, derepressed JNK activity stimulates JUN-mediated transcription, leading to aberrant MAPK pathway activation [31]. Interestingly, two other screen hits, *DET1* and *COP1*, are also negative regulators of JUN.

Originally described as regulators of light signaling in *Arabidopsis thaliana* [46], both *DET1* (de-etiolated homolog 1) and *COP1* (constitutive photomorphogenic 1, also known as *RFWD2*) mechanistically function as E3 ubiquitin-protein ligases and are evolutionarily conserved members of the COP-DET-FUS protein family.

Extensive biochemical studies have shown that COP1-DET1 complex targets JUN for ubiquitination and degradation [40]. Further characterization of *in vivo* models established the role of human *COP1* as a tumor suppressor [47-49]. Here we uncover a role for human *COP1* and *DET1* in resistance to MEK inhibitors via inhibition of the JNK-JUN pathway.

Since three of the genes identified in our resistance screen (*DUSP4*, *DET1* and *COP1*) are negative regulators of JUN, we propose that activated ERN1 leads to increased JUN activity, which then translates to cell proliferation despite the inhibition of MEK. ERN1 is linked to the JUN pathway via its binding factor TRAF2, which executes a signaling cascade resulting in the activation of JUN N-terminal kinase JNK [41]. Furthermore, our work demonstrates that the kinase and endonuclease domains of ERN1 are not responsible for the differential sensitivity to MEK inhibition. Recently we showed that cancers that fail to activate JNK-JUN, due to inactivating mutations in upstream kinases MAP3K1 and MAP2K4, are sensitive to MEK inhibition [50]. Here we demonstrate that *ERN1* KO cells also fail to activate the JNK-JUN pathway resulting in a similar sensitivity to MEK inhibition.

We propose that the JNK arm of MAPK signaling can functionally compensate for the inhibition of the MEK/ERK signaling axis. Conversely, under conditions of abrogated JNK signaling, such as in the presence of JNK or TAK1 inhibitors, cells become more dependent on the flux of signal through the MEK/ERK pathway. This dependency could then prove to be of therapeutic importance. We speculate that cells in which *ERN1* knockout does not sensitize to MEK inhibition (such as DLD1 cells, Additional file 1: Figures S2A-C) can activate JNK-JUN signaling through other pathways, thereby making such cells independent of ERN1 for their MEK inhibitor response. Alternatively, other pathways may be involved in MEK inhibitor resistance in these cells.

We report synergistic cell growth arrest when JNK and MEK inhibitors are combined. Moreover, inhibition of JNK itself (Figures 4D and E) or JNK activators, such as TAK1 (Figures 4G and H), might also be useful in preventing intrinsic resistance to MEK inhibitors. In this study, we made use of the resorcyclic lactone (5Z)-7-oxozeanol (5ZO) as a TAK1 inhibitor. However, considerable off-target effects render this molecule inadequate for therapeutic purposes. It remains to be seen whether recently developed TAK1 inhibitors [51] give a more favorable toxicologic profile in the clinic. Taken together, our findings identify an unexpected role for the Unfolded Protein Response executor ERN1 in determining the response to MEK inhibition in *KRAS*-driven colon cancer.

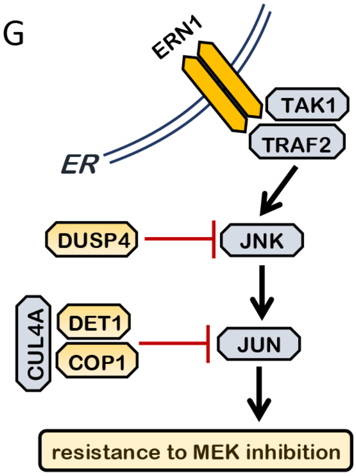

Figure 4. (G) Schematic representation of the signaling from the endoplasmic reticulum (ER) embedded ERN1 to JNK and JUN via its binding factor TRAF2 and TAK1. Shown in yellow are resistance screen hits DUSP4, DET1 and COP1, which are all negative regulators of JNK and JUN, respectively.

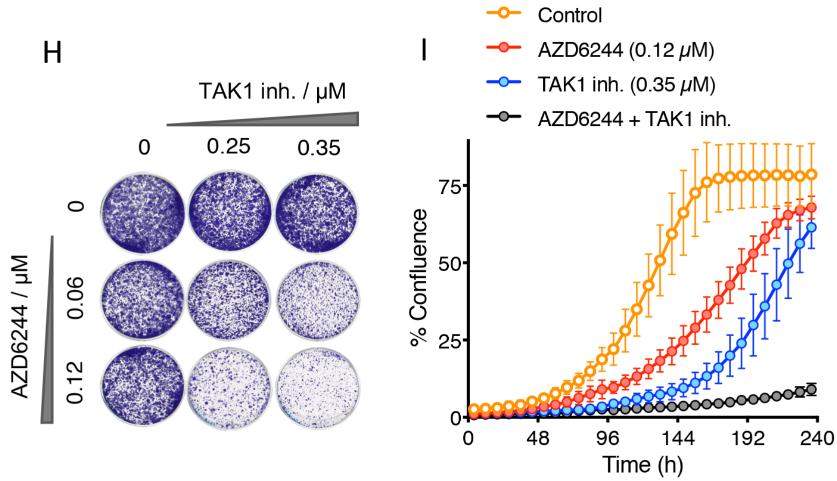

Figure 4. (H) A representative colony formation assay showing the effect of the TAK1 inhibitor (5Z)-7-oxozeanol (5ZO) on the proliferation of *KRAS* mutant LoVo cells in the presence of the indicated concentrations of the MEK inhibitor AZD6244.

(I) Live cell proliferation assay for the combination of the MEK inhibitor AZD6244 and TAK1 inhibitor 5ZO over the course of 10 days (240 hours). Yellow line shows vehicle treated control cells. Error bars indicate standard deviation calculated from three replicate experiments.

CONCLUSIONS

We identify here a set of genes involved in endosomal transport and ER stress that are synthetic lethal with mutant *RAS* in yeast. At the crossroads of these processes, we identify *IRE1* and *HAC1* that are not only synthetic lethal with hyperactivated RAS signaling in yeast, but also with *ERI1*, a non-essential component of the GPI-GnT enzyme which mediates ER stress response. The fact that *IRE1* and *HAC1* are both master regulators of the unfolded protein response (UPR) indicates that ER homeostasis is disturbed in mutant *RAS* expressing cells and that these cells are dependent on the UPR.

Moreover, in human colon cancer cell lines, we find that MAPK pathway shields *KRAS* mutant cells from synthetic lethality with *ERN1*, a human ortholog of *IRE1*. These interactions point to an evolutionarily conserved genetic network structure between RAS signaling and ER stress.

Finally, we find that ERN1 is an important regulator of JUN activity, which becomes crucial for survival in *KRAS* mutant colon cancer under conditions of abrogated MAPK signaling. We identify the ERN1-JNK-JUN pathway as a novel regulator of MEK inhibitor response in *KRAS* mutant colon cancer, and point to synthetic lethality of MEK inhibition with therapeutics targeting JUN activating kinases, TAK1 and JNK. The genetic network connecting JUN and MAPK signaling may explain why *KRAS* mutant tumor cells are traditionally seen as highly refractory to MEK inhibitor therapy, but these genetic interactions may also provide a therapeutically exploitable vulnerability.

List of abbreviations

Synthetic lethal (SL), endoplasmic reticulum (ER), wild-type (WT), selective ploidy ablation (SPA), unfolded protein response (UPR), regulated IRE1-dependent decay (RIDD), knockout (KO), non-targeting (NT), polyethylenimine (PEI), untreated (UT), thapsigargin (Tg), ERN1 inhibitor (ERN1i), MEK inhibitor (MEKi), JNK inhibitor (JNKi), (5Z)-7-oxozeanol (5ZO).

Availability of data and material

The datasets supporting the conclusions of this article are included within the online version of the article and its additional files (Additional file 1.pdf and Additional file 2.xslx).

https://genomemedicine.biomedcentral.com/articles/10.1186/s13073-018-0600-z#Sec17

Competing interests

The authors declare that they have no competing interests.

Funding

This study was supported by a Rubicon grant from the Netherlands Organisation for Scientific Research (NWO), grants from the Dutch Cancer Society and the Center for Cancer Genomics. SW was funded in part by research funding from Astex Pharmaceuticals (Cambridge, UK) under the Sustaining Innovation Post-Doctoral Programme. R.R. received support from the New York State Department of Health, Wadsworth Center Health Research Science Board (http://www.wads- worth.org/extramural, HRSB-C028248), the National Cancer Institute (NCI) (R33 CA125520) and the National Institute of General Medical Sciences (R35 GM118180). J.D. received support from an NCI training grant (T32 CA009503).

Authors' contributions

TS, SW, and EB generated the data. TS, SW, EB, RJDR, JD, CL and RLB analyzed the data. TS, SW, RR, LFAW and RB designed the study. TS, SW, RJDR and RR wrote the manuscript. All authors read and approved the final manuscript.

Acknowledgements

We thank all members of the Bernards, Beijersbergen, Wessels and Rothstein labs for helpful support and discussions. We acknowledge Samantha Ciccone and Bethany Andresen for their assistance with the yeast screening protocol. We also thank Bastiaan Evers for the initial analysis of the CRISPR screen output and for the dual vector doxycycline inducible CRISPR/Cas9 system mentioned in the methods section. We would like to thank Vishva Dixit and Genentech for kindly providing us with DET1 and COP1 antibodies.

REFERENCES

1. Karnoub AE, Weinberg RA. Ras oncogenes: split personalities. Nat Rev Mol Cell Biol. 2008;9:517–31.
2. Ostrem JM, Peters U, Sos ML, Wells JA, Shokat KM. K-Ras(G12C) inhibitors allosterically control GTP affinity and effector interactions. Nature. Nature Publishing Group; 2013;503:548–51.
3. Janes MR, Zhang J, Li L-S, Hansen R, Peters U, Guo X, et al. Targeting KRAS Mutant Cancers with a Covalent G12C-Specific Inhibitor. Cell. 2018;172:578–589.e17.
4. Kataoka T, Powers S, McGill C, Fasano O, Strathern J, Broach J, et al. Genetic analysis of yeast RAS1 and RAS2 genes. Cell. 1984;37:437–45.
5. Kataoka T, Powers S, Cameron S, Fasano O, Goldfarb M, Broach J, et al. Functional homology of mammalian and yeast RAS genes. Cell. 1985;40:19–26.
6. DeFeo-Jones D, Tatchell K, Robinson LC, Sigal IS, Vass WC, Lowy DR, et al. Mammalian and yeast ras gene products: biological function in their heterologous systems. Science. 1985;228:179–84.
7. Reid RJD, González-Barrera S, Sunjevaric I, Alvaro D, Ciccone S, Wagner M, et al. Selective ploidy ablation, a high-throughput plasmid transfer protocol, identifies new genes affecting topoisomerase I-induced DNA damage. Genome Res. Cold Spring Harbor Lab; 2011;21:477–86.
8. Gardner BM, Pincus D, Gotthardt K, Gallagher CM, Walter P. Endoplasmic reticulum stress sensing in the unfolded protein response. Cold Spring Harb Perspect Biol. 2013;5:a013169–9.
9. Yoshida H, Matsui T, Yamamoto A, Okada T, Mori K. XBP1 mRNA is induced by ATF6 and spliced by IRE1 in response to ER stress to produce a highly active transcription factor. Cell. 2001;107:881–91.
10. Reid RJD, Lisby M, Rothstein R. Cloning-free genome alterations in Saccharomyces cerevisiae using adaptamer-mediated PCR. Meth. Enzymol. 2002;350:258–77.
11. Winzeler EA, Shoemaker DD, Astromoff A, Liang H, Anderson K, Andre B, et al. Functional characterization of the S. cerevisiae genome by gene deletion and parallel analysis. Science. 1999;285:901–6.
12. Brunen D, de Vries RC, Lieftink C, Beijersbergen RL, Bernards R. PIM Kinases Are a Potential Prognostic Biomarker and Therapeutic Target in Neuroblastoma. Mol. Cancer Ther. 2018;17:849–57.
13. van Schadewijk A, van't Wout EFA, Stolk J, Hiemstra PS. A quantitative method for detection of spliced X-box binding protein-1 (XBP1) mRNA as a measure of endoplasmic reticulum (ER) stress. Cell Stress Chaperones. Springer Netherlands; 2012;17:275–9.

14. Herold MJ, van den Brandt J, Seibler J, Reichardt HM. Inducible and reversible gene silencing by stable integration of an shRNA-encoding lentivirus in transgenic rats. Proc. Natl. Acad. Sci. U.S.A. National Academy of Sciences; 2008;105:18507–12.

15. Prahallad A, Heynen GJJE, Germano G, Willems SM, Evers B, Vecchione L, et al. PTPN11 Is a Central Node in Intrinsic and Acquired Resistance to Targeted Cancer Drugs. CellReports. 2015;12:1978–85.

16. Sanjana NE, Shalem O, Zhang F. Improved vectors and genome-wide libraries for CRISPR screening. Nature Methods. Nature Publishing Group; 2014;11:783–4.

17. Evers B, Jastrzebski K, Heijmans JPM, Grernrum W, Beijersbergen RL, Bernards R. CRISPR knockout screening outperforms shRNA and CRISPRi in identifying essential genes. Nat Biotechnol. Nature Publishing Group; 2016;34:631–3.

18. Dittmar JC, Reid RJ, Rothstein R. ScreenMill: a freely available software suite for growth measurement, analysis and visualization of high-throughput screen data. BMC Bioinformatics. BioMed Central; 2010;11:353.

19. Dittmar JC, Pierce S, Rothstein R, Reid RJD. Physical and genetic-interaction density reveals functional organization and informs significance cutoffs in genome-wide screens. Proc. Natl. Acad. Sci. U.S.A. 2013;110:7389–94.

20. van Wageningen S, Kemmeren P, Lijnzaad P, Margaritis T, Benschop JJ, de Castro IJ, et al. Functional overlap and regulatory links shape genetic interactions between signaling pathways. Cell. 2010;143:991–1004.

21. Howard SC, Chang YW, Budovskaya YV, Herman PK. The Ras/PKA signaling pathway of Saccharomyces cerevisiae exhibits a functional interaction with the Sin4p complex of the RNA polymerase II holoenzyme. Genetics. Genetics Society of America; 2001;159:77–89.

22. Benschop JJ, Brabers N, van Leenen D, Bakker LV, van Deutekom HWM, van Berkum NL, et al. A consensus of core protein complex compositions for Saccharomyces cerevisiae. Mol. Cell. 2010;38:916–28.

23. Leber JH, Bernales S, Walter P. IRE1-independent gain control of the unfolded protein response. Steven McKnight, editor. PLoS Biol. Public Library of Science; 2004;2:E235.

24. Chen Y, Feldman DE, Deng C, Brown JA, De Giacomo AF, Gaw AF, et al. Identification of mitogen-activated protein kinase signaling pathways that confer resistance to endoplasmic reticulum stress in Saccharomyces cerevisiae. Mol. Cancer Res. 2005;3:669–77.

25. Sobering AK, Watanabe R, Romeo MJ, Yan BC, Specht CA, Orlean P, et al. Yeast Ras regulates the complex that catalyzes the first step in GPI-anchor biosynthesis at the ER. Cell. 2004;117:637–48.

26. Costanzo M, Baryshnikova A, Bellay J, Kim Y, Spear ED, Sevier CS, et al. The genetic landscape of a cell. Science. 2010;327:425–31.

27. Harrington PE, Biswas K, Malwitz D, Tasker AS, Mohr C, Andrews KL, et al. Unfolded Protein Response in Cancer: IRE1α Inhibition by Selective Kinase Ligands Does Not Impair Tumor Cell Viability. ACS Med Chem Lett. 2015;6:68–72.

28. Hollien J, Lin JH, Li H, Stevens N, Walter P, Weissman JS. Regulated Ire1-dependent decay of messenger RNAs in mammalian cells. J. Cell Biol. 2009;186:323–31.

29. Oikawa D, Tokuda M, Iwawaki T. Site-specific cleavage of CD59 mRNA by endoplasmic reticulum-localized ribonuclease, IRE1. Biochem. Biophys. Res. Commun. 2007;360:122–7.

30. Balko JM, Cook RS, Vaught DB, Kuba MG, Miller TW, Bhola NE, et al. Profiling of residual breast cancers after neoadjuvant chemotherapy identifies DUSP4 deficiency as a mechanism of drug resistance. Nat. Med. 2012;18:1052–9.

31. Balko JM, Schwarz LJ, Bhola NE, Kurupi R, Owens P, Miller TW, et al. Activation of MAPK pathways due to DUSP4 loss promotes cancer stem cell-like phenotypes in basal-like breast cancer. Cancer Research. American Association for Cancer Research; 2013;73:6346–58.

32. Huang J, Teng L, Liu T, Li L, Chen D, Li F, et al. Identification of a novel serine/threonine kinase that inhibits TNF-induced NF-kappaB activation and p53-induced transcription. Biochem. Biophys. Res. Commun. 2003;309:774–8.

33. Xu N, Meisgen F, Butler LM, Han G, Wang X-J, Söderberg-Nauclér C, et al. MicroRNA-31 is overexpressed in psoriasis and modulates inflammatory cytokine and chemokine production in keratinocytes via targeting serine/threonine kinase 40. J. Immunol. American Association of Immunologists; 2013;190:678–88.

34. Konieczkowski DJ, Johannessen CM, Abudayyeh O, Kim JW, Cooper ZA, Piris A, et al. A melanoma cell state distinction influences sensitivity to MAPK pathway inhibitors. Cancer Discovery. American Association for Cancer Research; 2014;4:816–27.

35. Mendoza-Villanueva D, Deng W, Lopez-Camacho C, Shore P. The Runx transcriptional co-activator, CBFβ, is essential for invasion of breast cancer cells. Mol Cancer. 2010;9:171–11.

36. Kundu M, Javed A, Jeon J-P, Horner A, Shum L, Eckhaus M, et al. Cbfβ interacts with Runx2 and has a critical role in bone development. Nature Genetics. 2002;32:639–44.

37. Lim K-E, Park N-R, Che X, Han M-S, Jeong J-H, Kim S-Y, et al. Core binding factor β of osteoblasts maintains cortical bone mass via stabilization of Runx2 in mice. J. Bone Miner. Res. 2015;30:715–22.

38. Qin X, Jiang Q, Matsuo Y, Kawane T, Komori H, Moriishi T, et al. Cbfb regulates bone development by stabilizing Runx family proteins. J. Bone Miner. Res. 2015;30:706–14.

39. Komori T. Requisite roles of Runx2 and Cbfb in skeletal development. J. Bone Miner. Res. 2003;21:193–7.

40. Wertz IE, O'Rourke KM, Zhang Z, Dornan D, Arnott D, Deshaies RJ, et al. Human De-etiolated-1 regulates c-Jun by assembling a CUL4A ubiquitin ligase. Science. American Association for the Advancement of Science; 2004;303:1371–4.

41. Urano F, Wang X, Bertolotti A, Zhang Y, Chung P, Harding HP, et al. Coupling of stress in the ER to activation of JNK protein kinases by transmembrane protein kinase IRE1. Science. 2000;287:664–6.

42. Iorio F, Knijnenburg TA, Vis DJ, Bignell GR, Menden MP, Schubert M, et al. A Landscape of Pharmacogenomic Interactions in Cancer. Cell. 2016;166:740–54.

43. Adjei AA, Cohen RB, Franklin W, Morris C, Wilson D, Molina JR, et al. Phase I pharmacokinetic and pharmacodynamic study of the oral, small-molecule mitogen-activated protein kinase kinase 1/2 inhibitor AZD6244 (ARRY-142886) in patients with advanced cancers. J. Clin. Oncol. American Society of Clinical Oncology; 2008;26:2139–46.

44. Migliardi G, Sassi F, Torti D, Galimi F, Zanella ER, Buscarino M, et al. Inhibition of MEK and PI3K/mTOR suppresses tumor growth but does not cause tumor regression in patient-derived xenografts of RAS-mutant colorectal carcinomas. Clinical Cancer Research. American Association for Cancer Research; 2012;18:2515–25.

45. Jänne PA, Shaw AT, Pereira JR, Jeannin G, Vansteenkiste J, Barrios C, et al. Selumetinib plus docetaxel for KRAS-mutant advanced non-small-cell lung cancer: a randomised, multicentre, placebo-controlled, phase 2 study. Lancet Oncol. 2013;14:38–47.

46. Wei N, Deng XW. Making sense of the COP9 signalosome. A regulatory protein complex conserved from Arabidopsis to human. Trends Genet. 1999;15:98–103.

47. Migliorini D, Bogaerts S, Defever D, Vyas R, Denecker G, Radaelli E, et al. Cop1 constitutively regulates c-Jun protein stability and functions as a tumor suppressor in mice. J. Clin. Invest. 2011;121:1329–43.

48. Vitari AC, Leong KG, Newton K, Yee C, O'Rourke K, Liu J, et al. COP1 is a tumour suppressor that causes degradation of ETS transcription factors. Nature. 2011;474:403–6.

49. Marine J-C. Spotlight on the role of COP1 in tumorigenesis. Nature Reviews Cancer. Nature Publishing Group; 2012;12:455–64.

50. Xue Z, Vis DJ, Bruna A, Sustic T, van Wageningen S, Batra AS, et al. MAP3K1 and MAP2K4 mutations are associated with sensitivity to MEK inhibitors in multiple cancer models. Cell Res. Nature Publishing Group; 2018;28:719–29.

51. Totzke J, Gurbani D, Raphemot R, Hughes PF, Bodoor K, Carlson DA, et al. Takinib, a Selective TAK1 Inhibitor, Broadens the Therapeutic Efficacy of TNF-α Inhibition for Cancer and Autoimmune Disease. Cell Chem Biol. 2017;24:1029–1039.e7.

SUPPLEMENTARY FIGURES (Additional file 1)

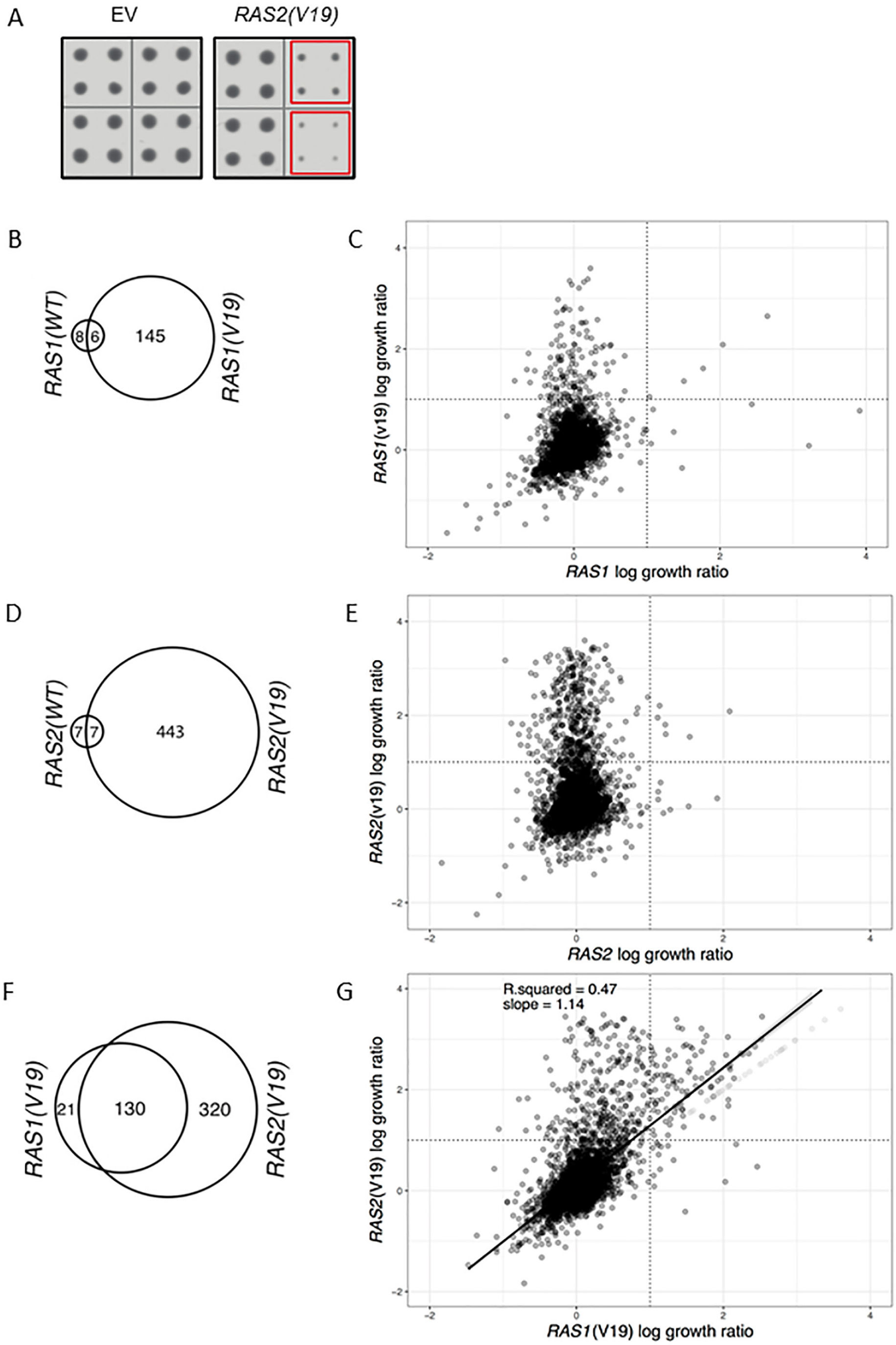

Figure S1. Genome-wide synthetic lethal screens with *RAS1(V19)* and *RAS2(V19)* identify overlapping sets of genes.

(A) Yeast strains containing the empty vector (EV) control (left) were used as a growth reference for the same strains expressing *RAS2(V19)* (right). Each of the ~4800 gene deletion strains is represented by 4 colonies. Two strains showing a growth defect in the presence of *RAS2(V19)* are outlined in red.

(B) Venn diagram showing the overlap between an SL screen with *RAS1* wild type (WT), that yielded 14 strains with a growth defect, and mutant *RAS1(V19)* screen that yielded 151 strains with a growth defect.

(C) Plot showing log growth ratios of the *RAS1* and *RAS1(V19)* SL screens. Ratios are calculated as the base 2 log of the growth ratio of the empty vector control divided by *RAS* plasmid, thus higher values represent slower growth when a *RAS* allele is expressed. Dotted lines show the 2-fold growth ratio difference from the population mean.

(D) Overlap between *RAS2* wild type (WT) screen and mutant *RAS2(V19)* screen.

(E) Plot of log growth ratios for the *RAS2* and *RAS2(V19)* SL screens.

(F) Venn diagram showing overlap between two screens with mutant *RAS*, *RAS1(V19)* and *RAS2(V19).* 130 out of 151 total synthetic lethal interactions from the *RAS1(V19)* screen are also present in the *RAS2(V19)* screen.

(G) Plot of log growth ratios and correlation between the *RAS1(V19)* and *RAS2(V19)* screens. The slow growth phenotype in the population of deletion mutants was overall more severe in the *RAS2(V19)* screen as compared with the *RAS1(V19)* screen. The solid line indicates the calculated correlation (slope and R2 value listed in inset). There are approximately 30 strains that show no growth with *RAS1(V19)* and *RAS2(V19)* and thus give identical growth ratios, i.e., slope = 1.0 (lighter gray points in the upper right quadrant).

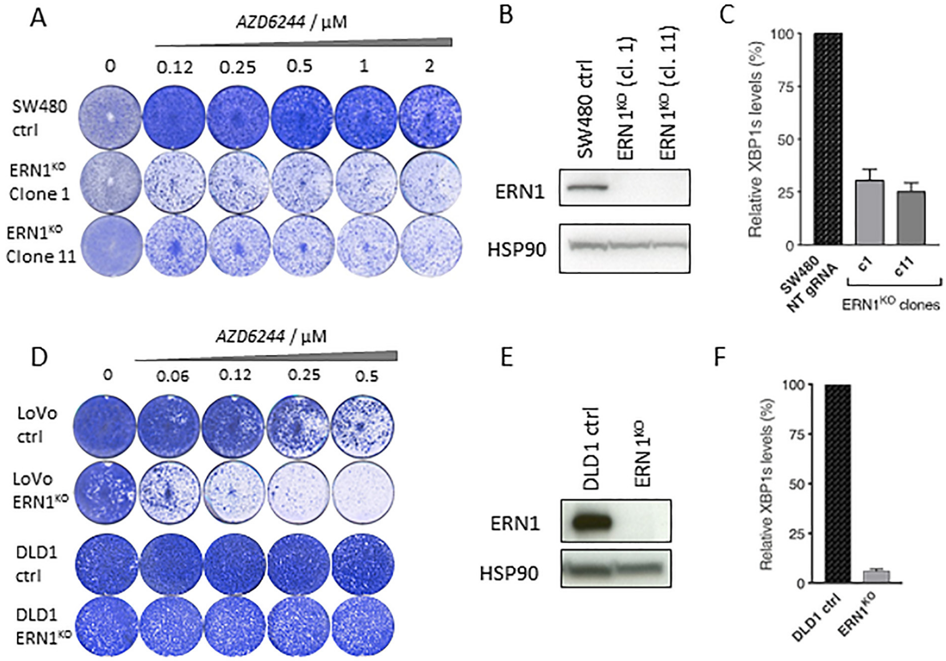

Figure S2. The response of SW480 *ERN1* KO and DLD1 *ERN1* KO *KRAS* mutant colon cancer cells to MEK inhibition.

(A) Colony formation assay of SW480 *ERN1* KO cells in indicated concentrations of the MEK inhibitor AZD6244.

(B) The expression of *ERN1* in SW480 *ERN1* KO cells.

(C) Quantification of spliced XBP1 mRNA (XBP1s) in SW480 *ERN1* KO clones.

(D) Colony formation assay of LoVo *ERN1* KO cells and DLD1 *ERN1* KO cells in indicated concentrations of the MEK inhibitor AZD6244.

(E) The expression of *ERN1* in DLD1 *ERN1* KO cells.

(F) Quantification of spliced XBP1 mRNA (XBP1s) in DLD1 *ERN1* KO clone.

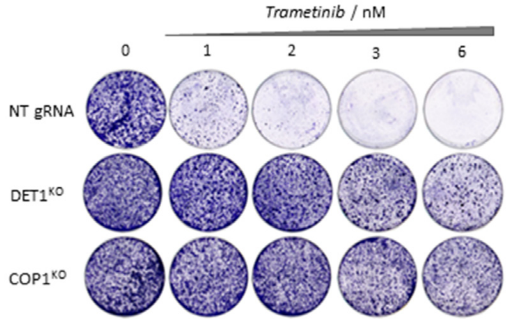

Figure S3. Colony formation assays of *DET1* and *COP1* knockout cells (in LoVo *ERN1* KO background) in the presence and absence of the MEK inhibitor trametinib are shown relative to control cells expressing non-targeting (NT) gRNA.

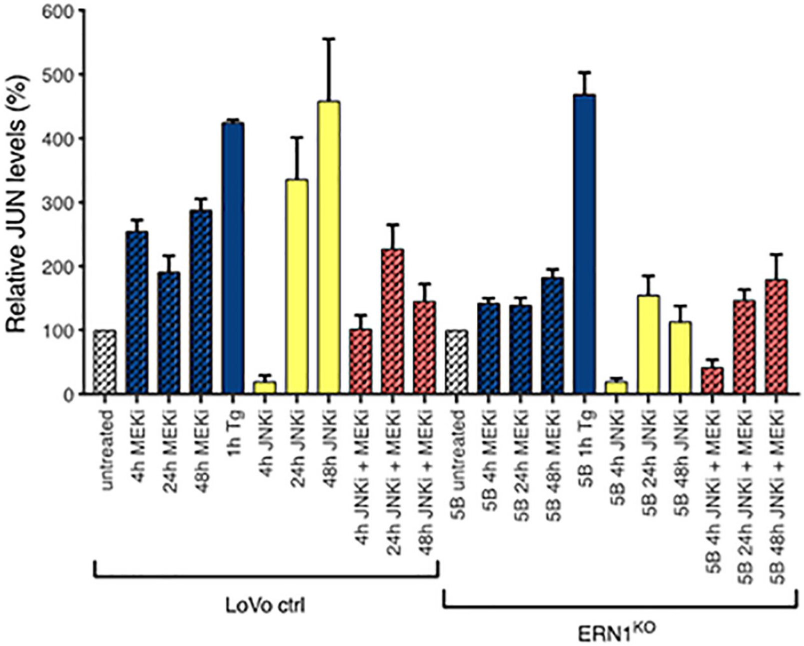

Figure S4. Quantification of *JUN* expression levels in MEK inhibitor (MEKi, 1 µM AZD6244), JNK inhibitor (JNKi, 1 µM SR-3306) and combination treatment (JNKi + MEKi). One hour thapsigargin treatment (Tg, 100 nM) was used as a control. Error bars represent standard deviation of three replicate experiments.

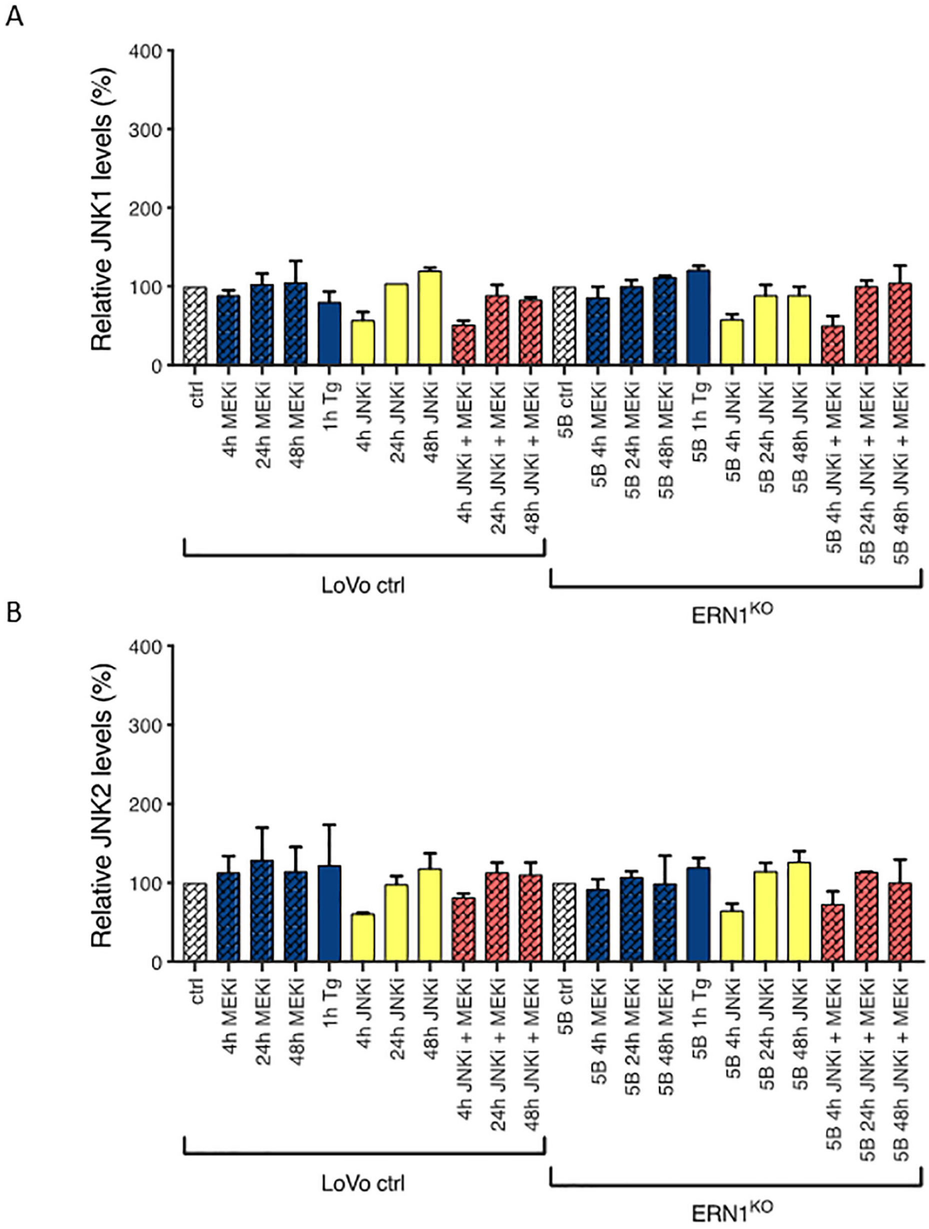

Figure S5. Quantification of *JNK1* **(A)** and *JNK2* **(B)** expression levels in MEK inhibitor (MEKi, 1 µM AZD6244), JNK inhibitor (JNKi, 1 µM SR-3306) and combination treatment (JNKi + MEKi). One hour thapsigargin treatment (Tg, 100 nM) was used as a control. Error bars represent standard deviation of three replicate experiments.

Chapter 4

RUNX2/CBFB modulates the response to MEK inhibitors through activation of receptor tyrosine kinases in *KRAS* mutant colorectal cancer

Tonći Šuštić [a], Evert Bosdriesz [a], Sake van Wageningen [a],
Lodewyk F.A. Wessels [a] and René Bernards [a,*]

[a] Division of Molecular Carcinogenesis, Oncode Institute, The Netherlands Cancer Institute, Plesmanlaan 121, Amsterdam 1066 CX, The Netherlands

* Corresponding author

Translational Oncology (2020); 13 (2): 201-211.

ABSTRACT

Intrinsic and acquired resistance are major hurdles preventing the effective use of MEK inhibitors for treatment of colorectal cancer (CRC). Some 35-45% of colorectal cancers are *KRAS* mutant and their treatment remains challenging as these cancers are refractory to MEK inhibitor treatment, due to feedback activation of receptor tyrosine kinases (RTKs). We reported previously that loss of *ERN1* sensitizes a subset of *KRAS* mutant colon cancer cells to MEK inhibition. Here we show that the loss of *RUNX2* or its cofactor *CBFB* can confer MEK inhibitor resistance in CRC cells. Mechanistically, we find that cells with genetically ablated *RUNX2* or *CBFB* activate multiple RTKs, which coincides with high SHP2 phosphatase activity, a phosphatase that relays signals from the cell membrane to downstream pathways governing growth and proliferation. Moreover, we show that high activity of SHP2 is causal to loss of *RUNX2*-induced MEK inhibitor resistance, as a small molecule SHP2 inhibitor reinstates sensitivity to MEK inhibitor in *RUNX2* knockout cells. Our results reveal an unexpected role for loss of *RUNX2*/*CBFB* in regulating RTK activity in colon cancer, resulting in reduced sensitivity to MEK inhibitors.

Keywords: MEK inhibitor resistance, colorectal cancer, ERN1, RUNX2, CBFB.

Abbreviations: colorectal cancer (CRC), receptor tyrosine kinase (RTK), knockout (KO), double knockout (DKO).

INTRODUCTION

KRAS mutant colorectal cancers (CRCs) are highly refractory to targeted treatments, including inhibition of direct downstream targets of KRAS, such as MEK [1-3]. We reported previously that genetic ablation of the endoplasmatic reticulum embedded kinase ERN1 sensitizes *KRAS* mutant colorectal cancer cells to MEK inhibition [4]. To reveal the mechanistic connection between ERN1 and the MAPK signalling pathway, we performed a genome-wide CRISPR/Cas9 genetic screen in *ERN1* knockout (KO) cells to find modulators of the MEK inhibitor response. Using this approach, we identified a number of genes whose inactivation can support the growth and proliferation of *ERN1* KO cells in the presence of MEK inhibitor [4]. Besides previously validated genes; *DUSP4*, *DET1* and *COP1*, we also identified in the same genetic screen *RUNX2* (formerly known as core-binding factor subunit alpha-1 or *CBFA1*) and its transcriptional co-activator; *CBFB* (core-binding factor subunit beta) as regulators of the MEK inhibitor response [4].

The RUNX (runt-related) family of transcription factors are heterodimeric proteins composed of a DNA-binding alpha subunit and a non-DNA binding beta subunit. All three mammalian RUNX proteins (RUNX1, RUNX2 and RUNX3) bind to a common DNA motif and heterodimerize with CBFβ, which facilitates DNA binding of RUNX proteins without making a direct contact with DNA itself [5]. The functional and mechanistic interaction between RUNX2/CBFA1 and CBFβ has been well documented using various *in vitro* [6] and *in vivo* model systems [7-10]. While all three RUNX proteins are involved in skeletal development and differentiation, RUNX2 is best characterized in terms of its role in control of bone cell proliferation and differentiation [11]. RUNX2 is often referred to as the principal osteogenic master switch, as it is essential for the formation of mature osteocytes and for controlling the expression of genes required for mineralization of the bone extracellular matrix. Heterozygous loss of *RUNX2* causes the skeletal disease cleidocranial dysplasia [12], while mice with a homozygous mutation in the *Runx2* locus die at birth without breathing, due to complete lack of ossification (bone formation) [13,14].

In normal development, *RUNX2* is robustly expressed during early embryogenesis, prior to formation of bone tissue, and its functional relevance at later stages of development remains less defined. It is, however, known that RUNX2 can regulate cell migration [15] and vascular invasion in bone tissue [16]. These were the first findings supporting the role of *RUNX2* in cell fate determination in cells that are not of osteogenic lineage.

RUNX2 is regulated by a number of post-transcriptional control mechanisms including selective proteolysis and phosphorylation. Specific ERK/MAPK phosphorylation sites on RUNX2 have been identified and functionally characterized, which suggest that RUNX2 is activated by the MAPK pathway [17,18]. Here, we set out to investigate how the loss of either *RUNX2* or *CBFB* can cause MEK inhibitor resistance in colorectal cancer. Our studies reveal an unexpected role for *RUNX2* in controlling signalling through the MAP kinase pathway through regulation of multiple RTKs.

MATERIALS AND METHODS

Cell culture, transfection and lentiviral infection

We used HEK293 cells, cultured in DMEM, for lentiviral production. All other cell lines were maintained in RPMI1640 medium containing 10% FBS and 1% penicillin/streptomycin at 37ºC and 5% CO2. All cell lines were purchased from the American Type Culture Collection (ATCC), STR profiled (by Eurofins Medigenomix Forensik GmbH, Ebersberg, Germany) and routinely tested negative for mycoplasma. Transfection of HEK293 cells with linear Polyethylenimine (PEI) 25K from Polysciences (cat# 23966-2) and subsequent infection of target cells was done as described previously [19]. For knockout of individual genes, the following single guide (sg) RNAs were cloned in the lenti CRISPR version 2.1 (LC2.1) vector by Gibson cloning: sgERN1, 5’-ACATCCCGAGACACGGTGGT-3’; sgRUNX2, 5’-GCTGTCGGTGCGGACGAGTT-3’; sgCBFB, 5’-GCCGACTTACGATTTCCGAG-3’. Non-targeting (NT) sgRNA 5’-ACGGAGGCTAAGCGTCGCAA-3’ was used as a control.

Cell proliferation assays and growth curves

For long-term cell proliferation assays cells were seeded in 6 well plates at densities of around 1×10^4 cells per well, in 12 well plates at around 5×10^3 cells per well, or in 48 well plates at around 2×10^3 cells per well, and cultured with or without inhibitors, as indicated. When control cells reached confluency, all cells were fixed in 4% formaldehyde and stained with 0.1% crystal violet (in water).

For short-term growth inhibition assays cells were seeded in 96-well plates at around 800 cells per well. Twenty-four hours after seeding, serial dilutions of AZD6244 were added to cells to final drug concentrations ranging from 0.04-10 µM. Cells were then incubated for 72 hours and cell viability was measured using the Cell Titer-Blue viability assay (Roche). Relative survival in the presence of AZD6244 was normalized to the untreated controls after subtracting the background.

Live cell growth was measured by automated determination of confluency every 4 hours using IncuCyte Zoom (Essen Bioscience). Between 600 and 800 cells were plated per well of a 96 well plate and all experiments were carried out in triplicates. MEK inhibitors selumetinib (AZD6244) and trametinib (GSK1120212) were purchased from Selleck chemicals and kept as 10mM stock solution aliquots in DMSO. SHP2 inhibitor SHP099 was synthesized as described previously [20]. Afatinib and pan-RAF inhibitor LY3009120 were purchased from MedKoo Inc. and neratinib was purchased from Bio-Connect BV. Anti-EGFR monoclonal antibody cetuximab was obtained from the Hospital Pharmacies at The Netherlands Cancer Institute.

Protein lysate preparation and western blot analysis

Cells were lysed and western blots performed as described previously [19]. Primary antibodies against HSP90 (H-114; sc-13119), ERK1 (C16; sc-93), ERK2 (C14; sc-154), p-ERK1/2 (E-4; sc-7383) and SHP2 (SH-PTP2 C-18; sc-280) were purchased from Santa Cruz Biotechnology. Antibodies against EGFR (ab40815), p-EGFR (Y1068; ab5644) and p-SHP2 (Y542; ab62322) were obtained from Abcam. Antibodies against ERN1 (3294), p-ERK1/2 (9101), RUNX2 (12556), CBFB (12902), JUN (9165), RSK1 (8408), p-p90 RSK (Ser380; 9335), and p-RET (3221) were purchased from

Cell Signaling. Antibody against p-RSK1 (Thr359/Ser363; 04-419) was obtained from Millipore. Secondary antibodies were obtained from Bio-Rad Laboratories. Human Phospho-Receptor Tyrosine Kinase Array Kit was purchased from R&D and processed according to manufacturer's instructions. All experiments shown, except RTK array analysis, were performed independently at least three times.

Computational analysis of drug response data

Drug response and (RMA normalized) *RUNX2* expression and mutation data in colorectal cancer cell lines from the GDSC1000 panel was downloaded from www.cancerrxgene.org [21]. IC50 values of the 5 MEK inhibitors in the panel were median centered to make them comparable. T-tests were performed to assess statistical significance of difference in response between groups.

Analysis of RNA-seq data

Transcriptomic analysis was performed using the R-package limma [22]. Non or lowly expressed genes (< 1 count per million in at least 2 samples) were removed before analysis. Read counts were transformed using the voom function. Multidimensional scaling (MDS) analysis was performed with the plotMDS function. Because of the transcriptional and phenotypic similarity, the *ERN1/CBFB* and *ERN1/RUNX2* DKO lines were treated as biological replicates. Differential gene expression analysis was performed using a linear model with drug-treatment, *CBFB/RUNX2* KO status, and the interaction between drug-treatment and KO status as variables, using the standard limma functions lmFit and eBayes. Raw and processed data from the next-generation RNA sequencing of samples have been deposited to the NCBI Gene Expression Omnibus (GEO) under accession number GSE139169.

RESULTS

We recently performed a genetic screen for MEK inhibitor resistance in *ERN1* null LoVo CRC cells, which identified both *RUNX2* and *CBFB* as potential modifiers of the response to MEK inhibitors [4]. To validate these findings, we asked whether loss of *RUNX2* or *CBFB* indeed confers resistance to MEK inhibitors in these cells. We introduced gRNAs targeting the *RUNX2* or *CBFB* genes in LoVo *ERN1* KO cells. After selection, we tested the growth of *ERN1/RUNX2* double knockout (DKO) and *ERN1/CBFB* DKO cells in the presence and absence of MEK inhibitors selumetinib and trametinib (Figure 1A). As predicted by the genetic screen, LoVo *ERN1* KO cells, that are sensitive to low nanomolar amounts of MEK inhibitor, showed strong resistance to MEK inhibitor treatment when gRNAs targeting *RUNX2* or *CBFB* were introduced. We also tested the effect of *RUNX2* or *CBFB* loss in HCT-116 *ERN1* KO cells as an additional model for *ERN1*-loss induced MEK inhibitor sensitivity. However, we observed no difference in MEK inhibitor response between HCT-116 *ERN1* KO cells transduced with non-targeting (NT) control sgRNA and sgRNAs targeting *RUNX2* or *CBFB* (Figure 1A). Biochemical analyses of protein cell lysates showed pronounced levels of RUNX2 protein in LoVo cells, but much lower levels in HCT-116 (Figure 1B), which might explain why we observed no change in MEK inhibitor response upon its loss. CBFβ shows similar levels of expression in LoVo and HCT-116 (Figure 1C), but its loss also failed to rescue the MEK inhibitor sensitivity of HCT-116 *ERN1* KO cells (Figure 1A). This could be explained by the notion that CBFβ acts through RUNX2, which is poorly expressed in HCT-116 cells.

We computationally analysed *RUNX2* expression in 45 colorectal cancer cell lines from the GDSC1000 panel according to *Iorio et al* [21]. Consistent with our Western blot data (Figure 1B), we found that HCT-116 cells, unlike LoVo, are on the lower end of the *RUNX2* gene expression scale (Figure 2A). Together, these data indicate that expression of *RUNX2* in CRC is rather heterogeneous.

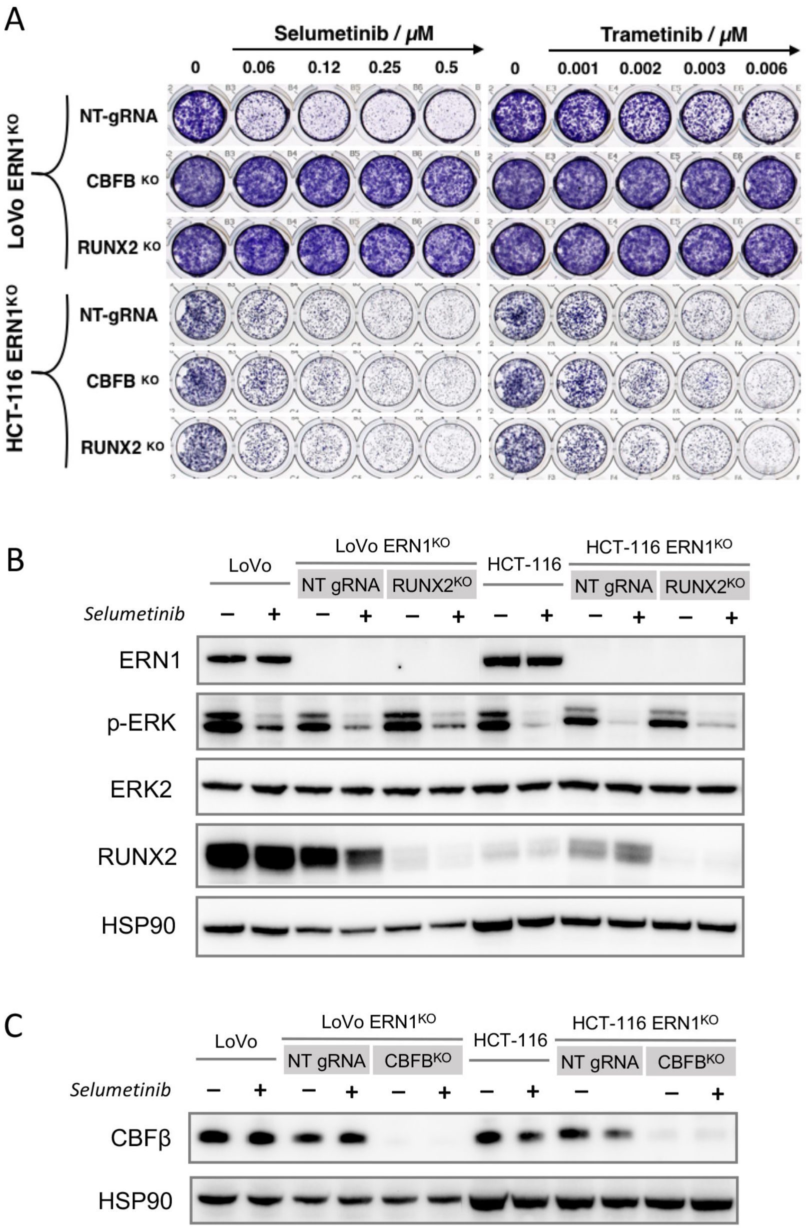

Figure 1. MEK inhibitor sensitivity of LoVo and HCT-116 *ERN1* knockout (KO) cells with loss of *RUNX2* or *CBFB*.

Figure 1.

(A) Colony formation assays comparing the growth of *CBFB* and *RUNX2* KO cells with cells expressing non-targeting (NT) gRNA in the presence of indicated concentrations of two different MEK inhibitors; selumetinib (left) and trametinib (right). After 10 days of culture, cells were fixed and stained. Image is representative of three independent experiments.

(B) Western blot analysis of LoVo and HCT-116 *ERN1/RUNX2* double KO cells compared to parental cells and cells expressing NT gRNA control. All (+) samples were treated with 1 μM of MEK inhibitor selumetinib for 24 hours before collection, and compared with vehicle treated (-) samples. Protein extracts were probed with specific antibodies against ERN1, phosphorylated ERK, ERK2, and RUNX2 (to estimate the efficiency of CRISPR editing in a polyclonal population). Specific antibody against HSP90 was used as a loading control.

(C) Western blot analysis of LoVo and HCT-116 *ERN1/CBFB* double KO cells compared to parental cells and cells expressing NT gRNA control. All (+) samples were treated with 1 μM of MEK inhibitor selumetinib for 24 hours before collection, and compared with vehicle treated (-) samples. Protein extracts were probed with specific antibodies against CBFβ (to estimate the efficiency of CRISPR editing), and HSP90 (as a loading control).

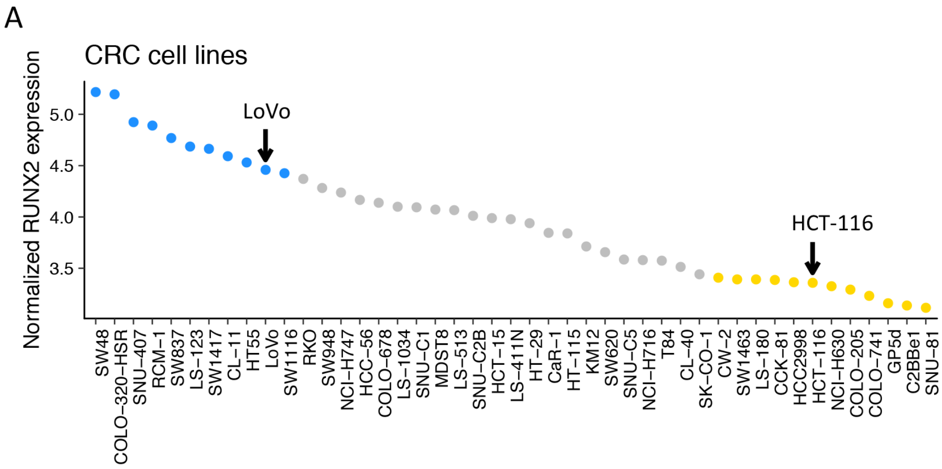

Figure 2. Analyses of *RUNX2* expression and mutation status in a CRC panel.

(A) *RUNX2* expression in colorectal cancer cell lines from the GDSC1000 panel. Blue dots represent cell lines in upper-most quantile and yellow dots lowest quantile of *RUNX2* expression.

Next, we compared the IC50 values of MEK inhibitors of the upper 25% of *RUNX2*-expressing cell lines with lower 25% (Supplemental Table 1). The data, represented in a box plot, indicate that *RUNX2* expression levels are not *per se* linked to MEK inhibitor response (Figure 2B). However, when we compared cell lines with *RUNX2* mutations to non-mutant cells, we found that *RUNX2* mutant cells have significantly higher MEK inhibitor IC50 values (Figure 2C). Considering that *RUNX2* gene does not have a hotspot mutation site, it is likely that the mutations are inactivating. These data suggest that loss of *RUNX2* leads to resistance to MEK inhibitors in CRC.

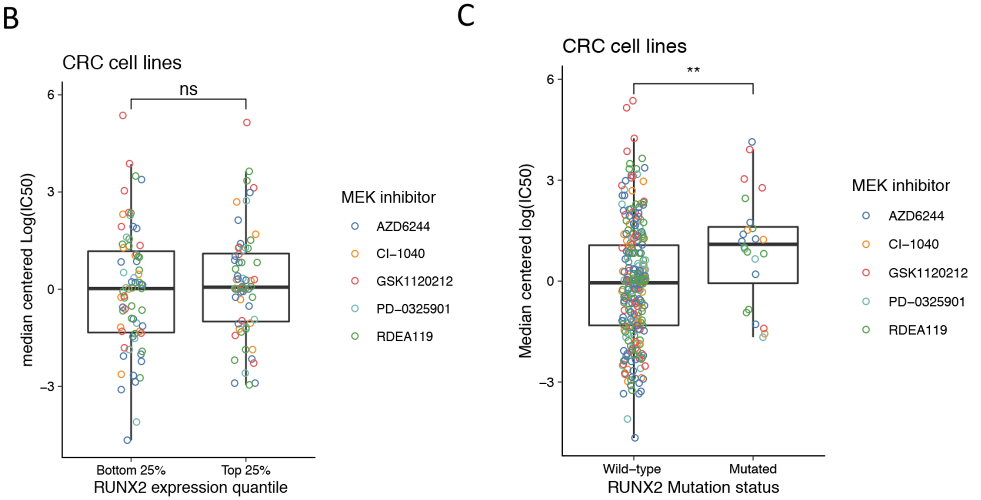

Figure 2. Analyses of *RUNX2* expression and mutation status in a CRC panel.

(B) IC50 values for five different MEK inhibitors in lowest 25% *RUNX2* expressing cells (C2BBe1, CCK-81, COLO-205, COLO-741, CW-2, GP5d, HCC-2998, HCT-116, LS-180, NCI-H630, SNU-81 and SW-1463; shown on the left) and highest 25% *RUNX2* expressing cells (CL-11, COLO-320-HSR, HT-55, LS-123, LoVo, RCM-1, SNU-407, SW-1116, SW-1417, SW-48 and SW-837; shown on the right).

(C) IC50 values for five different MEK inhibitors in four *RUNX2* mutant CRC cell lines (GP5d, HT-115, SW-620, SW-948; right) compared to non-mutant lines (41 *RUNX2* wild type CRC cell lines; left).

To test directly whether loss of *RUNX2* or *CBFB* could decrease the response of CRC cells to MEK inhibitors in the absence of *ERN1* loss, we made polyclonal populations of *RUNX2* and *CBFB* knockout cells in parental LoVo cells. As can be seen in Figure 2D, these polyclonal populations had reduced expression, but not complete loss, of RUNX2 and CBFβ. Nonetheless, this was sufficient to cause a marked increase in resistance to the MEK inhibitor selumetinib (Figure 2E). This indicates that *RUNX2* or *CBFB* can modulate MEK inhibitor responses in a broader context than just in cells having *ERN1* loss of function (Figures 2D and 2E).

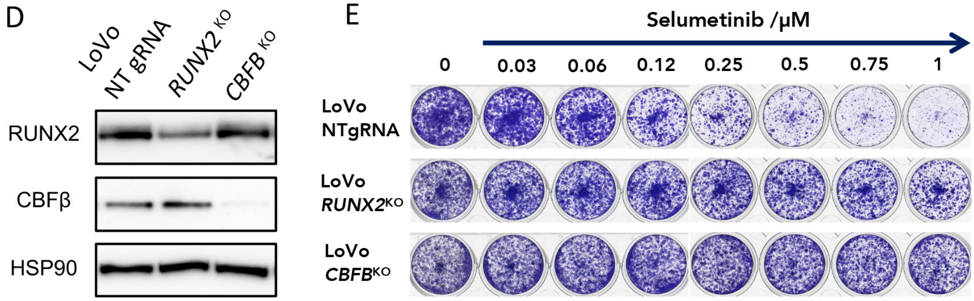

Figure 2. MEK inhibitor response of LoVo parental cells with loss of *RUNX2* or *CBFB*.
(D) Western blot of LoVo *RUNX2* KO and *CBFB* KO cells compared to NT gRNA controls.
(E) Colony formation assay of LoVo *RUNX2* KO and *CBFB* KO cells in the presence and absence of the MEK inhibitor selumetinib, relative to LoVo parental cells expressing non-targeting (NT) gRNA control. Shown is a representative example of three biological replicates.

To address the mechanism of loss-of-*RUNX2* induced MEK inhibitor resistance, we established a collection of *CBFB* and *RUNX2* KO clones in LoVo in an *ERN1* KO background (Figure 3A). For subsequent analyses, we used *CBFB* KO clone B and *RUNX2* KO clone A. We tested the growth properties of these clones in the presence of MEK inhibitor selumetinib using both a colony formation assay (Figure 3B) and an IC 50 assay (Figure 3C). These assays show that the MEK inhibitor resistance induced by the loss of *RUNX2* or *CBFB* surpasses intrinsic resistance of the parental line, as IC50 values of the parental line fall in between values for *ERN1* KO and *ERN1/RUNX2* DKO or *ERN1/CBFB* DKO cells.

To investigate possible transcriptomic changes giving rise to this drug resistance phenotype, we performed RNA sequencing of *CBFB* and *RUNX2* knockout clones (both in the presence and absence of MEK inhibitor). Analysis of RNA sequencing data revealed a strong transcriptional similarity between *CBFB* and *RUNX2* knockout clones indicating a similar resistance mechanism in both clones (Figure 3D).

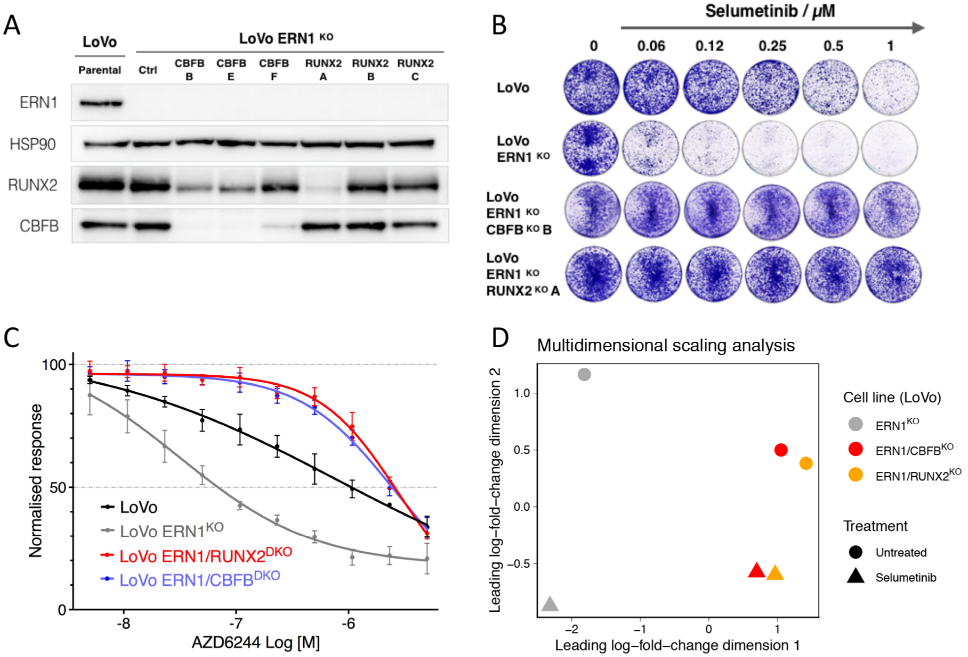

Figure 3. Characterization of LoVo *ERN1/RUNX2* and *ERN1/CBFB* double KO clones.

(A) Western blot analysis of LoVo *ERN1/RUNX2* and *ERN1/CBFB* double KO clones.

(B) Colony formation assay of ERN1/RUNX2 and ERN1/CBFB double KO cells in the presence and absence of the MEK inhibitor selumetinib, relative to control ERN1 KO cells and LoVo parental cells. Shown is a representative example of three biological replicates.

(C) IC50 growth curves of LoVo *ERN1/RUNX2* and *ERN1/CBFB* double KO cells as compared to LoVo *ERN1* KO and LoVo parental cells in the presence of indicated concentrations of AZD6244 (selumetinib). Error bars represent standard deviation of three independent experiments.

(D) Multidimensional scaling (MDS) plot of RNA sequencing data from *ERN1* KO, *ERN1/CBFB* KO and *ERN1/RUNX2* KO cells treated with 1 µM MEK inhibitor selumetinib or vehicle control.

Interestingly, *DKK-1* (Dickkopf-1), a secreted inhibitor of the WNT/β-catenin pathway, is the most significant differentially expressed gene when comparing *CBFB* and *RUNX2* knockouts with their parental counterparts (false discovery rate $<10^{-6}$), as shown by a volcano plot in Figure S1A. In both treated and untreated conditions, expression levels of *DKK-1* were significantly higher in knockout clones (Figure S1B), indicating that RUNX2 might act as a repressor of *DKK-1*.

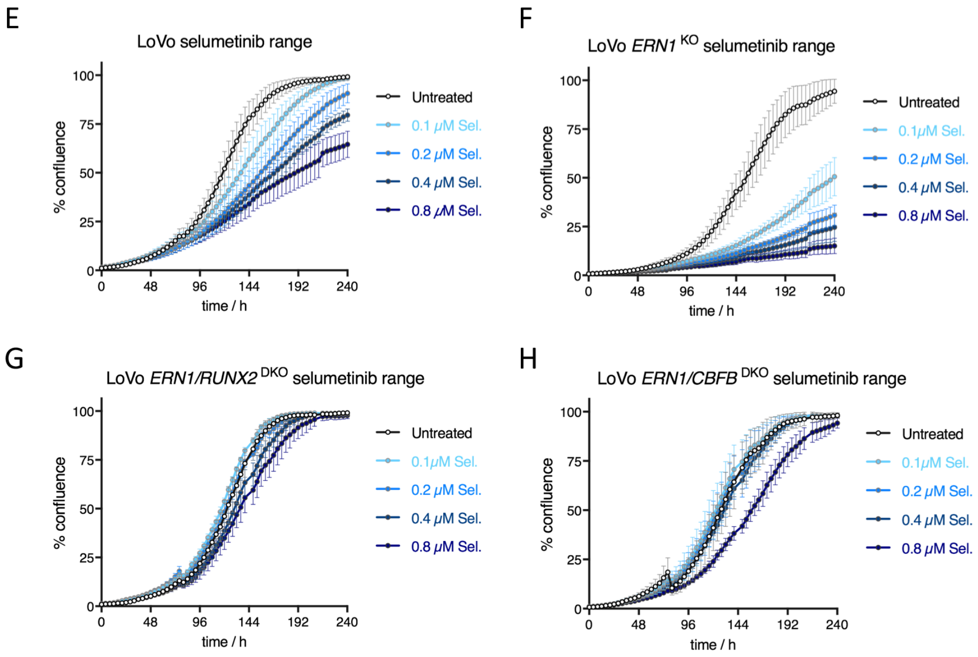

Figure 3. Characterization of LoVo *ERN1/RUNX2* and *ERN1/CBFB* double KO clones.

(E-H) Live cell proliferation assays of **(E)** LoVo parental, **(F)** LoVo *ERN1* KO, **(G)** LoVo *ERN1/RUNX2* double KO, and **(H)** LoVo *ERN1/CBFB* double KO cells in the presence and absence of indicated concentrations of MEK inhibitor AZD6244 (selumetinib).

Error bars show standard deviation of three experiments.

To further quantify the degree of MEK inhibitor resistance in *CBFB* and *RUNX2* KO cells, we performed IncuCyte® real time cell proliferation assays using a dose range of the MEK inhibitors selumetinib and trametinib. We compared the response of parental cells to *ERN1* KO cells and confirmed their increased sensitivity to a wide concentration range of the MEK inhibitors selumetinib (Figures 3E and 3F) and trametinib (Figures S2A and S2B). On the other hand, *ERN1/RUNX2* DKO cells and *ERN1/CBFB* DKO cells showed uninhibited proliferation in the presence of selumetinib (Figures 3G and 3H) or trametinib (Figures S2C and S2D) treatment.

In order to delineate the mechanism of *RUNX2*-loss induced MEK inhibitor resistance, we first analysed phosphorylation status of a panel of receptor tyrosine kinases using a Human Phospho-Receptor Tyrosine Kinase Array Kit (R&D). The results showed that *ERN1/RUNX2* DKO cells exhibit higher levels of phospho-HER3 (ERBB3) and phospho-RET compared to their parental *ERN1* KO cells, and these differences were even more pronounced under selumetinib treatment (Figure 4A).

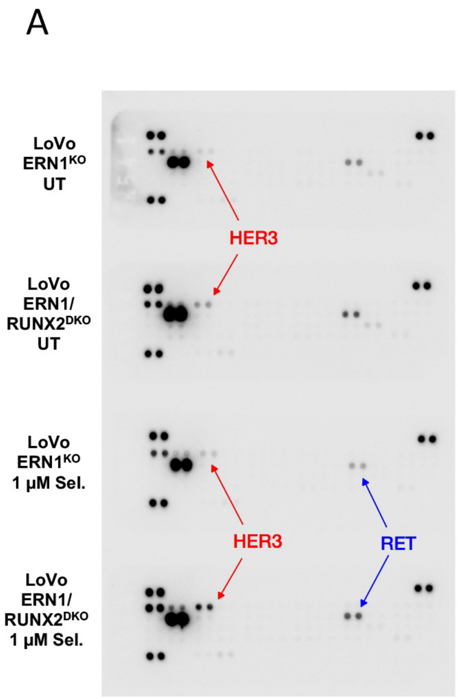

Figure 4. Loss of *RUNX2* induces multiple receptor tyrosine kinases (RTKs).

(A) LoVo *ERN1* KO and *ERN1/RUNX2* KO cells were cultured in the presence or absence (untreated = UT) of 1 µM MEK inhibitor selumetinib (1 µM Sel.).

After 24 hours, cells were collected and protein lysates were processed with Human Phospho-Receptor Tyrosine Kinase (RTK) Array Kit (R&D) according to manufacturer's instructions.

We validated these results by immunoblotting with specific antibodies in both long-term (Figure 4B) and short-term assays (Figure 4C). Interestingly, prolonged treatment of LoVo cells with MEK inhibitor (14 days) resulted in markedly reduced levels of RUNX2 protein, suggesting that low *RUNX2* expressing cells were positively selected under MEK inhibitor pressure (Figure 4B). In addition, we note that *ERN1/RUNX2* DKO cells exhibit sustained levels of phospho-ERK and phospho-RSK despite MEK inhibitor treatment, explaining their poor response to these drugs.

Interestingly, this is correlated with high phospho-EGFR as compared to parental LoVo and *ERN1* KO cells. To further confirm the intensity of RTK signalling in *RUNX2* and *CBFB* KO cells, we blotted for phospho-SHP2 (encoded by the *PTPN11* gene), which is essential in signal transduction from the receptor tyrosine kinases in the cell membrane to the RAS-MEK-ERK pathway [23]. Our results show persistent SHP2 activity in *RUNX2* and *CBFB* KO cells compared to MEK inhibitor sensitive *ERN1* KO counterparts. On the other hand, parental LoVo cells exhibit intermediate levels of phospho-SHP2 (Figure 4C).

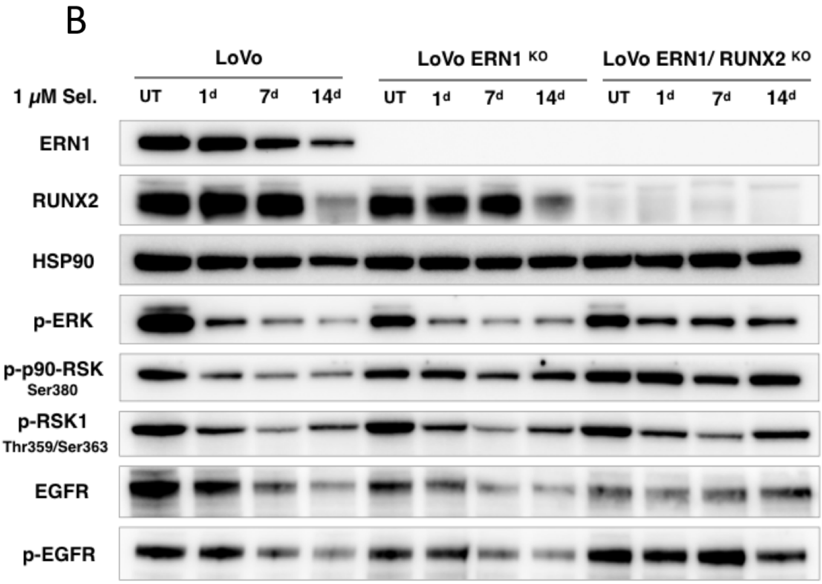

Figure 4. Loss of *RUNX2* induces multiple receptor tyrosine kinases (RTKs).

(B) Western blot showing the effects of long-term MEK inhibitor treatment on LoVo, *ERN1* KO and *ERN1/RUNX2* double KO cells. Cells were cultured in the presence and absence of 1 μM selumetinib for the indicated time (in days).

In order to find out whether SHP2 activity is causally related to MEK inhibitor resistance observed in *RUNX2* negative cells, we used SHP2 inhibitor SHP099 and combined it with MEK inhibitor selumetinib in LoVo *ERN1* KO (Figure 5A) and *ERN1/RUNX2* DKO cells (Figure 5B). As expected, LoVo *ERN1* KO cells were not growing even in relatively modest amounts of selumetinib. However, *ERN1/RUNX2* DKO cells, whose growth was uninhibited in MEK inhibitor alone, exhibited complete growth arrest when SHP2 inhibitor was combined with the MEK inhibitor (Figure 5B). Considering that we observed high activity of ERBB3/HER3 in *ERN1/RUNX2* DKO cells (Figure 4A), and that ERBB3 is a kinase impaired protein that signals through obligatory heterodimers with other members of the ERBB receptor family, we used EGFR and HER2 inhibitors to see if those could recapitulate the effects of SHP2 inhibition. Interestingly however, we could not identify a single RTK

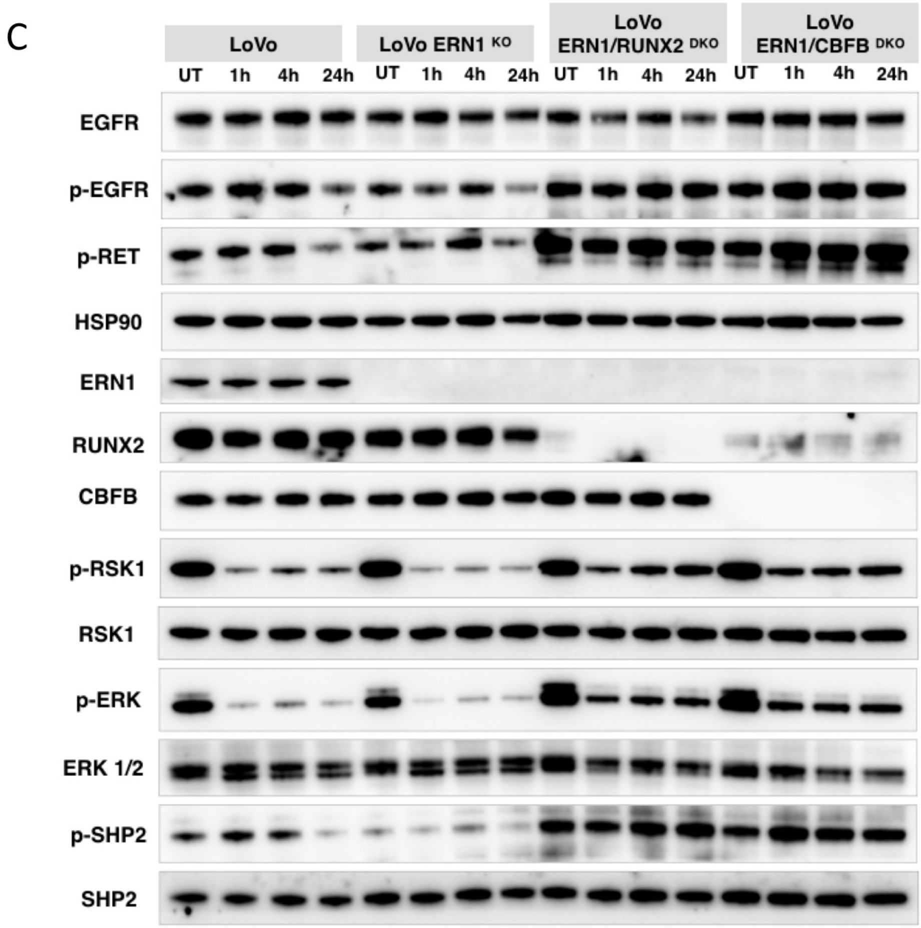
C
LoVo
LoVo ERN1 KO
LoVo ERN1/RUNX2 DKO
LoVo ERN1/CBFB DKO
UT
1h
4h
24h
EGFR
p-EGFR
p-RET
HSP90
ERN1
RUNX2
CBFB
p-RSK1
RSK1
p-ERK
ERK 1/2
p-SHP2
SHP2

Figure 4. Loss of RUN*X2* induces multiple receptor tyrosine kinases (RTKs).

(C) Western blot showing the effects of short-term treatment with MEK inhibitor on LoVo parental and LoVo ERN1 KO cells compared to LoVo ERN1/RUNX2 and ERN1/CBFB double KO cells. Cells were cultured in the presence and absence of 1 µM selumetinib for the indicated time (in hours). All experiments shown, except RTK array analysis, were performed independently at least twice.

inhibitor that could mimic the phenotype observed with SHP2 inhibition (Figures S3 A-C). Only combination of MEK inhibitor with pan-RAF inhibitor could replicate synthetic lethality observed with SHP2 and MEK inhibitor combination (Figure 5C).

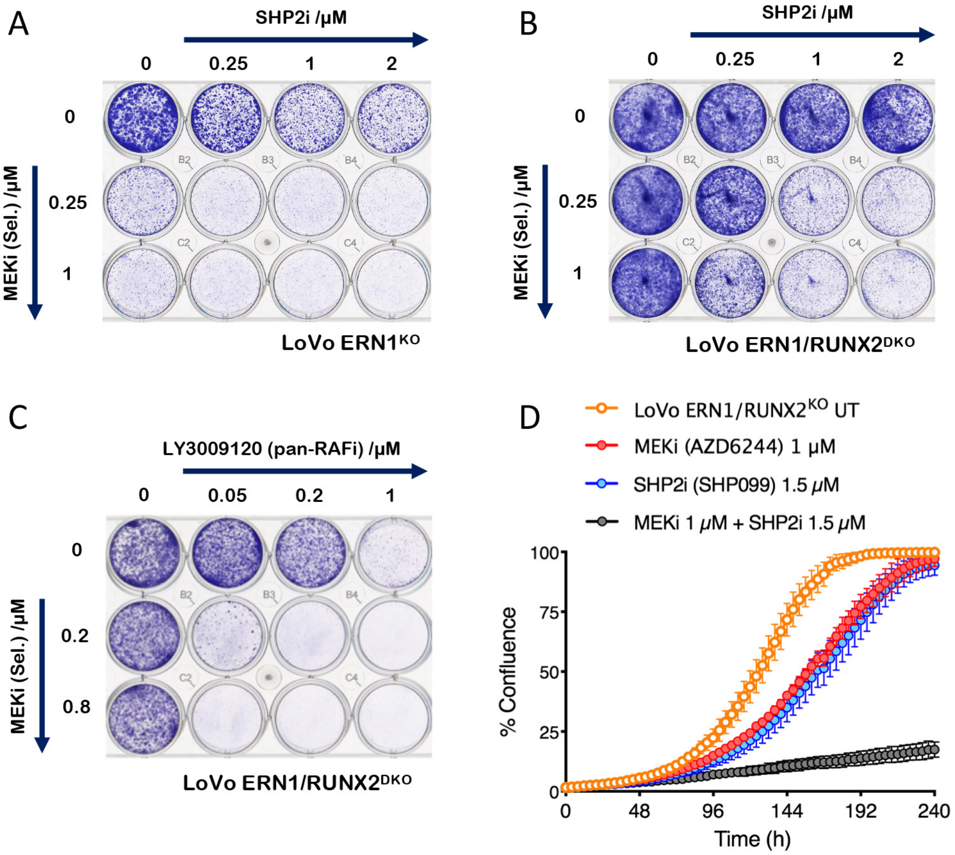

Figure 5. SHP2 is an essential driver of loss-of-RUNX2 induced MEK inhibitor sensitivity.

(A) Colony formation assay of LoVo ERN1 KO cells in the presence of indicated concentrations of the SHP2 inhibitor SHP099 and MEK inhibitor selumetinib.

(B-C) Colony formation assays of LoVo *ERN1/RUNX2* double knockout (DKO) cells in the presence and absence of the MEK inhibitor selumetinib (shown vertically) and in the indicated concentrations of **(B)** SHP2 inhibitor SHP099, and **(C)** pan-RAF inhibitor LY3009120. Shown are representative examples of three biological replicates.

(D) Live cell proliferation assay comparing the growth of LoVo *ERN1/RUNX2* double KO cells in the presence and absence of indicated concentrations of MEK inhibitor selumetinib (AZD6244), SHP2 inhibitor SHP099 and their combination (UT = untreated). Error bars show standard deviation of three experiments.

To quantify these effects in time-dependent fashion, we used IncuCyte® real time cell proliferation imaging and quantified cell confluence for LoVo *ERN1/RUNX2* DKO cells in the presence and absence of MEK inhibitor selumetinib, SHP2 inhibitor, or their combination. These data again indicated that the combination of a SHP2 and a MEK inhibitor is highly effective in the context of *RUNX2* null colorectal cancer cells (Figure 5D), highlighting the central role of RTK signalling in the resistance to MEK inhibitors of *RUNX2* KO cells.

DISCUSSION

This study reveals that RUNX2, a critical transcription factor for bone development, and its cofactor CBFβ can regulate MEK inhibitor response in colorectal cancer cells. Previous work has shown that *RUNX2* is aberrantly expressed in cancer cells as compared to normal mammary epithelial cells [24]. In cancer cells RUNX2 has thus far been shown to regulate beta-casein [25], osteopontin [26], sialoprotein [27], calcitonin, and RANKL [28]. More recently, RUNX2 was shown to be required for the growth of multiple myeloma, a malignancy driven by the accumulation and proliferation of abnormal plasma cells in the bone marrow. The suppression of *RUNX2* inhibited the progression of the disease and the expression of metastasis-promoting RUNX2 target genes *RANKL* and *DKK-1* [29]. However, the role of RUNX2 in regulating the expression or activation of receptor-tyrosine kinases or MEK inhibitor sensitivity, in the context of colorectal cancer, has thus far not been identified. In melanoma, however, *RUNX2* knockdown by short hairpin RNAs resulted in RTK downregulation [30]. The same study demonstrated that melanoma cells resistant to the BRAF V600E inhibitor PLX4720 had a significant increase in *RUNX2* expression which was associated with an increase in both RTK expression and activation. This is the opposite of the RUNX2 effect on RTK activity we find in *KRAS* mutant colorectal cancer cells. A differential response between melanoma cells and colon cancer cells in terms of their response to inhibition of the MAPK pathway has been shown before by our lab and others [31-33]. In colorectal cancer, unlike melanoma, BRAF inhibition causes rapid feedback activation through the epidermal growth factor receptor (EGFR). For this reason, BRAF inhibitor treatment is ineffective as a monotherapy in colorectal cancer and combination treatment approach is needed. A combination of BRAF inhibitor encorafenib, MEK inhibitor binimetinib and an EGFR inhibitor cetuximab recently resulted in a successfully completed phase 3 clinical trial [34], underscoring the importance of the regulation of RTK activity in colorectal cancer.

A study by Kim et al. [35] has shown that deletion of *Mek1* and *Mek2* kinases resulted in severe osteopenia and cleidocranial dysplasia, similar to that seen in humans and mice with impaired Runx2 function. In the present study, we show that RUNX2 directly controls MAPK pathway activity. We first show that loss of *RUNX2* reverts the MEK inhibitor sensitivity phenotype of LoVo *ERN1* KO cells. Moreover, lack of *RUNX2* expression increased resistance of parental LoVo cells as well, and this was also confirmed for its binding factor CBFβ. Interestingly, all *CBFB* knockout clones display reduced levels of RUNX2 protein confirming previous findings that CBFβ plays an important role in the stabilization of RUNX proteins by inhibiting ubiquitination-mediated degradation [8,9]. This could explain why whole exome sequencing efforts identified CBFB as one of six most significantly-mutated genes in breast cancer, right after *TP53*, *PIK3CA* and *AKT1* [36]. More studies are required to investigate whether *CBFB* loss of function mutations in breast cancer are also associated with increased RTK activity.

Differential gene expression analysis of RNA sequencing data point to genes whose expression pattern changes under MEK inhibitor treatment. Interestingly, transcriptional analysis of *CBFB* and *RUNX2* knockout clones (in the presence and absence of MEK inhibitor) revealed *DKK-1* (Dickkopf-1), a secreted inhibitor of the WNT/β-catenin pathway and a negative regulator of bone formation, as the most significant differentially expressed gene when comparing *CBFB* and *RUNX2* knockouts with their parental counterparts. In both treated and untreated conditions, expression levels of *DKK-1* are significantly higher in knockout clones, indicating that RUNX2 might act as a repressor of *DKK-1*. By contrast, *Gowda et al.* [29] found that reduced expression of *RUNX2* correlates with a reduction in *DKK-1* in multiple myeloma. Our results suggest context specificity of *DKK-1* regulation by RUNX2. This is potentially significant as it impacts our understanding of WNT signaling regulation in colorectal cancer. For example, *Tentler et al.*[37] have shown that *DKK-1* is among the core genes in the WNT pathway with increased expression in *KRAS* mutant CRC cells resistant to AZD6244 (selumetinib).

In this work, we demonstrate that RUNX2 functions as a repressor of RTK activity in LoVo colorectal cancer cells. We observed sustained levels of MEK/ERK signaling in *CBFB* or *RUNX2*-null cells, even in the presence of MEK inhibitor. These sustained levels of phospho-ERK (resulting in continued proliferation) coincide with high phosphorylation status of EGFR, ERBB3 and RET in RUNX2-null cells. These findings complement our previous work showing that high RTK activity confers resistance to MEK inhibitors in colon cancer cells [38]. Moreover, here we report high levels of phosho-SHP2 in MEK inhibitor treated *RUNX2*-null cells indicating persistent signaling from the cell membrane which helps to explain the observed resistance phenotype.

To validate the functional significance of SHP2 activity in *RUNX2* negative cells, we used SHP2 inhibitor in combination with MEK inhibitor. The observed synthetic lethality demonstrated that RTK activation in *RUNX2* negative cells is causal to their lack of sensitivity to MEK inhibition. The MEK and SHP2 inhibitor combination has already been demonstrated as a powerful treatment strategy to overcome RTK activity-driven MEK inhibitor resistance; in the context of pancreatic ductal adenocarcinoma [39], *KRAS*-mutant non-small-cell lung cancer [40] and in wild-type *KRAS*-amplified gastroesophageal cancer [41]. In these cancers, combination of SHP2 and MEK inhibitors was shown to synergistically inhibit signaling through the MAPK pathway.

Results presented here suggest that resistance to MEK inhibition via loss or downregulation of *RUNX2* can be circumvented by concomitant treatment with SHP2 inhibitor. This is particularly relevant when we consider that deep deletions of *CBFB* are seen in around 6% of malignant peripheral nerve sheath tumors and in 5% of metastatic prostate cancers (cbioportal.org). Moreover, mutations in *RUNX2* are seen in ~10% of small-cell lung cancer and in ~10% of desmoplastic melanomas [42]. Our data reveal an unexpected relationship between loss of function mutations in

RUNX2 and *CBFB* and activity of RTKs in colon cancer. These data may help explain why loss of function mutations in these two genes are seen in a variety of cancers.

Based on our findings and those in the literature, we propose a model for MAPK pathway regulation by RUNX2 (Figure 5E). Previous work has shown that *RUNX2* expression and activity are positively regulated by the PI3K and MAPK pathways [17,18,43]. Moreover, RUNX2 has been shown to repress RTK signalling [44]. Our present data add to this by showing that the RUNX2/CBFB complex acts as a repressor of RTK activity. Thus, inhibition of MEK has a dual effect on RTK activity. First, ERK inhibition leads to activation of RTK signalling, as previously demonstrated [35, 42]. Second, ERK inhibition, by inhibition RUNX2/CBFB activity, also leads to RTK activation (Figure 4). These two effects both counteract the effect of the MEK inhibitor, contributing to drug resistance. In summary, our data are compatible with a model in which *RUNX2* mutant tumors are resistant to MEK inhibitors, but respond to the combination of MEK and SHP2 inhibitors.

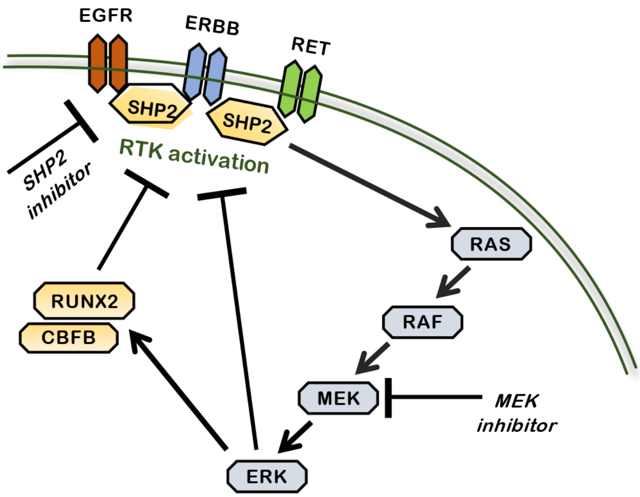

Figure 5. SHP2 is an essential driver of loss-of-RUNX2 induced MEK inhibitor sensitivity.

(E) Model showing the interplay between RTK activation, SHP2, RUNX2 and RAS/RAF/MEK/ERK signaling pathway.

REFERENCES

[1] A.A. Adjei, R.B. Cohen, W. Franklin, C. Morris, D. Wilson, J.R. Molina, et al., Phase I pharmacokinetic and pharmacodynamic study of the oral, small-molecule mitogen-activated protein kinase kinase 1/2 inhibitor AZD6244 (ARRY-142886) in patients with advanced cancers, J. Clin. Oncol. 26 (2008) 2139–2146. doi:10.1200/JCO.2007.14.4956.

[2] G. Migliardi, F. Sassi, D. Torti, F. Galimi, E.R. Zanella, M. Buscarino, et al., Inhibition of MEK and PI3K/mTOR suppresses tumor growth but does not cause tumor regression in patient-derived xenografts of RAS-mutant colorectal carcinomas, Clinical Cancer Research. 18 (2012) 2515–2525. doi:10.1158/1078-0432.CCR-11-2683.

[3] P.A. Jänne, A.T. Shaw, J.R. Pereira, G. Jeannin, J. Vansteenkiste, C. Barrios, et al., Selumetinib plus docetaxel for KRAS-mutant advanced non-small-cell lung cancer: a randomised, multicentre, placebo-controlled, phase 2 study, Lancet Oncol. 14 (2013) 38–47. doi:10.1016/S1470-2045(12)70489-8.

[4] T. Sustic, S. van Wageningen, E. Bosdriesz, R.J.D. Reid, J. Dittmar, C. Lieftink, et al., A role for the unfolded protein response stress sensor ERN1 in regulating the response to MEK inhibitors in KRAS mutant colon cancers, Genome Med. 10 (2018) 90. doi:10.1186/s13073-018-0600-z.

[5] M.M. Cohen, Perspectives on RUNX genes: an update, Am. J. Med. Genet. A. 149A (2009) 2629–2646. doi:10.1002/ajmg.a.33021.

[6] D. Mendoza-Villanueva, W. Deng, C. Lopez-Camacho, P. Shore, The Runx transcriptional co-activator, CBFβ, is essential for invasion of breast cancer cells, Mol Cancer. 9 (2010) 171–11. doi:10.1186/1476-4598-9-171.

[7] M. Kundu, A. Javed, J.-P. Jeon, A. Horner, L. Shum, M. Eckhaus, et al., Cbfβ interacts with Runx2 and has a critical role in bone development, Nature Genetics. 32 (2002) 639–644. doi:10.1038/ng1050.

[8] K.-E. Lim, N.-R. Park, X. Che, M.-S. Han, J.-H. Jeong, S.-Y. Kim, et al., Core binding factor β of osteoblasts maintains cortical bone mass via stabilization of Runx2 in mice, J. Bone Miner. Res. 30 (2015) 715–722. doi:10.1002/jbmr.2397.

[9] X. Qin, Q. Jiang, Y. Matsuo, T. Kawane, H. Komori, T. Moriishi, et al., Cbfb regulates bone development by stabilizing Runx family proteins, J. Bone Miner. Res. 30 (2015) 706–714. doi:10.1002/jbmr.2379.

[10] T. Komori, Requisite roles of Runx2 and Cbfb in skeletal development, J. Bone Miner. Res. 21 (2003) 193–197.

[11] G.S. Stein, J.B. Lian, A.J. van Wijnen, J.L. Stein, M. Montecino, A. Javed, et al., Runx2 control of organization, assembly and activity of the regulatory machinery for skeletal gene expression, Oncogene. 23 (2004) 4315–4329. doi:10.1038/sj.onc.1207676.

[12] S. Mundlos, F. Otto, C. Mundlos, J.B. Mulliken, A.S. Aylsworth, S. Albright, et al., Mutations involving the transcription factor CBFA1 cause cleidocranial dysplasia, Cell. 89 (1997) 773–779.

[13] T. Komori, H. Yagi, S. Nomura, A. Yamaguchi, K. Sasaki, K. Deguchi, et al., Targeted disruption of Cbfa1 results in a complete lack of bone formation owing to maturational arrest of osteoblasts, Cell. 89 (1997) 755–764.

[14] F. Otto, A.P. Thornell, T. Crompton, A. Denzel, K.C. Gilmour, I.R. Rosewell, et al., Cbfa1, a candidate gene for cleidocranial dysplasia syndrome, is essential for osteoblast differentiation and bone development, Cell. 89 (1997) 765–771.

[15] L. Sun, M. Vitolo, A. Passaniti, Runt-related gene 2 in endothelial cells: inducible expression and specific regulation of cell migration and invasion, Cancer Research. 61 (2001) 4994–5001.

[16] E. Zelzer, D.J. Glotzer, C. Hartmann, D. Thomas, N. Fukai, S. Soker, et al., Tissue specific regulation of VEGF expression during bone development requires Cbfa1/Runx2, Mech. Dev. 106 (2001) 97–106.

[17] G. Xiao, D. Jiang, P. Thomas, M.D. Benson, K. Guan, G. Karsenty, et al., MAPK pathways activate and phosphorylate the osteoblast-specific transcription factor, Cbfa1, Journal of Biological Chemistry. 275 (2000) 4453–4459. doi:10.1074/jbc.275.6.4453.

[18] C. Ge, G. Xiao, D. Jiang, Q. Yang, N.E. Hatch, H. Roca, et al., Identification and functional characterization of ERK/MAPK phosphorylation sites in the Runx2 transcription factor, J. Biol. Chem. 284 (2009) 32533–32543. doi:10.1074/jbc.M109.040980.

[19] D. Brunen, R.C. de Vries, C. Lieftink, R.L. Beijersbergen, R. Bernards, PIM Kinases Are a Potential Prognostic Biomarker and Therapeutic Target in Neuroblastoma, Mol. Cancer Ther. 17 (2018) 849–857. doi:10.1158/1535-7163.MCT-17-0868.

[20] J. Garcia Fortanet, C.H.-T. Chen, Y.-N.P. Chen, Z. Chen, Z. Deng, B. Firestone, et al., Allosteric Inhibition of SHP2: Identification of a Potent, Selective, and Orally Efficacious Phosphatase Inhibitor, J. Med. Chem. 59 (2016) 7773–7782. doi:10.1021/acs.jmedchem.6b00680.

[21] F. Iorio, T.A. Knijnenburg, D.J. Vis, G.R. Bignell, M.P. Menden, M. Schubert, et al., A Landscape of Pharmacogenomic Interactions in Cancer, Cell. 166 (2016) 740–754. doi:10.1016/j.cell.2016.06.017.

[22] M.E. Ritchie, B. Phipson, D. Wu, Y. Hu, C.W. Law, W. Shi, et al., limma powers differential expression analyses for RNA-sequencing and microarray studies, Nucleic Acids Res. 43 (2015) e47–e47. doi:10.1093/nar/gkv007.

[23] A. Prahallad, G.J.J.E. Heynen, G. Germano, S.M. Willems, B. Evers, L. Vecchione, et al., PTPN11 Is a Central Node in Intrinsic and Acquired Resistance to Targeted Cancer Drugs, CellReports. 12 (2015) 1978–1985. doi:10.1016/j.celrep.2015.08.037.

[24] M. Tandon, Z. Chen, J. Pratap, Runx2 activates PI3K/Akt signaling via mTORC2 regulation in invasive breast cancer cells, Breast Cancer Res. 16 (2014) R16. doi:10.1186/bcr3611.

[25] C.K. Inman, N. Li, P. Shore, Oct-1 counteracts autoinhibition of Runx2 DNA binding to form a novel Runx2/Oct-1 complex on the promoter of the mammary gland-specific gene beta-casein, Molecular and Cellular Biology. 25 (2005) 3182–3193. doi:10.1128/MCB.25.8.3182-3193.2005.

[26] C.K. Inman, P. Shore, The osteoblast transcription factor Runx2 is expressed in mammary epithelial cells and mediates osteopontin expression, Journal of Biological Chemistry. 278 (2003) 48684–48689. doi:10.1074/jbc.M308001200.

[27] G.L. Barnes, A. Javed, S.M. Waller, M.H. Kamal, K.E. Hebert, M.Q. Hassan, et al., Osteoblast-related transcription factors Runx2 (Cbfa1/AML3) and MSX2 mediate the expression of bone sialoprotein in human metastatic breast cancer cells, Cancer Research. 63 (2003) 2631–2637.

[28] T.J. Martin, M.T. Gillespie, Receptor activator of nuclear factor kappa B ligand (RANKL): another link between breast and bone, Trends Endocrinol. Metab. 12 (2001) 2–4.

[29] P.S. Gowda, B.J. Wildman, T.N. Trotter, X. Xu, X. Hao, M.Q. Hassan, et al., Runx2 Suppression by miR-342 and miR-363 Inhibits Multiple Myeloma Progression, Molecular Cancer Research. 16 (2018) 1138–1148. doi:10.1158/1541-7786.MCR-17-0606.

[30] R.K. Boregowda, D.J. Medina, E. Markert, M.A. Bryan, W. Chen, S. Chen, et al., The transcription factor RUNX2 regulates receptor tyrosine kinase expression in melanoma, Oncotarget. 7 (2016) 29689–29707. doi:10.18632/oncotarget.8822.

[31] A. Prahallad, C. Sun, S. Huang, F. Di Nicolantonio, R. Salazar, D. Zecchin, et al., Unresponsiveness of colon cancer to BRAF(V600E)inhibition through feedback activation of EGFR, Nature. 482 (2013) 100–103. doi:10.1038/nature10868.

[32] M. Mao, F. Tian, J.M. Mariadason, C.C. Tsao, R. Lemos, F. Dayyani, et al., Resistance to BRAF inhibition in BRAF-mutant colon cancer can be overcome with PI3K inhibition or demethylating agents, Clinical Cancer Research. 19 (2013) 657–667. doi:10.1158/1078-0432.CCR-11-1446.

[33] R.B. Corcoran, C.E. Atreya, G.S. Falchook, E.L. Kwak, D.P. Ryan, J.C. Bendell, et al., Combined BRAF and MEK Inhibition With Dabrafenib and Trametinib in BRAF V600-Mutant Colorectal Cancer, J. Clin. Oncol. 33 (2015) 4023–4031. doi:10.1200/JCO.2015.63.2471.

[34] S. Kopetz, A. Grothey, R. Yaeger, E. Van Cutsem, J. Desai, T. Yoshino, et al., Encorafenib, Binimetinib, and Cetuximab in BRAFV600E–Mutated Colorectal Cancer, N Engl J Med. (2019) NEJMoa1908075–12. doi:10.1056/NEJMoa1908075.

[35] J.-M. Kim, Y.-S. Yang, K.H. Park, H. Oh, M.B. Greenblatt, J.-H. Shim, The ERK MAPK Pathway Is Essential for Skeletal Development and Homeostasis, Int J Mol Sci. 20 (2019) 1803. doi:10.3390/ijms20081803.

[36] S. Banerji, K. Cibulskis, C. Rangel-Escareno, K.K. Brown, S.L. Carter, A.M. Frederick, et al., Sequence analysis of mutations and translocations across breast cancer subtypes, Nature. 486 (2012) 405–409. doi:10.1038/nature11154.

[37] J.J. Tentler, S. Nallapareddy, A.C. Tan, A. Spreafico, T.M. Pitts, M.P. Morelli, et al., Identification of predictive markers of response to the MEK1/2 inhibitor selumetinib (AZD6244) in K-ras-mutated colorectal cancer, Mol. Cancer Ther. 9 (2010) 3351–3362. doi:10.1158/1535-7163.MCT-10-0376.

[38] C. Sun, S. Hobor, A. Bertotti, D. Zecchin, S. Huang, F. Galimi, et al., Intrinsic Resistance to MEK Inhibitionin KRAS Mutant Lung and Colon Cancer through Transcriptional Induction of ERBB3, CellReports. 7 (2014) 86–93. doi:10.1016/j.celrep.2014.02.045.

[39] D.A. Ruess, G.J. Heynen, K.J. Ciecielski, J. Ai, A. Berninger, D. Kabacaoglu, et al., Mutant KRAS-driven cancers depend on PTPN11/SHP2 phosphatase, Nat. Med. 24 (2018) 954–960. doi:10.1038/s41591-018-0024-8.

[40] S. Mainardi, A. Mulero-Sánchez, A. Prahallad, G. Germano, A. Bosma, P. Krimpenfort, et al., SHP2 is required for growth of KRAS-mutant non-small-cell lung cancer in vivo, Nat. Med. 24 (2018) 961–967. doi:10.1038/s41591-018-0023-9.

[41] G.S. Wong, J. Zhou, J.B. Liu, Z. Wu, X. Xu, T. Li, et al., Targeting wild-type KRAS-amplified gastroesophageal cancer through combined MEK and SHP2 inhibition, Nat. Med. 24 (2018) 968–977. doi:10.1038/s41591-018-0022-x.

[42] A.H. Shain, M. Garrido, T. Botton, E. Talevich, I. Yeh, J.Z. Sanborn, et al., Exome sequencing of desmoplastic melanoma identifies recurrent NFKBIE promoter mutations and diverse activating mutations in the MAPK pathway, Nature Genetics. 47 (2015) 1194–1199. doi:10.1038/ng.3382.

[43] K.A. Cohen-Solal, R.K. Boregowda, A. Lasfar, RUNX2 and the PI3K/AKT axis reciprocal activation as a driving force for tumor progression, Mol Cancer. (2015) 1–10. doi:10.1186/s12943-015-0404-3.

[44] M. Tandon, Z. Chen, J. Pratap, Role of Runx2 in crosstalk between Mek/Erk and PI3K/Akt signaling in MCF-10A cells, J. Cell. Biochem. 115 (2014) 2208–2217. doi:10.1002/jcb.24939.

ACKNOWLEDGEMENTS

We thank Cor Lieftink for quality control analysis of the RNA sequencing data and all members of the Bernards, Beijersbergen, van der Heijden and Wessels groups; in particular Sander Palit and Roderick Beijersbergen for helpful support and discussions. This work was supported by a grant from the Dutch Cancer Society through the Oncode Institute.

CONFLICT OF INTEREST

The authors declare no conflict of interest.

CRediT AUTHOR STATEMENT

Tonći Šuštić: Conceptualization, Investigation, Methodology, Validation, Writing – original draft preparation. Evert Bosdriesz: Formal Analysis, Software, Validation, Data curation, Visualization. Sake van Wageningen: Methodology, Validation. Lodewyk F.A. Wessels: Supervision, René Bernards: Conceptualization, Writing – Reviewing and Editing, Supervision, Funding Acquisition.

SUPPLEMENTARY FIGURES

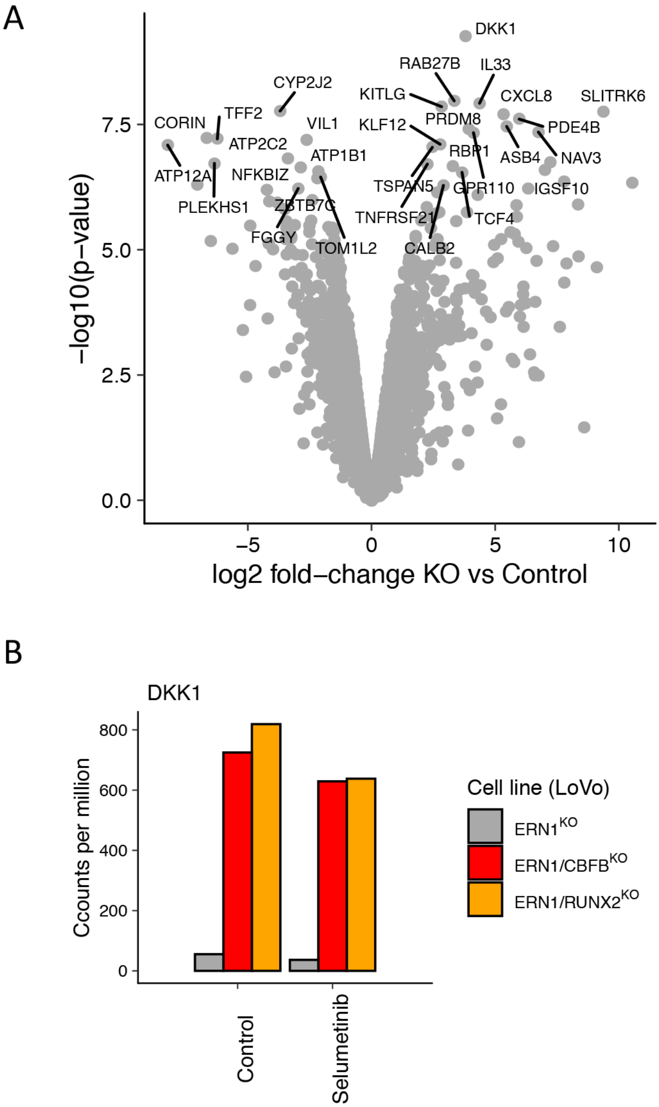

Supplemental Figure 1. Gene expression of ERN1/RUNX2 and ERN1/CBFB KO cells treated with selumetinib.

(A) Volcano plot comparing E*RN1/RUNX2* or *ERN1/CBFB* KO with *ERN1* KO cells.

(B) Expression of *DKK-1* in *RUNX2* and *CBFB* KO clones (orange and red, respectively) compared with *ERN1* KO clone (gray).

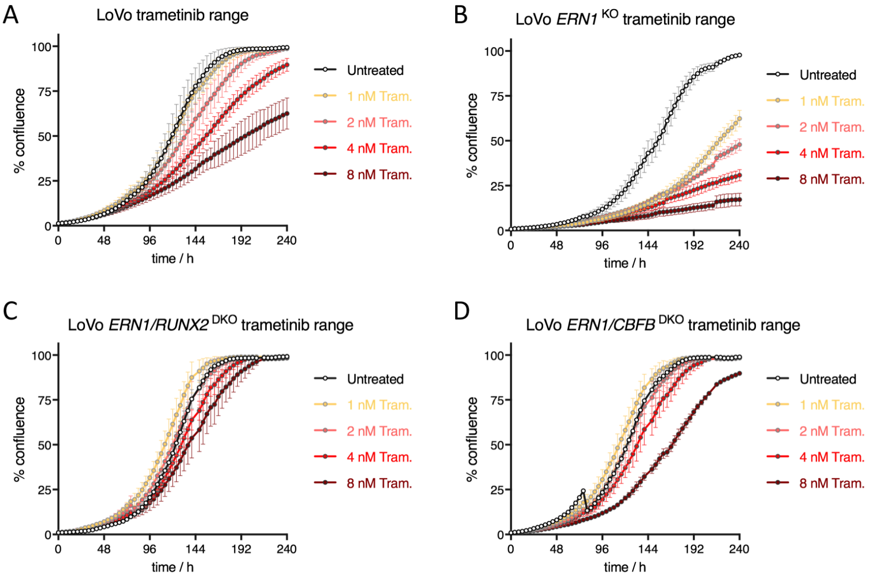

Supplemental Figure 2. (A-D) Live cell proliferation assays of **(A)** LoVo parental, **(B)** LoVo *ERN1* KO, **(C)** LoVo *ERN1/RUNX2* double KO, and **(D)** LoVo *ERN1/CBFB* double KO cells in the presence and absence of indicated concentrations of MEK inhibitor trametinib. Error bars show standard deviation of three experiments.

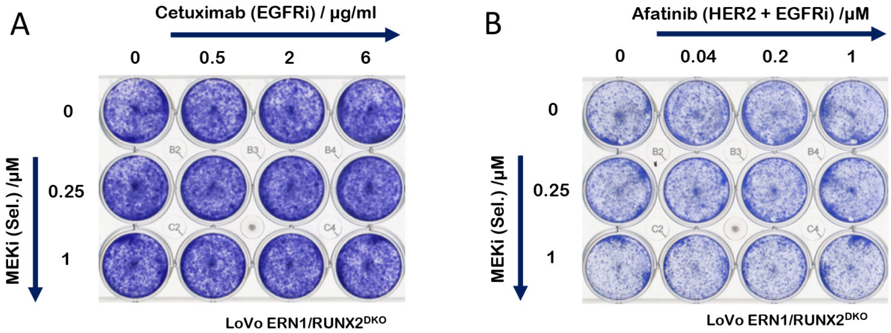
A
Cetuximab (EGFRi) / µg/ml
0
0.5
2
6
MEKi (Sel.) /µM
0
0.25
1
LoVo ERN1/RUNX2DKO
B
Afatinib (HER2 + EGFRi) /µM
0
0.04
0.2
1
MEKi (Sel.) /µM
0
0.25
1
LoVo ERN1/RUNX2DKO

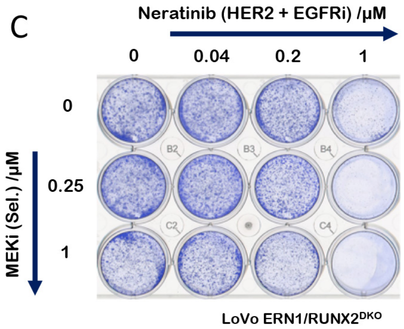
C
Neratinib (HER2 + EGFRi) /µM
0
0.04
0.2
1
MEKi (Sel.) /µM
0
0.25
1
LoVo ERN1/RUNX2DKO

Supplemental Figure 3. Colony formation assays of LoVo *ERN1/RUNX2* double KO cells in the presence and absence of the MEK inhibitor selumetinib (shown vertically) and in the indicated concentrations of **(A)** EGFR inhibitor cetuximab, **(B)** afatinib and **(C)** neratinib. Shown are representative examples of three biological replicates.

SUPPLEMENTARY TABLE

Supplemental Table 1. A panel of colorectal cancer cell lines divided in quantiles with respect to *RUNX2* expression.

Cell line	*RUNX2* expression	Quantile
SNU-81	3,11569	1
C2BBe1	3,13466	1
GP5d	3,15577	1
COLO-741	3,22882	1
COLO-205	3,29088	1
NCI-H630	3,32234	1
HCT-116	3,35529	1
HCC2998	3,36015	1
CCK-81	3,38233	1
LS-180	3,38852	1
SW1463	3,39257	1
CW-2	3,40487	1
SK-CO-1	3,44219	2
CL-40	3,51146	2
T84	3,57002	2
NCI-H716	3,57767	2
SNU-C5	3,58600	2
SW620	3,65693	2
KM12	3,71203	2
HT-115	3,83962	2
CaR-1	3,84102	2
HT-29	3,93743	2
LS-411N	3,97634	2
HCT-15	3,98812	3
SNU-C2B	4,00756	3
LS-513	4,06738	3
MDST8	4,07168	3
SNU-C1	4,09417	3
LS-1034	4,09972	3
COLO-678	4,13520	3
HCC-56	4,16193	3
NCI-H747	4,23788	3
SW948	4,28065	3
RKO	4,36646	3
SW1116	4,42349	4
LoVo	4,45570	4
HT55	4,52987	4
CL-11	4,59071	4
SW1417	4,66423	4
LS-123	4,68570	4
SW837	4,76686	4
RCM-1	4,88769	4
SNU-407	4,92105	4
COLO-320-HSR	5,19569	4
SW48	5,21461	4

Chapter 5

General discussion

Current clinical development status of the PI3K and FGFR inhibitors

Growth factor signaling is mediated through a series of intracellular kinases, and one of the most studied are phosphatidylinositol 3-kinases (PI3Ks). Aberrant activation of PI3K signaling represents a molecular signature underlying the development of metabolic diseases (such as diabetes and obesity), tumor predisposition syndromes (e.g. tuberous sclerosis complex), and somatic human cancers. This observation, together with the actionable nature of the PI3K/AKT/mTOR signaling network, resulted in expectations that PI3K inhibitors would lead to major clinical advances. With the exception of a handful of encouraging examples, which will be mentioned below, we now know that most clinical trials performed with PI3K inhibitors have fallen short of this expectation. These inhibitors were designed to target various isoforms of catalytic subunits of the PI3K called p110. Catalytic isoforms p110-α and p110-β are ubiquitously expressed, whereas the p110-δ subunit is found primarily in leukocytes (Chantry et al., 1997; Vanhaesebroeck et al., 1997). Interestingly, only p110-α, encoded by the *PIK3CA* gene, has been found to be frequently mutated in human tumors (Bachman et al., 2004), suggesting distinct roles for the individual PI3Ks in both normal signaling and oncogenic transformation. In 2006, Zhao and colleagues (Zhao et al., 2006) reported that cells deficient in the p110-α isoform are resistant to oncogenic transformation induced by a variety of oncogenic receptor tyrosine kinases (RTKs). This focused drug development efforts around the p110-α isoform specifically, although most currently available PI3K inhibitors target all isoforms with varied degrees of selectivity.

In Chapter 2 of this thesis we used BKM120 (buparlisib) as an orally available pan-class I, reversible inhibitor of PI3K. Besides potent antiproliferative effect in human cancer cell lines, buparlisib exhibits good oral bioavailability and significant antitumor activity in human tumor xenograft models at tolerated doses (Maira et al., 2012). In addition, BKM120 inhibits all four class I PI3K isoforms in biochemical assays with at least 50-fold selectivity against other protein kinases (Maira et al., 2012). This is why we used this inhibitor in our xenograft cohort (L. Wang et al., 2017). Moreover, the maximum tolerated dose (MTD) of BKM120 was already established at 100 mg daily in a phase I dose-escalation study in patients with advanced solid tumors (Bendell et al., 2012). This MTD was later confirmed in a follow-up study with the dose-escalation and dose-expansion arms (Rodon et al., 2014). However, treatment-related adverse events (AEs) in both the studies included decreased appetite, diarrhea, nausea, hyperglycemia, rash, mood alteration and even abnormal hepatic function.

Subsequent clinical trials investigated the effects of the combination of buparlisib with the chemotherapeutic agents carboplatin and paclitaxel. A phase Ib clinical trial showed that this combination is well tolerated in patients with solid tumors and recorded objective response in 5 out of 25 patients (Hyman et al., 2015). However, subsequent dose expansion study concluded that the addition of buparlisib to high dose carboplatin and paclitaxel was not tolerable (Smyth et al., 2017). Combinations of buparlisib with other targeted agents were also tested in clinical studies. For example, the combination of buparlisib with the MEK inhibitor trametinib displayed promising antitumor activity in patients with *KRAS*-mutant ovarian cancer, but only modest activity in patients with non-small cell lung cancer and pancreatic cancer (Bedard et al., 2015). The same study found that long-term tolerability of the combination at recommended phase II dose (buparlisib 60 mg + trametinib 1.5 mg daily) was challenging due to toxicity that required frequent dose interruptions. Similar results were seen in a study that investigated the combination of buparlisib with the PARP inhibitor olaparib. A phase I dose escalation study reported anticancer activity in patients with breast and high-grade serous ovarian cancer, but warned that the combination required attenuation of the BKM120 dose due to toxicity (Matulonis et al., 2017). Major toxicity was also found in a phase II study that concluded that buparlisib was associated with a poor safety profile and minimal antitumor activity in advanced or recurrent endometrial carcinoma. That clinical trial was stopped before end of recruitment for toxicity (Heudel et al., 2017). The results of these clinical trials on BKM120 were made public only after our study, reported here in Chapter 2, was already accepted for publication (L. Wang et al., 2017).

Clinical trials combining buparlisib with endocrine therapies in postmenopausal women with endocrine-resistant, hormone receptor-positive, HER2-negative advanced breast cancer have reached phase 3. BELLE-2, a phase 3, randomized and placebo-controlled trial, concluded that combination regimen of buparlisib with fulvestrant resulted in meaningful clinical benefits in patients with *PIK3CA* mutations found in circulating tumor DNA (Baselga et al., 2017), but no further studies were recommended because of the toxicity associated with that combination. A related study, BELLE-3, aimed at assessing the efficacy of buparlisib or placebo in combination with fulvestrant in hormone receptor-positive, HER2-negative, advanced breast cancer patients who had relapsed on or after endocrine therapy and mTOR inhibitors, similarly concluded that the safety profile of buparlisib plus fulvestrant does not support the further development of that combination in the investigated setting (Di Leo et al., 2018). However, the documented efficacy of buparlisib supported the rationale for the use of PI3K inhibitors with endocrine therapy in patients with *PIK3CA* mutations. An emerging hope for a more favorable toxicity profile is given by the development of a so-called β-sparing PI3K inhibitor taselisib (GDC-0032), that potently inhibits p110-α, p110-γ and p110-δ, but has a 30-fold lower potency against p110-β (Ndubaku et al., 2013). Phase 1b POSEIDON trial confirmed the antitumor activity of taselisib in both PIK3CA mutant and wild-type cancers, while concluding that it can be safely combined with tamoxifen in patients with ER-positive, metastatic breast cancer who had failed prior endocrine therapy (Baird et al., 2019).

As it is becoming increasingly clear that PI3K inhibitors are effective in inhibiting tumor progression, many other PI3K pathway-targeted agents have been tested in oncology trials (reviewed by (Yang et al., 2019)), but only three of them have thus far been approved by regulatory agencies (idelalisib, duvelisib and copanlisib). Idelalisib (CAL-101), δ isoform specific PI3K inhibitor, was the first PI3K inhibitor approved by regulatory agencies for treatment of specific blood cancers (Gopal et al., 2014; Markham, 2014; Smith et al., 2017). Duvelisib (IPI-145), like idelalisib, is also an orally available inhibitor, but with dual activity against PI3K-δ and PI3K-γ isoforms that performed exceptionally well in preclinical studies in primary chronic lymphocytic leukemia cells (Dong et al., 2014). In a phase II study performed on patients with relapsed or refractory indolent non-Hodgkin lymphoma, duvelisib demonstrated clinically meaningful activity and a manageable safety profile (Flinn et al., 2019). Phase 3 randomized DUO trial for patients with relapsed or refractory chronic lymphocytic leukemia and small lymphocytic lymphoma met primary study end point by significantly improving progression-free survival in duvelisib treated patients compared to ofatumumab monotherapy (Flinn et al., 2018). This led to the approval of duvelisib by the United States Food and Drug Administration (FDA) in September 2018. Copanlisib (BAY 80-6946) is a highly selective and reversible pan-class I PI3K inhibitor with dominant activity against p110-α and p110-δ isoforms (Liu et al., 2013). Already phase I study of copanlisib monotherapy showed promising anti-tumor activity in patients with advanced solid tumors and non-Hodgkin's lymphomas (Patnaik et al., 2016). Phase II studies that followed (Dreyling et al., 2017a; 2017b) led to accelerated approval of copanlisib for relapsed follicular lymphoma (Markham, 2017). Phase 3 trials are still ongoing.

Varied degrees of toxicity observed in different clinical trials using different PI3K inhibitors are likely due to the fact that PI3K catalytic and regulatory subunits have roles in normal cell function such as the regulation of cellular metabolism and also in immune system functions (Fruman et al., 2017). Dose-limiting toxicities prevent sufficient target engagement in tumor tissues to maintain pathway suppression. Moreover, intrinsic or acquired resistance to PI3K pathway inhibitors is commonly associated with activation of growth factor receptors that stimulate both PI3K and MAPK signaling. In addition, PI3K pathway itself is activated by various cell surface receptors, and cancer cells show remarkable plasticity when it comes to amplifying upstream mechanisms to maintain signal flow in the presence of pharmacological inhibitors. In Chapter 2 we demonstrated the efficacy of PI3K inhibitors to overcome incomplete responses observed with FGFR inhibitors in *FGFR*-driven solid cancers (L. Wang et al., 2017), but the reverse is true as well. Hyperactivation of the FGFR signaling in the form of *FGFR* mutations or amplifications can be seen as an intrinsic mechanism of resistance to PI3K inhibitors. In line with that, Herrera-Abreu and coworkers (Herrera-Abreu et al., 2013) have observed the downregulation of phospho-AKT (which can be seen as an effector of the PI3K activity) in the presence of the FGFR inhibitor PD173074, showing how closely intertwined the two pathways are in *FGFR*-driven bladder cancer cells.

In Chapter 2 we propose direct pharmacological inhibition of the PI3K pathway in conjunction with the FGFR inhibitors for *FGFR*-driven bladder and lung cancers, which is important considering that PI3K inhibition on its own is frequently followed by the induction of adaptive (non-genetic) resistance mechanisms (Thorpe et al., 2015). Previous studies have shown that increased transcription of genes encoding diverse receptor tyrosine kinases (RTKs), most notably HER3, EGFR, and INSR/IGFR1 is a frequent mechanism cancer cells resort to in response to PI3K pathway inhibitors (Chakrabarty et al., 2012; Chandarlapaty et al., 2011; Muranen et al., 2012). Those studies all suggest that PI3K antagonists will inhibit AKT and thus relieve suppression of RTK expression and their activity. As a consequence, PI3K pathway inhibitors have limited clinical activity if used as single agents. For this reason, several studies have been designed to investigate combinations of PI3K pathway inhibitors with RTK inhibitors. Garcia-Garcia and coworkers tested the hypothesis that the suppression of the PI3K/AKT/mTOR pathway results in sensitization to anti-HER2 agents in HER2-positive breast cancer that is refractory to anti-HER2 therapy (García-García et al., 2012). They found that mTOR inhibitor INK-128 induces phosphorylation of both HER2 and HER3, and this is prevented with the addition of lapatinib, a small molecule inhibitor of the HER2 intracellular kinase domain. Moreover, the dual blockade produced synergistic induction of cell death in HER2-positive cell lines *in vitro* and in patient-derived xenograft models, without signs of toxicity. In another study, Garrett *et al* examined the effects of LJM716, a HER3 neutralizing antibody that inhibits HER3 dimerization, as a single agent and in combination with BYL719, an ATP competitive PI3K catalytic subunit p110-α-specific inhibitor. They found that dual blockade of HER3 and PI3K is an effective treatment approach against HER2-overexpressing breast and gastric cancers (Garrett et al., 2013). Collectively, these studies indicate that one of the greatest challenges in the clinical practice is to predict and target the specific RTKs conferring PI3K inhibitor resistance in individual patients. Our work presented in Chapter 2 contributes to addressing this challenge by clearly pointing to the FGFR-PI3K co-dependency in *FGFR*-driven bladder and lung cancers. Moreover, we suggest that hyperactivated FGFR can be used as a biomarker for the efficacy of this combination (L. Wang et al., 2017).

In our study (Chapter 2) we used the pan-PI3K inhibitor BKM120 because one or more of the remaining class I PI3Ks may assume the signalling functions of the drug-inhibited PI3K isoform when isoform-selective PI3K inhibitors are used. The concept of PI3K inhibitor-mediated feedback regulation of RTKs was explained mechanistically in renal cancer cells where the PI3K-AKT pathway is a validated therapeutic target (Lin et al., 2014). More specifically, Lin *et al* showed that PI3K inhibitor treatment promotes AKT phosphorylation at Ser473 via FOXO transcription factors that also upregulate the expression of RICTOR, an essential component of the mTOR complex 2 (Lin et al., 2014). That study also points to FOXO as a potential biomarker that can be used to stratify renal cell carcinoma patients that would benefit from PI3K or AKT inhibitor treatment. However, the clinical utility of a transcription factor as a novel therapeutic target, is limited due to the poor drug-ability of these proteins. The advantage of combination treatment of PI3K with an RTK, such as FGFR, that we propose in chapter 2, is in the fact that inhibitors are already commercially available, and clinically tested. Moreover, various clinical studies published in recent years (presented above) have informed us about the toxicity profiles of different PI3K inhibitors enabling a better-informed test compound selection.

The development of FGFR inhibitors also made clinical advances in recent years. In 2017, Perera *at al* reported the discovery and pharmacological characterization of JNJ-42756493 (Erdafitinib) (Perera et al., 2017). It is an orally active small molecule with potent tyrosine kinase inhibitory activity against all four FGFR family members and selectivity versus other highly related kinases. Erdafitinib shows rapid uptake into the lysosomal compartment of cells in culture, which is associated with prolonged inhibition of FGFR signalling, most likely due to sustained release of the inhibitor. In July 2019, a phase 2 clinical study reports that the use of erdafitinib is associated with an objective tumor response in 40% of previously treated patients with locally advanced and metastatic urothelial carcinoma with *FGFR* alterations (Loriot et al., 2019). Moreover, the same study suggests the use of erdafitinib over immunotherapy given the better response rate, similar rates of overall survival, and lower activity of immunotherapy in patients with *FGFR* mutations. These results led to the accelerated approval of erdafitinib by the Food and Drug Administration (FDA) in April 2019 for the treatment of patients with locally advanced or metastatic *FGFR*-mutant urothelial carcinoma (Markham, 2019), even though more work is needed to establish the *FGFR* mutation status as a biomarker for resistance to immunotherapy. Also, nearly half of the erdafitinib treated patients suffered from treatment-related grade 3 or higher adverse events (Loriot et al., 2019). However, the results of reported trials have provided a solid proof-of-concept for the use of FGFR inhibitors in the treatment of urothelial carcinoma with *FGFR* alterations. Erdafitinib is currently being investigated as a treatment for other cancers including cholangiocarcinoma, liver cancer, non-small cell lung cancer, prostate cancer, lymphoma and oesophageal cancer (Markham, 2019).

Penetrance of synthetic lethality

Synthetic lethality refers to a situation where perturbation of individual genes is well tolerated, but perturbation of combinations of genes results in cell death. The concept was initially used to describe an incompatibility between pairs of alleles in fruit flies, and the first clinical application, described in the introduction (Chapter 1) led to regulatory approval of PARP inhibitors for the treatment of breast or ovarian cancers with mutations in the *BRCA1* or *BRCA2* tumor-suppressor genes (Lord and Ashworth, 2017). Despite the development of targeted therapeutics designed to target specific cancer-driving mutations, the vast majority of patients are still treated either by surgery, chemotherapy or radiotherapy, or combination thereof. After more than a decade of concentrated effort aimed at developing synthetic lethal treatments for cancer, we only have a handful of successful examples. One of the possible reasons could be attributed to the limitations of the RNAi technology, that used to be the primary technology used to identify synthetic lethal effects. In Chapter 2, we resorted to short hairpin RNA (shRNA), which is also one of the RNAi technologies, to search for synthetic lethal interactions with FGFR inhibitor. Short hairpin RNAs, like other RNAi approaches, are limited by ‘off-target’ effects, which means that the reagent used can inhibit other genes, in addition to the target gene (Echeverri et al., 2006). Second major challenge of the

RNAi technology is in its efficiency, as most RNAi reagents do not inhibit the target to any significant extent. As a consequence, each individual RNAi construct needs to be validated separately in the specific cell line model in question. This limits the researcher's ability to simultaneously test large panels of cell lines and opens the possibility of reporting false positives and false negatives as synthetic lethal partners (Kaelin, 2012). In fact, many drug targets identified by RNAi technologies in academic laboratories were not validated by robust approaches of industrial laboratories (Begley and Ellis, 2012; Prinz et al., 2011).

The development of CRISPR/Cas9 gene editing technology sparked new enthusiasm for identification of synthetic lethal interactions, due to improved targeting efficiency and reduced off-target effects (Mullard, 2017). For these reasons, we also switched from RNAi technology (in Chapter 2) to CRISPR/Cas9 based technologies (in Chapters 3 and 4 of this thesis). However, when it comes to identifying novel synthetic lethal interactions of notable clinical applicability, a much greater hurdle lies in the extensive molecular heterogeneity of tumors. As a result, most synthetic lethal interactions identified in a single model system are not highly penetrant, which means that they are not robustly applicable to diverse biological systems (Ashworth et al., 2011; Ryan et al., 2018). Even in model organisms, such as budding yeast, most screens are performed in a single defined genetic background (Chapter 3). As a result, it is challenging to estimate how dependent synthetic lethal effects are upon their genetic background, or how penetrant they might be across different backgrounds (Gasch et al., 2016). For example, in Chapter 2 we report that even some *FGFR* mutant cancer cell lines display a partial or complete lack of responsiveness to the combination of the FGFR and PI3K inhibitors, if they harbor mutations in the downstream effector of the PI3K, AKT1. This mutation allows cancer cells to maintain their proliferative capacity despite upstream inhibitions (L. Wang et al., 2017).

RAS synthetic lethality

The study of *RAS* genes and its interactions has been at the forefront of signal transduction and molecular oncology since pioneering work with acute transforming retroviruses to the current post-genomic period (Malumbres and Barbacid, 2003). Genetic dependencies associated with mutant RAS have been thoroughly investigated, mainly to circumvent the inability to directly inhibit most mutant RAS proteins with small molecules (Simanshu et al., 2017). As a result, a whole series of approaches were designed to indirectly target RAS-driven cancers through synthetic lethal (SL) genetic vulnerabilities that are selectively necessary for the maintenance of a RAS-mutated cell state.

Driven by the idea that synthetic lethality screens can identify genes that are essential only in the context of specific cancer-causing mutations, several groups have invested considerable efforts to identify synthetic lethal interactions with mutant *RAS*. This came as a direct application of the concepts first proposed by Hartwell *et al.* (Hartwell et al., 1997), and later reiterated by Brummelkamp and Bernards (Brummelkamp and Bernards, 2003), and others (Kaelin, 2005). These authors postulated that genetic screens can be used to identify protein targets that would create a therapeutic advantage in a mutant compared with a wild type genotype by screening for second site mutations that are lethal in the mutant strain but not in the wild-type strain. Mutant *RAS* is an exciting model to study synthetic lethal interactions as approximately 20% of all cancers are driven by deregulated activity of one of mutant *RAS* isoforms (Downward, 2015). In principle, synthetic lethality with mutant *RAS* would enable selective targeting of tumor cells while sparing the patient's nonmalignant cells.

One of the earliest examples of a *RAS* synthetic lethality screen was a kinome-centered short hairpin RNA (shRNA) screen which identified the non-canonical IκB kinase *TBK1* as selectively essential in mutant *KRAS*-driven non-small-cell lung cancer cells (Barbie et al., 2009). Considering that TBK1 can activate NF-κB anti-apoptotic signals that are essential for cell survival, this finding pointed to NF-κB signaling as essential in *KRAS* mutant tumors. Interestingly, our genome-wide MEK inhibitor resistance screen presented in Chapter 3 identified serine-threonine kinase *STK40* (Sustic et al., 2018), which has been described as a negative regulator of the NF-κB signaling (Huang et al., 2003; Xu et al., 2013). Subsequent validations have confirmed that the loss of *STK40* (and hence, presumably, sustained activation of the NF-κB signaling) renders *KRAS* mutant colorectal cancer (CRC) cells resistant to MEK inhibitors. This is in line with the finding that NF-κB activity can directly modulate resistance to several different MAPK pathway inhibitors (Konieczkowski et al., 2014). Given that NF-κB pathway can also regulate AP-1 transcriptional output (Fujioka et al., 2004) it is tempting to speculate that the loss of *STK40* might de-repress not only NF-κB, but also JUN, a component of the AP-1 transcription factor. If this would be the case, it would explain why *STK40* loss yields the same or similar functional consequences under MEK inhibitor as the loss of DET1 and COP1, established negative regulators of JUN (Sustic et al., 2018).

Over the years, different studies reported different synthetic lethal partners of mutant *RAS*. One of the most prominent examples was given by a series of shRNA screens in eight human cancer cell lines that identified serine-threonine kinase *STK33* as a synthetic lethal partner of mutant *RAS* (Scholl et al., 2009). Unfortunately, follow-up studies have failed to broadly validate this interaction leading to the conclusion that *RAS* synthetic lethal interaction with *STK33* is not widely applicable and most likely specific to model systems tested (Frohling and Scholl, 2011; T. Luo et al., 2012). Several other reported synthetic lethal interactions have also later been confirmed as highly context-dependent (Barbie et al., 2009; J. Luo et al., 2009; Scholl et al., 2009; Singh et al., 2012). This means that their clinical utility, if any, would be limited to a very specific group of patients, provided that such patients can be reliably identified as responders to a given synthetic lethal drug combination. Moreover, there is a very limited overlap between synthetic lethal effects identified by different screens. There are numerous reasons for why this could be the case, ranging from cellular heterogeneity and differences between individual *RAS* mutations to methodological differences and the difficulties of validating 2D cell culture data *in vivo* (Downward, 2015).

Despite all of these challenges, in 2017, Sabatini and coworkers reported a handful of *RAS* synthetic lethal interactions in acute myeloid leukemia (AML) cells involving genes required for RAS processing and MAPK signaling (T. Wang et al., 2017). However, to come to these findings they performed genome-wide CRISPR-Cas9 screens in 14 different AML cell lines. This allowed them to compare a panel of *KRAS*-mutant or *NRAS*-mutant cell lines with *KRAS*- (and *NRAS*-) wild-type cells, thus illustrating the scale of the efforts needed to identify and validate novel synthetic lethal interactions. For this reason, deeper molecular understanding of the mechanisms of gene interdependence in various model systems is an invaluable resource that could lead to the identification of novel vulnerabilities induced specifically by the oncogene-limited state.

Conclusion

Lessons learned from a series of concentrated efforts to identify synthetic lethal interactors with mutant *RAS* in human cells, systematically reviewed by Ashworth and Lord (Ashworth and Lord, 2018), have led to the establishment of a series of guidelines that might either assist in the discovery of robust synthetic lethal effects in other systems, or help us transcend towards higher-order synthetic lethality effects such as collateral dependencies (described in Chapter 1). An example of a newly discovered higher-order synthetic lethality is given in Chapter 3, as genetic inactivation of the unfolded protein response (UPR) executor *ERN1* in *KRAS*-mutant colorectal cancers can be regarded as a collateral dependency of MEK-inhibited cancer cell state (Sustic et al., 2018). Moreover, in Chapter 3, we use the acquired resistance as a tool to understand the molecular mechanism of drug sensitivity. On the other hand, in Chapter 4, we use acquired resistance (to MEK inhibitors) as a tool to unravel specific vulnerabilities of the drug-resistant state (Sustic et al., 2020).

REFERENCES

Ashworth, A., Lord, C.J., 2018. Synthetic lethal therapies for cancer: what's next after PARP inhibitors? Nat Rev Clin Oncol 1–13. doi:10.1038/s41571-018-0055-6

Ashworth, A., Lord, C.J., Reis-Filho, J.S., 2011. Genetic interactions in cancer progression and treatment. Cell 145, 30–38. doi:10.1016/j.cell.2011.03.020

Bachman, K.E., Argani, P., Samuels, Y., Silliman, N., Ptak, J., Szabo, S., Konishi, H., Karakas, B., Blair, B.G., Lin, C., Peters, B.A., Velculescu, V.E., Park, B.H., 2004. The PIK3CA gene is mutated with high frequency in human breast cancers. Cancer Biol. Ther. 3, 772–775. doi:10.4161/cbt.3.8.994

Baird, R.D., van Rossum, A.G.J., Oliveira, M., Beelen, K., Gao, M., Schrier, M., Mandjes, I.A.M., Garcia-Corbacho, J., Vallier, A.-L., Dougall, G., van Werkhoven, E., Linossi, C., Kumar, S., van Tinteren, H., Callari, M., Beddowes, E., Perez-Garcia, J.-M., Rosing, H., Platte, E., Nederlof, P., Schot, M., de Vries Schultink, A., Bernards, R., Saura, C., Gallagher, W., Cortés, J., Caldas, C., Linn, S.C., 2019. POSEIDON Trial Phase 1b Results: Safety, Efficacy and Circulating Tumor DNA Response of the Beta Isoform-Sparing PI3K Inhibitor Taselisib (GDC-0032) Combined with Tamoxifen in Hormone Receptor Positive Metastatic Breast Cancer Patients. Clinical Cancer Research 25, 6598–6605. doi:10.1158/1078-0432.CCR-19-0508

Barbie, D.A., Tamayo, P., Boehm, J.S., Kim, S.Y., Moody, S.E., Dunn, I.F., Schinzel, A.C., Sandy, P., Meylan, E., Scholl, C., Frohling, S., Chan, E.M., Sos, M.L., Michel, K., Mermel, C., Silver, S.J., Weir, B.A., Reiling, J.H., Sheng, Q., Gupta, P.B., Wadlow, R.C., Le, H., Hoersch, S., Wittner, B.S., Ramaswamy, S., Livingston, D.M., Sabatini, D.M., Meyerson, M., Thomas, R.K., Lander, E.S., Mesirov, J.P., Root, D.E., Gilliland, D.G., Jacks, T., Hahn, W.C., 2009. Systematic RNA interference reveals that oncogenic KRAS-driven cancers require TBK1. Nature 462, 108–112. doi:10.1038/nature08460

Baselga, J., Im, S.-A., Iwata, H., Cortés, J., De Laurentiis, M., Jiang, Z., Arteaga, C.L., Jonat, W., Clemons, M., Ito, Y., Awada, A., Chia, S., Jagiełło-Gruszfeld, A., Pistilli, B., Tseng, L.-M., Hurvitz, S., Masuda, N., Takahashi, M., Vuylsteke, P., Hachemi, S., Dharan, B., Di Tomaso, E., Urban, P., Massacesi, C., Campone, M., 2017. Buparlisib plus fulvestrant versus placebo plus fulvestrant in postmenopausal, hormone receptor-positive, HER2-negative, advanced breast cancer (BELLE-2): a randomised, double-blind, placebo-controlled, phase 3 trial. Lancet Oncol. 18, 904–916. doi:10.1016/S1470-2045(17)30376-5

Bedard, P.L., Tabernero, J., Janku, F., Wainberg, Z.A., Paz-Ares, L., Vansteenkiste, J., Van Cutsem, E., Pérez-García, J., Stathis, A., Britten, C.D., Le, N., Carter, K., Demanse, D., Csonka, D., Peters, M., Zubel, A., Nauwelaerts, H., Sessa, C., 2015. A phase Ib dose-escalation study of the oral pan-PI3K inhibitor buparlisib (BKM120) in combination with the oral MEK1/2 inhibitor trametinib (GSK1120212) in patients with selected advanced solid tumors. Clinical Cancer Research 21, 730–738. doi:10.1158/1078-0432.CCR-14-1814

Begley, C.G., Ellis, L.M., 2012. Drug development: Raise standards for preclinical cancer research. Nature 483, 531–533. doi:10.1038/483531a

Bendell, J.C., Rodon, J., Burris, H.A., de Jonge, M., Verweij, J., Birle, D., Demanse, D., De Buck, S.S., Ru, Q.C., Peters, M., Goldbrunner, M., Baselga, J., 2012. Phase I, dose-escalation study of BKM120, an oral pan-Class I PI3K inhibitor, in patients with advanced solid tumors. J. Clin. Oncol. 30, 282–290. doi:10.1200/JCO.2011.36.1360

Brummelkamp, T.R., Bernards, R., 2003. New tools for functional mammalian cancer genetics. Nature Reviews Cancer 3, 781–789. doi:10.1038/nrc1191

Chakrabarty, A., Sánchez, V., Kuba, M.G., Rinehart, C., Arteaga, C.L., 2012. Feedback upregulation of HER3 (ErbB3) expression and activity attenuates antitumor effect of PI3K inhibitors. Proc. Natl. Acad. Sci. U.S.A. 109, 2718–2723. doi:10.1073/pnas.1018001108

Chandarlapaty, S., Sawai, A., Scaltriti, M., Rodrik-Outmezguine, V., Grbovic-Huezo, O., Serra, V., Majumder, P.K., Baselga, J., Rosen, N., 2011. AKT inhibition relieves feedback suppression of receptor tyrosine kinase expression and activity. Cancer Cell 19, 58–71. doi:10.1016/j.ccr.2010.10.031

Chantry, D., Vojtek, A., Kashishian, A., Holtzman, D.A., Wood, C., Gray, P.W., Cooper, J.A., Hoekstra, M.F., 1997. p110delta, a novel phosphatidylinositol 3-kinase catalytic subunit that associates with p85 and is expressed predominantly in leukocytes. Journal of Biological Chemistry 272, 19236–19241. doi:10.1074/jbc.272.31.19236

Di Leo, A., Johnston, S., Lee, K.S., Ciruelos, E., Lønning, P.E., Janni, W., O'Regan, R., Mouret-Reynier, M.-A., Kalev, D., Egle, D., Csőszi, T., Bordonaro, R., Decker, T., Tjan-Heijnen, V.C.G., Blau, S., Schirone, A., Weber, D., El-Hashimy, M., Dharan, B., Sellami, D., Bachelot, T., 2018. Buparlisib plus fulvestrant in postmenopausal women with hormone-receptor-positive, HER2-negative, advanced breast cancer progressing on or after mTOR inhibition (BELLE-3): a randomised, double-blind, placebo-controlled, phase 3 trial. Lancet Oncol. 19, 87–100. doi:10.1016/S1470-2045(17)30688-5

Dong, S., Guinn, D., Dubovsky, J.A., Zhong, Y., Lehman, A., Kutok, J., Woyach, J.A., Byrd, J.C., Johnson, A.J., 2014. IPI-145 antagonizes intrinsic and extrinsic survival signals in chronic lymphocytic leukemia cells. Blood 124, 3583–3586. doi:10.1182/blood-2014-07-587279

Downward, J., 2015. RAS Synthetic Lethal Screens Revisited: Still Seeking the Elusive Prize? Clinical Cancer Research 21, 1802–1809. doi:10.1158/1078-0432.CCR-14-2180

Dreyling, M., Morschhauser, F., Bouabdallah, K., Bron, D., Cunningham, D., Assouline, S.E., Verhoef, G., Linton, K., Thieblemont, C., Vitolo, U., Hiemeyer, F., Giurescu, M., Garcia-Vargas, J., Gorbatchevsky, I., Liu, L., Koechert, K., Peña, C., Neves, M., Childs, B.H., Zinzani, P.L., 2017a. Phase II study of copanlisib, a PI3K inhibitor, in relapsed or refractory, indolent or aggressive lymphoma. Ann. Oncol. 28, 2169–2178. doi:10.1093/annonc/mdx289

Dreyling, M., Santoro, A., Mollica, L., Leppä, S., Follows, G.A., Lenz, G., Kim, W.S., Nagler, A., Panayiotidis, P., Demeter, J., Özcan, M., Kosinova, M., Bouabdallah, K., Morschhauser, F., Stevens, D.A., Trevarthen, D., Giurescu, M., Cupit, L., Liu, L., Köchert, K., Seidel, H., Peña, C., Yin, S., Hiemeyer, F., Garcia-Vargas, J., Childs, B.H., Zinzani, P.L., 2017b. Phosphatidylinositol 3-Kinase Inhibition by Copanlisib in Relapsed or Refractory Indolent Lymphoma. J. Clin. Oncol. 35, 3898–3905. doi:10.1200/JCO.2017.75.4648

Echeverri, C.J., Beachy, P.A., Baum, B., Boutros, M., Buchholz, F., Chanda, S.K., Downward, J., Ellenberg, J., Fraser, A.G., Hacohen, N., Hahn, W.C., Jackson, A.L., Kiger, A., Linsley, P.S., Lum, L., Ma, Y., Mathey-Prévôt, B., Root, D.E., Sabatini, D.M., Taipale, J., Perrimon, N., Bernards, R., 2006. Minimizing the risk of reporting false positives in large-scale RNAi screens. Nature Methods 3, 777–779. doi:10.1038/nmeth1006-777

Flinn, I.W., Hillmen, P., Montillo, M., Nagy, Z., Illés, Á., Etienne, G., Delgado, J., Kuss, B.J., Tam, C.S., Gasztonyi, Z., Offner, F., Lunin, S., Bosch, F., Davids, M.S., Lamanna, N., Jaeger, U., Ghia, P., Cymbalista, F., Portell, C.A., Skarbnik, A.P., Cashen, A.F., Weaver, D.T., Kelly, V.M., Turnbull, B., Stilgenbauer, S., 2018. The phase 3 DUO trial: duvelisib vs ofatumumab in relapsed and refractory CLL/SLL. Blood 132, 2446–2455. doi:10.1182/blood-2018-05-850461

Flinn, I.W., Miller, C.B., Ardeshna, K.M., Tetreault, S., Assouline, S.E., Mayer, J., Merli, M., Lunin, S.D., Pettitt, A.R., Nagy, Z., Tournilhac, O., Abou-Nassar, K.-E., Crump, M., Jacobsen, E.D., de Vos, S., Kelly, V.M., Shi, W., Steelman, L., Le, N., Weaver, D.T., Lustgarten, S., Wagner-Johnston, N.D., Zinzani, P.L., 2019. DYNAMO: A Phase II Study of Duvelisib (IPI-145) in Patients With Refractory Indolent Non-Hodgkin Lymphoma. J. Clin. Oncol. 37, 912–922. doi:10.1200/JCO.18.00915

Frohling, S., Scholl, C., 2011. STK33 kinase is not essential in KRAS-dependent cells--letter. Cancer Research 71, 7716–author reply 7717. doi:10.1158/0008-5472.CAN-11-2495

Fruman, D.A., Chiu, H., Hopkins, B.D., Bagrodia, S., Cantley, L.C., Abraham, R.T., 2017. The PI3K Pathway in Human Disease. Cell 170, 605–635. doi:10.1016/j.cell.2017.07.029

Fujioka, S., Niu, J., Schmidt, C., Sclabas, G.M., Peng, B., Uwagawa, T., Li, Z., Evans, D.B., Abbruzzese, J.L., Chiao, P.J., 2004. NF-kappaB and AP-1 connection: mechanism of NF-kappaB-dependent regulation of AP-1 activity. Molecular and Cellular Biology 24, 7806–7819. doi:10.1128/MCB.24.17.7806-7819.2004

García-García, C., Ibrahim, Y.H., Serra, V., Calvo, M.T., Guzmán, M., Grueso, J., Aura, C., Pérez, J., Jessen, K., Liu, Y., Rommel, C., Tabernero, J., Baselga, J., Scaltriti, M., 2012. Dual mTORC1/2 and HER2 blockade results in antitumor activity in preclinical models of breast cancer resistant to anti-HER2 therapy. Clinical Cancer Research 18, 2603–2612. doi:10.1158/1078-0432.CCR-11-2750

Garrett, J.T., Sutton, C.R., Kurupi, R., Bialucha, C.U., Ettenberg, S.A., Collins, S.D., Sheng, Q., Wallweber, J., Defazio-Eli, L., Arteaga, C.L., 2013. Combination of antibody that inhibits ligand-independent HER3 dimerization and a p110α inhibitor potently blocks PI3K signaling and growth of HER2+ breast cancers. Cancer Research 73, 6013–6023. doi:10.1158/0008-5472.CAN-13-1191

Gasch, A.P., Payseur, B.A., Pool, J.E., 2016. The Power of Natural Variation for Model Organism Biology. Trends Genet. 32, 147–154. doi:10.1016/j.tig.2015.12.003

Gopal, A.K., Kahl, B.S., de Vos, S., Wagner-Johnston, N.D., Schuster, S.J., Jurczak, W.J., Flinn, I.W., Flowers, C.R., Martin, P., Viardot, A., Blum, K.A., Goy, A.H., Davies, A.J., Zinzani, P.L., Dreyling, M., Johnson, D., Miller, L.L., Holes, L., Li, D., Dansey, R.D., Godfrey, W.R., Salles, G.A., 2014. PI3Kδ inhibition by idelalisib in patients with relapsed indolent lymphoma. N Engl J Med 370, 1008–1018. doi:10.1056/NEJMoa1314583

Hartwell, L.H., Szankasi, P., Roberts, C.J., Murray, A.W., Friend, S.H., 1997. Integrating genetic approaches into the discovery of anticancer drugs. Science 278, 1064–1068. doi:10.1126/science.278.5340.1064

Herrera-Abreu, M.T., Pearson, A., Campbell, J., Shnyder, S.D., Knowles, M.A., Ashworth, A., Turner, N.C., 2013. Parallel RNA interference screens identify EGFR activation as an escape mechanism in FGFR3-mutant cancer. Cancer Discovery 3, 1058–1071. doi:10.1158/2159-8290.CD-12-0569

Heudel, P.-E., Fabbro, M., Roemer-Becuwe, C., Kaminsky, M.C., Arnaud, A., Joly, F., Roche-Forestier, S., Meunier, J., Foa, C., You, B., Priou, F., Tazi, Y., Floquet, A., Selle, F., Berton-Rigaud, D., Lesoin, A., Kalbacher, E., Lortholary, A., Favier, L., Treilleux, I., Ray-Coquard, I., 2017. Phase II study of the PI3K inhibitor BKM120 in patients with advanced or recurrent endometrial carcinoma: a stratified type I-type II study from the GINECO group. British Journal of Cancer 116, 303–309. doi:10.1038/bjc.2016.430

Huang, J., Teng, L., Liu, T., Li, L., Chen, D., Li, F., Xu, L.-G., Zhai, Z., Shu, H.-B., 2003. Identification of a novel serine/threonine kinase that inhibits TNF-induced NF-kappaB activation and p53-induced transcription. Biochem. Biophys. Res. Commun. 309, 774–778.

Hyman, D.M., Snyder, A.E., Carvajal, R.D., Gerecitano, J.F., Voss, M.H., Ho, A.L., Konner, J., Winkelmann, J.L., Stasi, M.A., Monson, K.R., Iasonos, A., Spriggs, D.R., Bialer, P., Lacouture, M.E., Teitcher, J.B., Katabi, N., Fury, M.G., 2015. Parallel phase Ib studies of two schedules of buparlisib (BKM120) plus carboplatin and paclitaxel (q21 days or q28 days) for patients with advanced solid tumors. Cancer Chemother. Pharmacol. 75, 747–755. doi:10.1007/s00280-015-2693-z

Kaelin, W.G., 2012. Molecular biology. Use and abuse of RNAi to study mammalian gene function. Science 337, 421–422. doi:10.1126/science.1225787

Kaelin, W.G., 2005. The concept of synthetic lethality in the context of anticancer therapy. Nature Reviews Cancer 5, 689–698. doi:10.1038/nrc1691

Konieczkowski, D.J., Johannessen, C.M., Abudayyeh, O., Kim, J.W., Cooper, Z.A., Piris, A., Frederick, D.T., Barzily-Rokni, M., Straussman, R., Haq, R., Fisher, D.E., Mesirov, J.P., Hahn, W.C., Flaherty, K.T., Wargo, J.A., Tamayo, P., Garraway, L.A., 2014. A melanoma cell state distinction influences sensitivity to MAPK pathway inhibitors. Cancer Discovery 4, 816–827. doi:10.1158/2159-8290.CD-13-0424

Lin, A., Piao, H.-L., Zhuang, L., Sarbassov, D.D., Ma, L., Gan, B., 2014. FoxO transcription factors promote AKT Ser473 phosphorylation and renal tumor growth in response to pharmacologic inhibition of the PI3K-AKT pathway. Cancer Research 74, 1682–1693. doi:10.1158/0008-5472.CAN-13-1729

Liu, N., Rowley, B.R., Bull, C.O., Schneider, C., Haegebarth, A., Schatz, C.A., Fracasso, P.R., Wilkie, D.P., Hentemann, M., Wilhelm, S.M., Scott, W.J., Mumberg, D., Ziegelbauer, K., 2013. BAY 80-6946 is a highly selective intravenous PI3K inhibitor with potent p110α and p110δ activities in tumor cell lines and xenograft models. Mol. Cancer Ther. 12, 2319–2330. doi:10.1158/1535-7163.MCT-12-0993-T

Lord, C.J., Ashworth, A., 2017. PARP inhibitors: Synthetic lethality in the clinic. Science 355, 1152–1158. doi:10.1126/science.aam7344

Loriot, Y., Necchi, A., Park, S.H., Garcia-Donas, J., Huddart, R., Burgess, E., Fleming, M., Rezazadeh, A., Mellado, B., Varlamov, S., Joshi, M., Duran, I., Tagawa, S.T., Zakharia, Y., Zhong, B., Stuyckens, K., Santiago-Walker, A., De Porre, P., O'Hagan, A., Avadhani, A., Siefker-Radtke, A.O., BLC2001 Study Group, 2019. Erdafitinib in Locally Advanced or Metastatic Urothelial Carcinoma. N Engl J Med 381, 338–348. doi:10.1056/NEJMoa1817323

Luo, J., Emanuele, M.J., Li, D., Creighton, C.J., Schlabach, M.R., Westbrook, T.F., Wong, K.-K., Elledge, S.J., 2009. A Genome-wide RNAi Screen Identifies Multiple Synthetic Lethal Interactions with the Ras Oncogene. Cell 137, 835–848. doi:10.1016/j.cell.2009.05.006

Luo, T., Masson, K., Jaffe, J.D., Silkworth, W., Ross, N.T., Scherer, C.A., Scholl, C., Frohling, S., Carr, S.A., Stern, A.M., Schreiber, S.L., Golub, T.R., 2012. STK33 kinase inhibitor BRD-8899 has no effect on KRAS-dependent cancer cell viability. Proc. Natl. Acad. Sci. U.S.A. 109, 2860–2865. doi:10.1073/pnas.1120589109

Maira, S.-M., Pecchi, S., Huang, A., Burger, M., Knapp, M., Sterker, D., Schnell, C., Guthy, D., Nagel, T., Wiesmann, M., Brachmann, S., Fritsch, C., Dorsch, M., Chène, P., Shoemaker, K., De Pover, A., Menezes, D., Martiny-Baron, G., Fabbro, D., Wilson, C.J., Schlegel, R., Hofmann, F., García-Echeverría, C., Sellers, W.R., Voliva, C.F., 2012. Identification and characterization of NVP-BKM120, an orally available pan-class I PI3-kinase inhibitor. Mol. Cancer Ther. 11, 317–328. doi:10.1158/1535-7163.MCT-11-0474

Malumbres, M., Barbacid, M., 2003. RAS oncogenes: the first 30 years. Nature Reviews Cancer 3, 459–465. doi:10.1038/nrc1097

Markham, A., 2019. Erdafitinib: First Global Approval. Drugs 79, 1017–1021. doi:10.1007/s40265-019-01142-9

Markham, A., 2017. Copanlisib: First Global Approval. Drugs 77, 2057–2062. doi:10.1007/s40265-017-0838-6

Markham, A., 2014. Idelalisib: first global approval. Drugs 74, 1701–1707. doi:10.1007/s40265-014-0285-6

Matulonis, U.A., Wulf, G.M., Barry, W.T., Birrer, M., Westin, S.N., Farooq, S., Bell-McGuinn, K.M., Obermayer, E., Whalen, C., Spagnoletti, T., Luo, W., Liu, H., Hok, R.C., Aghajanian, C., Solit, D.B., Mills, G.B., Taylor, B.S., Won, H., Berger, M.F., Palakurthi, S., Liu, J., Cantley, L.C., Winer, E., 2017. Phase I dose escalation study of the PI3kinase pathway inhibitor BKM120 and the oral poly (ADP ribose) polymerase (PARP) inhibitor olaparib for the treatment of high-grade serous ovarian and breast cancer. Ann. Oncol. 28, 512–518. doi:10.1093/annonc/mdw672

Mullard, A., 2017. Synthetic lethality screens point the way to new cancer drug targets. Nature Reviews Drug Discovery 16, 589–591. doi:10.1038/nrd.2017.165

Muranen, T., Selfors, L.M., Worster, D.T., Iwanicki, M.P., Song, L., Morales, F.C., Gao, S., Mills, G.B., Brugge, J.S., 2012. Inhibition of PI3K/mTOR leads to adaptive resistance in matrix-attached cancer cells. Cancer Cell 21, 227–239. doi:10.1016/j.ccr.2011.12.024

Ndubaku, C.O., Heffron, T.P., Staben, S.T., Baumgardner, M., Blaquiere, N., Bradley, E., Bull, R., Do, S., Dotson, J., Dudley, D., Edgar, K.A., Friedman, L.S., Goldsmith, R., Heald, R.A., Kolesnikov, A., Lee, L., Lewis, C., Nannini, M., Nonomiya, J., Pang, J., Price, S., Prior, W.W., Salphati, L., Sideris, S., Wallin, J.J., Wang, L., Wei, B., Sampath, D., Olivero, A.G., 2013. Discovery of 2-{3-[2-(1-isopropyl-3-methyl-1H-1,2-4-triazol-5-yl)-5,6-dihydrobenzo[f]imidazo[1,2-d][1,4]oxazepin-9-yl]-1H-pyrazol-1-yl}-2-methylpropanamide (GDC-0032): a β-sparing phosphoinositide 3-kinase inhibitor with high unbound exposure and robust in vivo antitumor activity. J. Med. Chem. 56, 4597–4610. doi:10.1021/jm4003632

Patnaik, A., Appleman, L.J., Tolcher, A.W., Papadopoulos, K.P., Beeram, M., Rasco, D.W., Weiss, G.J., Sachdev, J.C., Chadha, M., Fulk, M., Ejadi, S., Mountz, J.M., Lotze, M.T., Toledo, F.G.S., Chu, E., Jeffers, M., Peña, C., Xia, C., Reif, S., Genvresse, I., Ramanathan, R.K., 2016. First-in-human phase I study of copanlisib (BAY 80-6946), an intravenous pan-class I phosphatidylinositol 3-kinase inhibitor, in patients with advanced solid tumors and non-Hodgkin's lymphomas. Ann. Oncol. 27, 1928–1940. doi:10.1093/annonc/mdw282

Perera, T.P.S., Jovcheva, E., Mevellec, L., Vialard, J., De Lange, D., Verhulst, T., Paulussen, C., Van De Ven, K., King, P., Freyne, E., Rees, D.C., Squires, M., Saxty, G., Page, M., Murray, C.W., Gilissen, R., Ward, G., Thompson, N.T., Newell, D.R., Cheng, N., Xie, L., Yang, J., Platero, S.J., Karkera, J.D., Moy, C., Angibaud, P., Laquerre, S., Lorenzi, M.V., 2017. Discovery and Pharmacological Characterization of JNJ-42756493 (Erdafitinib), a Functionally Selective Small-Molecule FGFR Family Inhibitor. Mol. Cancer Ther. 16, 1010–1020. doi:10.1158/1535-7163.MCT-16-0589

Prinz, F., Schlange, T., Asadullah, K., 2011. Believe it or not: how much can we rely on published data on potential drug targets? Nature Reviews Drug Discovery 10, 712–712. doi:10.1038/nrd3439-c1

Rodon, J., Braña, I., Siu, L.L., De Jonge, M.J., Homji, N., Mills, D., Di Tomaso, E., Sarr, C., Trandafir, L., Massacesi, C., Eskens, F., Bendell, J.C., 2014. Phase I dose-escalation and -expansion study of buparlisib (BKM120), an oral pan-Class I PI3K inhibitor, in patients with advanced solid tumors. Invest New Drugs 32, 670–681. doi:10.1007/s10637-014-0082-9

Ryan, C.J., Bajrami, I., Lord, C.J., 2018. Synthetic Lethality and Cancer – Penetrance as the Major Barrier. Trends Cancer 1–13. doi:10.1016/j.trecan.2018.08.003

Scholl, C., Frohling, S., Dunn, I.F., Schinzel, A.C., Barbie, D.A., Kim, S.Y., Silver, S.J., Tamayo, P., Wadlow, R.C., Ramaswamy, S., DOhner, K., Bullinger, L., Sandy, P., Boehm, J.S., Root, D.E., Jacks, T., Hahn, W.C., Gilliland, D.G., 2009. Synthetic Lethal Interaction between Oncogenic KRAS Dependency and STK33 Suppression in Human Cancer Cells. Cell 137, 821–834. doi:10.1016/j.cell.2009.03.017

Simanshu, D.K., Nissley, D.V., McCormick, F., 2017. RAS Proteins and Their Regulators in Human Disease. Cell 170, 17–33. doi:10.1016/j.cell.2017.06.009

Singh, A., Sweeney, M.F., Yu, M., Burger, A., Greninger, P., Benes, C., Haber, D.A., Settleman, J., 2012. TAK1 inhibition promotes apoptosis in KRAS-dependent colon cancers. Cell 148, 639–650. doi:10.1016/j.cell.2011.12.033

Smith, S.M., Pitcher, B.N., Jung, S.-H., Bartlett, N.L., Wagner-Johnston, N., Park, S.I., Richards, K.L., Cashen, A.F., Jaslowski, A., Smith, S.E., Cheson, B.D., Hsi, E., Leonard, J.P., 2017. Safety and tolerability of idelalisib, lenalidomide, and rituximab in relapsed and refractory lymphoma: the Alliance for Clinical Trials in Oncology A051201 and A051202 phase 1 trials. Lancet Haematol 4, e176–e182. doi:10.1016/S2352-3026(17)30028-5

Smyth, L.M., Monson, K.R., Jhaveri, K., Drilon, A., Li, B.T., Abida, W., Iyer, G., Gerecitano, J.F., Gounder, M., Harding, J.J., Voss, M.H., Makker, V., Ho, A.L., Razavi, P., Iasonos, A., Bialer, P., Lacouture, M.E., Teitcher, J.B., Erinjeri, J.P., Katabi, N., Fury, M.G., Hyman, D.M., 2017. A phase 1b dose expansion study of the pan-class I PI3K inhibitor buparlisib (BKM120) plus carboplatin and paclitaxel in PTEN deficient tumors and with dose intensified carboplatin and paclitaxel. Invest New Drugs 35, 742–750. doi:10.1007/s10637-017-0445-0

Sustic, T., Bosdriesz, E., van Wageningen, S., Wessels, L.F.A., Bernards, R., 2020. RUNX2/CBFB modulates the response to MEK inhibitors through activation of receptor tyrosine kinases in KRAS-mutant colorectal cancer. Transl Oncol 13, 201–211. doi:10.1016/j.tranon.2019.10.006

Sustic, T., van Wageningen, S., Bosdriesz, E., Reid, R.J.D., Dittmar, J., Lieftink, C., Beijersbergen, R.L., Wessels, L.F.A., Rothstein, R., Bernards, R., 2018. A role for the unfolded protein response stress sensor ERN1 in regulating the response to MEK inhibitors in KRAS mutant colon cancers. Genome Med 10, 90. doi:10.1186/s13073-018-0600-z

Thorpe, L.M., Yuzugullu, H., Zhao, J.J., 2015. PI3K in cancer: divergent roles of isoforms, modes of activation and therapeutic targeting. Nature Reviews Cancer 15, 7–24. doi:10.1038/nrc3860

Vanhaesebroeck, B., Welham, M.J., Kotani, K., Stein, R., Warne, P.H., Zvelebil, M.J., Higashi, K., Volinia, S., Downward, J., Waterfield, M.D., 1997. P110delta, a novel phosphoinositide 3-kinase in leukocytes. Proceedings of the National Academy of Sciences 94, 4330–4335. doi:10.1073/pnas.94.9.4330

Wang, L., Sustic, T., Leite de Oliveira, R., Lieftink, C., Halonen, P., van de Ven, M., Beijersbergen, R.L., van den Heuvel, M.M., Bernards, R., van der Heijden, M.S., 2017. A Functional Genetic Screen Identifies the Phosphoinositide 3-kinase Pathway as a Determinant of Resistance to Fibroblast Growth Factor Receptor Inhibitors in FGFR Mutant Urothelial Cell Carcinoma. European Urology 71, 858–862. doi:10.1016/j.eururo.2017.01.021

Wang, T., Yu, H., Hughes, N.W., Liu, B., Kendirli, A., Klein, K., Chen, W.W., Lander, E.S., Sabatini, D.M., 2017. Gene Essentiality Profiling Reveals Gene Networks and Synthetic Lethal Interactions with Oncogenic Ras. Cell 168, 890–903.e15. doi:10.1016/j.cell.2017.01.013

Xu, N., Meisgen, F., Butler, L.M., Han, G., Wang, X.-J., Söderberg-Nauclér, C., Ståhle, M., Pivarcsi, A., Sonkoly, E., 2013. MicroRNA-31 is overexpressed in psoriasis and modulates inflammatory cytokine and chemokine production in keratinocytes via targeting serine/threonine kinase 40. J. Immunol. 190, 678–688. doi:10.4049/jimmunol.1202695

Yang, J., Nie, J., Ma, X., Wei, Y., Peng, Y., Wei, X., 2019. Targeting PI3K in cancer: mechanisms and advances in clinical trials. Mol Cancer 18, 26–28. doi:10.1186/s12943-019-0954-x

Zhao, J.J., Cheng, H., Jia, S., Wang, L., Gjoerup, O.V., Mikami, A., Roberts, T.M., 2006. The p110alpha isoform of PI3K is essential for proper growth factor signaling and oncogenic transformation. Proceedings of the National Academy of Sciences 103, 16296–16300. doi:10.1073/pnas.0607899103

Appendix

Nederlandse samenvatting

Summary *(in English)*

Curriculum vitae

Publication list

Acknowledgments

Nederlandse samenvatting

Kanker werd historisch gezien als een genetische ziekte gekarakteriseerd door ongeremde proliferatie van getransformeerde cellen met invasieve eigenschappen leidend tot metastases in verschillende organen van het menselijk lichaam. Tientallen jaren onderzoek naar kanker heeft ons verregaande inzichten gegeven waardoor het beeld van kanker als dodelijke ziekte wordt uitgedaagd. De ontdekking van "driver" mutaties bracht specifieke kwetsbaarheden van kankercellen aan het licht, genaamd *oncogene addiction*, en creëerde interesse in het ontwikkelen en het toepassen van geneesmiddelen die specifiek het veranderde eiwit zelf of de signaleringsroute die het aanstuurt blokkeert en de progressie van kanker remt. Deze gerichte geneesmiddelen zijn bedoeld om de afwijkende signalering, waaraan kankercellen verslaafd zijn, te blokkeren of te verstoren. Hierbij wordt toxiciteit voor normale cellen gereduceerd. Sommige van deze geneesmiddelen worden al met succes in de kliniek gebruikt, voornamelijk in het verlengen van progressievrije overleving, maar met beperkte verbeteringen in de totale overleving door het ontstaan van resistentie.

Hoofdstuk 1 geeft een overzicht van de belangrijkste strategieën die gebruikt worden om de ontwikkeling van resistentie tegen doelgerichte geneesmiddelen tegen te gaan. Het gaat hier onder andere om behandelingen waarbij combinaties van geneesmiddelen worden gebruikt die gebaseerd zijn op de genetische concepten van *synthetic lethality* en *higher-order synthetic lethality* interactie, onlangs genoemd *collateral dependency*. Het verschil tussen *collateral dependency* en *synthetic lethality* kan gezien worden als semantiek, zoals in het voorbeeld bij de BRAF en EGFR remmer synergie in colorectale kanker. BRAF en EGFR remmers vertonen geen significante effecten in colorectale kanker wanneer deze middelen apart worden toegepast, echter in combinatie vertonen zij synergie. Deze combinatie was vastgesteld als een *synthetic lethal* geneesmiddelen combinatie. Anderzijds, geactiveerde EGFR kan worden beschouwd als collaterale afhankelijkheid van een BRAF geinhibeerde colorectale kankercel, omdat de remming van EGFR zorgt voor preventie van de *synthetic rescue effect* dat veroorzaakt word door de *feedback* reactivatie van receptor tyrosine kinases (RTKs). Tenslotte, het concept van collaterale kwetsbaarheid is voorgelegd omdat het mogelijkheden biedt voor innovatieve therapeutische interventies die gericht zijn op behandelings-resistente kankercellen.

Hoofdstuk 2 beschrijft de ontdekking van *synthetic lethal* combinatie van geneesmiddelen bestaande uit FGFR en PI3K remmers in *FGFR-driven* long- en blaaskanker. Deze ontdekking was gebaseerd op een functionele genetische *screen*, een onafhankelijke benadering die ontworpen is om genen te vinden die, wanneer ze worden geremd, de sensitiviteit van FGFR remmers versterken. We identificeerden meerdere componenten van de PI3K signaleringsroute en valideerden onze bevindingen *in vitro*, waarbij we zowel een genetische als een farmacologische aanpak gebruikten. Voor *in vivo* validatie gebruikten we xenograft muizen modellen. Ook ontdekten wij het moleculaire mechanisme achter deze synergie, die liet zien dat de remming van FGFR een snelle feedback activatie van EGFR en HER3 veroorzaakt. De re-activatie van deze RTKs is gereflecteerd in de verhoogde activiteit van de PI3K signaleringsroute, dus geeft het een solide grondslag voor het klinisch testen van FGFR remmers in combinatie met PI3K remmers in kanker die aangestuurd wordt door genetische activatie van FGFR genen.

Hoofdstuk 3 begint met het ambitieuze doel om de *synthetic lethal* interacties te vinden die specifiek gericht zijn het gemuteerde RAS eiwit. Daarbij maakten we gebruik van de resultaten van *genome-wide genetische screens* in gist en valideerde ze in *KRAS* gemuteerde colorectale kankercellen. Onze resultaten lieten zien dat het verlies van de endoplasmatic reticulum (ER) stress sensor *ERN1* geen invloed heeft op de groei, maar zorgt voor sensibilisatie voor MEK remming. Om te onderzoeken hoe *ERN1* de MEK remmer reacties moduleert, hebben we genetische *screens* uitgevoerd in *ERN1 knockout KRAS* gemuteerde colon kanker cellen om de genen te identificeren wiens inactivatie resistentie veroorzaakt tegen MEK remming. Vervolgens identificeerden we meerdere negatieve regulatoren van JUN N-terminal kinase (JNK)/JUN signalering en constateerde we de ERN1-JNK-JUN route als een nieuwe regulator van de MEK remmer respons in KRAS gemuteerde colon kanker. Meerdere signaleeringsroutes kunnen JUN activeren, deze ontdekking verklaart de resistentie van *KRAS* gemuteerde tumor cellen naar MEK remming behandeling. Ook lieten we zien dat JUN geactiveerde kinases, zoals TAK1 en JNK, een functioneren als collaterale afhankelijkheden van MEK remmende-behandelde *KRAS* gemuteerde kankercellen.

Hoofdstuk 4 beschrijft de onverwachte connectie tussen de osteogene master regulator transcriptiefactor RUNX2 en de cofactor CBFB, met de MAPK signaleringsroute. In dit hoofdstuk laten we zien dat het verlies van RUNX2 of CBFB, resistentie tegen MEK remmers in colorectale kankercellen kan veroorzaken. Mechanistisch, vonden we dat de inactivatie van deze genen resulteerden in de activatie van meerdere RTKs, dat blijkt door de hoge SHP2 fosfatase-activiteit. Vervolgens, maakten we gebruik van een SHP2 remmer om te onderzoeken of hoge SHP2 activiteit een causale rol heeft met betrekking tot het verlies van *RUNX2*-geinduceerde MEK remmer resistentie. Uiteindelijke, vonden we dat de SHP2 remmer de gevoeligheid voor MEK remmers herstelt in *RUNX2 knockout KRAS* gemuteerde colorectale kanker cellen. Deze bevinding is een aanvulling op eerdere studies van onze groep en anderen die het therapeutische potentieel van deze combinatie ook hebben aangetoond.

Hoofdstuk 5 geeft een kort overzicht van recentelijk-gerapporteerde klinische studies over de PI3K remmer buparlisib die gebruikt werd in hoofdstuk 2. Dit is relevant voor een beter begrip van de toekomstperspectieven van onze bevindingen uit hoofdstuk 2, gezien het feit dat het werk 4 jaar geleden voltooid was voor de voltooiing van dit proefschrift. Met de ontwikkeling van de nieuwe, minder toxische, PI3K en FGFR remmers, zal het mogelijk worden om klinische studies uit te voeren die de werkzaamheid van de voorgestelde combinatie te evalueren. Tenslotte bespreek ik daar de beperkingen van *synthetic lethality* als een concept en geven verschillende voorbeelden van *RAS synthetic lethality* studies, waardoor ik ons werk uit hoofdstuk 3 in een bredere context plaats.

Summary *(in English)*

Cancer has been historically referred to as a genetic disease characterized by the unrestrained proliferation of transformed cells and often also by invasion beyond tissue boundaries and metastasis to different organs of the human body. Decades of research on cancer have given us a solid foundation to challenge the perception of cancer as a deadly disease. In particular, the discovery of “driver” mutations revealed specific vulnerabilities of cancer cells, termed oncogene addiction, and sparked interest in developing and applying drugs that target specifically the protein product of a given mutated gene “driving” the progression of cancer. These targeted agents are meant to block or disrupt the aberrant signaling to which cancer cells are addicted, sparing the normal cells from collateral toxicity. Some of these agents have made a significant clinical success, especially in terms of prolonging progression-free survival, but with limited improvements in overall survival due to the emergence of resistance.

Chapter 1 gives an overview of main strategies used to overcome the development of resistance to targeted agents, such as drug combination treatments based on the genetic concepts of synthetic lethality and higher-order synthetic lethality interactions, recently termed “collateral dependency”. I note that the difference between collateral dependency and synthetic lethality can be a matter of semantics, as in the example of the BRAF and EGFR inhibitor synergy in colorectal cancer. Considering that neither BRAF nor EGFR inhibitors have significant effects in colorectal cancer when applied in isolation, but together exhibit synergy, this combination was established as a synthetic lethal drug combination. On the other hand, activated EGFR can be considered as a collateral dependency of a BRAF inhibited colorectal cancer cell state, as the inhibition of EGFR prevents synthetic rescue effect triggered by the feedback reactivation of receptor tyrosine kinases (RTKs). Finally, the concept of collateral vulnerability is presented as it opens possibilities for innovative therapeutic interventions targeting treatment-resistant cancer cell population.

Chapter 2 presents the discovery of a synthetic lethal drug combination of FGFR and PI3K inhibitors in *FGFR*-driven lung and bladder cancer. This finding was based on a functional genetic screen, an unbiased approach designed to find enhancers of sensitivity to FGFR inhibitors. We identified multiple components of the PI3K pathway and validated our findings in vitro, using both genetic and pharmacological approach, and *in vivo* using xenograft mouse models. We also uncover the molecular mechanism underlying this synergy, showing that the inhibition of FGFR causes a rapid feedback activation of EGFR and HER3. The reactivation of these RTKs is reflected in the enhanced activity of the PI3K pathway, thus giving a solid rationale for clinical testing of FGFR inhibitors in combination with PI3K inhibitors in cancers driven by the genetic activation of the FGFR genes.

Chapter 3 starts with an ambitious goal to find synthetic lethal interactions specific to mutant *RAS*. We make use of the results from genome-wide genetic screens in yeast, and validate them in *KRAS* mutant colorectal cancer cells. We find that the loss of the endoplasmatic reticulum (ER) stress sensor *ERN1* does not affect growth, but sensitizes to MEK inhibition. To investigate how *ERN1* modulates MEK inhibitor responses, we performed genetic screens in *ERN1* knockout *KRAS* mutant colon cancer cells to identify genes whose inactivation confers resistance to MEK inhibition. We subsequently identify multiple negative regulators of JUN N-terminal kinase (JNK) /JUN signalling and establish ERN1-JNK-JUN pathway as a novel regulator of MEK inhibitor response in *KRAS* mutant colon cancer. As multiple signalling pathways can activate JUN, this finding contributes to explaining the resistance of *KRAS* mutant tumor cells to MEK inhibitor treatment. We also demonstrate that JUN activating kinases, such as TAK1 and JNK, function as collateral dependencies of MEK inhibitor-treated *KRAS* mutant cancer cells.

Chapter 4 uncovers the unexpected connection between the osteogenic master regulator transcription factor *RUNX2* and its cofactor *CBFB*, with the MAPK pathway. In this chapter, we show that the loss of RUNX2 or CBFB can confer MEK inhibitor resistance in colorectal cancer cells. Mechanistically, we find that the inactivation of these genes, results in activation of multiple RTKs which is mirrored by the high SHP2 phosphatase activity. Next, we make use of a small molecule SHP2 inhibitor to investigate if high SHP2 activity has a causal role to loss of *RUNX2*-induced MEK inhibitor resistance. Finally, we find that SHP2 inhibitor reinstates sensitivity to MEK inhibitor in *RUNX2* knockout *KRAS* mutant colorectal cancer cells. This finding complements previous works from our group and others reiterating the therapeutic potential of this combination.

Chapter 5 first gives a brief overview of the recently reported clinical studies on PI3K inhibitor buparlisib used in Chapter 2. This is relevant for better understanding of future perspectives of our findings from Chapter 2, considering that the work described in Chapter 2 has been completed 4 years before completion of this thesis. With the development of novel PI3K and FGFR inhibitors with safer toxicity profiles, it is now possible to set up clinical studies that can evaluate the efficacy of the proposed combination. Finally, I discuss the limitations of the synthetic lethality as a concept, and give several examples of *RAS* synthetic lethality studies, thus putting our work from Chapter 3 in a broader context.

Curriculum vitae

Tonći Šuštić was born on the 21st of February 1984 to Anka and Siniša Šuštić in Split, Croatia. He completed his primary school education at the elementary school *Dobri*, Split, and high school at the *IV. gimnazija Marko Marulić*, Split. In 2002, he enrolled the molecular biology study program at the Department of Biology, Faculty of Science and Mathematics, University of Zagreb. From 1998 to 2004 he was financially supported by the scholarship of the city of Split, and from 2004 to 2006 he was a recipient of the Croatian State Scholarship as one of the top performing students nation-wide. He gained his first hands-on research experience at the Department of Biochemistry, where he joined the project studying seryl-tRNA synthetase structure-function relationship, under the supervision of the late Prof Ivana Weygand-Đurašević, from October 2005 till February 2006. From January to July 2006, he worked part-time as a teacher of biology and chemistry at the First High School of Computational Technology, in Zagreb. In 2006 he received the Dean's Award for Excellence, at the Faculty of Science and Mathematics, University of Zagreb, and the *'Top Scholarship for Top Students'* by NCL Media Group, which was the most prestigious scholarship in the country at that time. This allowed him to take his second internship at the Molecular Pathology Unit of the Massachusetts General Hospital in Boston, MA, United States of America. There, he studied the role of *HOXB13* in ovarian cancer progression with Prof Sandra Oršulić from July 2006 till February 2007. In 2007, he got accepted to the *Ecole Polytechnique Fédérale de Lausanne* (EPFL) Summer Research Program at the Swiss Institute for Experimental Cancer Research in Lausanne, Switzerland. There, he joined the research group of Prof Pierre Gönczy where he applied *in vivo* imaging techniques to study nuclear envelope breakdown in one cell stage *C. elegans* embryos under various RNAi conditions. In the following year, 2008, he did another summer placement to study the effects of copper toxicity on *D. melanogaster* development with the group of Prof Walter Schaffner, at the Institute of Molecular Life Sciences, University of Zurich, Switzerland.

In 2009 he received the poster award at the 2nd EMBO Young Scientists Forum, in Zagreb, Croatia. The practical aspect of the award included participation at the EMBO Meeting 2009 in Amsterdam, The Netherlands. There, he developed interest in cellular senescence which led him to obtain a Cancer Research UK International PhD Scholarship. In December 2009 he graduated from the University of Zagreb and in 2010 he joined the research group of Dr Masashi Narita at the Cancer Research UK, Cambridge Institute, where he studied the metabolomics of oncogene-induced senescence in collaboration with Prof John Griffiths and Prof Simon Tavaré. In 2010 Tonći Šuštić matriculated at the St. John's College of the University of Cambridge as a graduate student. In 2012, he obtained a Masters' degree (MPhil) in Medical Science (Oncology), at the University of Cambridge.

From May 2012 till July 2013 he worked as a Research Assistant to Prof Brian Huntly at the Department of Haematology, Cambridge Institute for Medical Research, University of Cambridge. In September 2013 he moved to the Netherlands to conduct his PhD on mechanisms of resistance to targeted therapies with Prof René Bernards, at the Netherlands Cancer Institute. Most of the results of the research that followed are presented in this thesis. In February 2020, he joined the immunoglobulin research group to study the mechanisms and functional consequences of antibody glycosylation under supervision of Dr Gestur Vidarsson and Prof Ellen van der Schoot at the Sanquin blood supply foundation in Amsterdam, the Netherlands.

Publication list

Key publications

Šuštić, T., Bosdriesz, E., van Wageningen, S., Wessels, L.F.A., and Bernards, R. (2020). RUNX2/CBFB modulates the response to MEK inhibitors through activation of receptor tyrosine kinases in *KRAS*-mutant colorectal cancer. *Translational Oncology.* 13(2): 201-211.

Šuštić, T.*, van Wageningen, S.*, Bosdriesz, E., Reid, R.J.D., Dittmar, J., Lieftink, C., Beijersbergen, R.L., Wessels, L.F.A., Rothstein, R., and Bernards, R. (2018). A role for the unfolded protein response stress sensor ERN1 in regulating the response to MEK inhibitors in KRAS mutant colon cancers. *Genome Medicine.* 10(1): 90.

Wang, L.*, **Šuštić, T.***, Leite de Oliveira, R.*, Lieftink, C., Halonen, P., van de Ven, M., Beijersbergen, R.L., van den Heuvel, M.M., Bernards, R., and van der Heijden, M.S. (2017). A Functional Genetic Screen Identifies the Phosphoinositide 3-kinase Pathway as a Determinant of Resistance to Fibroblast Growth Factor Receptor Inhibitors in *FGFR* Mutant Urothelial Cell Carcinoma. *European Urology.* 71(6): 858–862.

*equal contributions

Other published contributions

Palit, S.A., Vis, D., Stelloo, S., Lieftink, C., Prekovic, S., Bekers, E., Hofland, I., **Šuštić, T.**, Wolters, L., Beijersbergen, R., Bergman, A.M., Győrffy, B., Wessels, L.F., Zwart, W., and van der Heijden, M.S. (2019). TLE3 loss confers AR inhibitor resistance by facilitating GR-mediated human prostate cancer cell growth. *eLife.* 8: e47430.

Xue, Z., Vis, D.J., Bruna, A., **Šuštić, T.**, van Wageningen, S., Batra, A.S., Rueda, O.M., Bosdriesz, E., Caldas, C., Wessels, L.F.A., and Bernards, R. (2018). MAP3K1 and MAP2K4 mutations are associated with sensitivity to MEK inhibitors in multiple cancer models. *Cell Research.* 28(7): 719–729.

Horton, S.J., Giotopoulos, G., Yun, H., Vohra, S., Sheppard, O., Bashford-Rogers, R., Rashid, M., Clipson, A., Chan, W.-I., Sasca, D., Yiangou, L., Osaki, H., Basheer, F., Gallipoli, P., Burrows, N., Erdem, A., Sybrina, A., Foerster, S., Zhao, W., **Šuštić, T.**, Petrunkina Harrison, A., Laurenti, E., Okosun, J., Hodson, D., Wright, P., Smith, K.G., Maxwell, P., Fitzgibbon, J., Du, M.Q., Adams, D.J., and Huntly, B.J.P. (2017). Early loss of Crebbp confers malignant stem cell properties on lymphoid progenitors. *Nature Cell Biology.* 19(9): 1093–1104.

Theelen, W.S., Mittempergher, L., Willems, S.M., Bosma, A.J., Peters, D.D., van der Noort, V., Japenga, E.J., Peeters, T., Koole, K., **Šuštić, T.**, Blaauwgeers, J.L., van Noesel, C.J., Bernards, R., and van den Heuvel, M.M. (2016). FGFR1, 2 and 3 protein overexpression and molecular aberrations of FGFR3 in early stage non-small cell lung cancer. *J Pathol Clin Res.* 2(4): 223–233.

Alhomsi, K., Selig, M., **Šuštić, T.**, Katrangi, E., Weissig, V., and Laposata, M. (2008). Induction of apoptosis and necrosis in human peripheral blood mononuclear cells by fatty acid ethyl esters. *Alcohol Clin Exp Res.* 32(3): 534–543.

Acknowledgements

None of the work presented in this thesis would have been possible without the support of many people who trusted in my ability to design, conduct and report independent and original research. In large part, the results presented in this thesis were a fruit of well orchestrated team work. First and foremost, I would like to thank the person who orchestrated it all, **René Bernards**. Thank you, René, for the opportunity to become part of your team. In your lab I was able to learn from the many talented and committed people who inspired me to rise above my personal limitations and achieve more than I thought was possible. Thank you, René, for being an exceptional mentor, for never failing to recognize the perfect moment to motivate me and inspire me to think and find solutions outside the box.

Secondly, I owe my deepest gratitude to **Michel van den Heuvel**, my co-supervisor in the first two years of this PhD who made sure that my research efforts are rooted in clinical reality. Thanks to your initiative, I kept my work as translational as it can possibly get. I would also like to thank **Michiel van der Heijden** who interviewed me for this PhD position, together with René and Michel. Thank you, Michiel, for being an example of hard work and commitment. You did more for me than you think.

Among the many of my peers who helped me in this process, I would first like to thank **Liqin Wang**. Thank you, Liqin, for supervising my first months on B7, thank you for painting a very clear picture for me of the high standard that was expected of me as a PhD student and as a Bernards lab team member. Through your guidance, I learned how to practically manage long and complex experiments, how to organize and plan a series of experiments at once, and, most of all, how to stand up for myself. You thought me how important it is not only to perform experiments, analyze the data, but also to write up and report the results in as short of a time as possible. I thank **Pasi Halonen**, you helped me when I needed it most. Thank you **Ben Morris** and **Rodrigo Leite de Oliveira** for your support in crucial aspects of the FGFR work.

I would especially like to thank **Sake van Wageningen**. Thank you, Sake, for introducing me to the project you started and to which you dedicated many years of your work. Together, we made the project flow in a new direction. Thank you for being open to those changes, and to me as a colleague. Your gentle approach took me a long way. I also owe my gratitute to **Evert Bosdriesz**. Thank you, Evert, for sharing your expertize and making it so easy to work with you. Thank you **Lodewyk Wessels**, for teaming me up with Evert, I felt priviledged and humbled by that opportunity. Finally, I am deeply grateful to our collaborators, most especially to Prof **Rodney Rothstein** and **Robert Reid**. Without your support in crucial phases of the work it would not have been possible to wrap up in a such an elegant way.

To **Roderick Beijersbergen**, thank you. You are the kind of scientist that I always wanted to become. I admired your work, appreciated your comments and tried to absorb as much knowledge from you as I possibly could. Because of you, I feel that my PhD was too short. I would have loved to spend many more years learning from you. To **Cor Lieftink**, thank you for always taking the time to comprehend, analyze and process large amounts of data in record time. My impression is that one Cor is more valuable than an entire core facility. Without your commitment, we would never be as fast and as efficient as we were. **Wouter Nijkamp**, thank you for being the best office mate I ever had. Thank you for not holding anything back, for being open and direct about what you think. It is through your support that I learned to not depend on others, but to trust myself and my own abilities. Working with you was challenging, but every moment was worth the effort.

To **Bastiaan Evers**, thank you for sharing your insights and your reagents with me. Had it not been for your unique and elegant gene knockout system, it would have been impossible to do a CRISPR screen in a knockout clone in such a short time. That screen brought new life to my PhD and inspired me to perform more. You are one of the best, and for the experience of working with you, I remain grateful. Along the lines of thanking the best, **Chong Sun**, thank you for always finding time to talk to me, for all your insight and suggestions. This was invaluable support in all stages of my PhD. I wish you every success in managing your new team. I am sure your most productive days are yet to come.

I would also like to acknowledge **Loredana Vecchione** for being more then a colleague. In you, I knew that I always had a friend. Thank you **Begoña Diosdado**, for sharing so much of your knowledge and experience. Your enthusiasm is more contagious than COVID-19. Thank you **Sara Mainardi** and **Astrid Bosma** for making it so pleasant to work with you. Thank you **Marielle Hijmans**, **Katrien Berns** and **Annemieke Gennissen**, for accepting me in your tissue culture lab. Sharing workspace with you was a joy. Thank you **Anirudh Prahallad**, you have been an inspiration I could only hope for. You showed me how to finalize a PhD with grace and elegance, and how to make most out of it. You opened the doors that many of us will follow. I thank **Michael Cloesmeijer** for helping out with the first draft of the *Nederlandse samenvatting*. Your support and your example meant a world to me. Without you, it would not have been the same.

I acknowledge all of my fellow PhD students for their insights and comments. Thank you, **Živa**, **Antonio**, **Fleur**, **João**, **Jeroen**, **Sander** and **Robin** – I hope you all graduate soon. Thank you, Robin, for having the courage to continue on the footsteps of these projects. It was an exciting journey for me, and I am sure it will be no less exciting for you as well. Wish you all the best.

Sander Palit, you have been by my side for most of this PhD, it is as much your achievement as it is mine. Thank you for your trust and for your open heart. This work is the result of our journey together, of our commitment and passion. Please know that you can do even better and I look forward to your potential unfolding, and to reading your thesis.

Finally, I would like to acknowledge the people who supported my personal development. For me, these people were a source of peace, joy, strength and love. They are all my family as they shaped me in the kind of person I am today.

Dr. Vladimir Ivanov, no words can express how much your support and guidance means to me. I remember your advice: if you see water in front of you – jump in and swim! You inspired me to drop hesitating, to embrace whatever challenges life decides to put in front of us. You showed me how to walk on the burning fire of my own heart. Through the fire, you walked first, but you did not walk alone. My feet learned from your feet, and my breath learned from your breath. Here-now, I am with you, and I look forward to those two cakes! ...which brings me to thank late **Elizabeta Josipović**, wherever you are – thank you, thank you for showing me that it is possible to leave this world with a smile on the face. I am sorry I did not graduate in time for you to see it. But you left me the greatest gift, you showed me how much strength one can get from simply making a vow and sticking to it – no matter what, till the last day. The strength of your commitment was a guiding star in a dark night. This thesis is dedicated to you.

On the topic of dark nights, I thank **Teal Swan**, those precious moments with you were an eternity to me. You broke me down, and helped me get up. You destroyed me, and made me laugh, and you pushed me to fall deeper than I ever thought would be possible. You encouraged me to see what I was refusing to see. I feel so humbled for having bathed in your splendor, in your beauty and your grace. You opened up a river inside of me, a river of joy, gratitude and bliss.

In third place, of course, to complete the triangle, I thank **Alberto Varela**, for teaching me how to make a clear cut difference between what does not work, and that what works. So simple, so obvious, and yet I never even thought about it that way before. You inspired me to look beyond the veil of illusion, and to dare to face the eye of reality. Thank you, Alverto, for recognizing my potential, for trusting me, and, most especially, for giving me the opportunity to collaborate with you and your family – it has been an incredible experience!

My greatest and final gratitude goes to my parents, **Anka** and **Siniša Šuštić**. Thank you mother, thank you father, for showing me that it is possible to overcome even the most dire challenges. You carried me unscratched through years of famine and war, I do not think I will ever be able to understand how you managed. All those challenges fade away in the flame of your committment to life. Thank you for being a living example that it is never too late to drop the old and make space for the new. Thank you for daring to look inside, I know now that your relationship is the fertile land on which any seed would blossom. You inspire me to be grateful for everything. Everything was, is and will be – perfect.

End of the thesis

6th April 2020